

John Carlin
Site Vice President

R.E. Ginna Nuclear Power Plant, LLC
1503 Lake Road
Ontario, New York 14519-9364
585.771.5200
585.771.3943 Fax
John.carlin@constellation.com



U. S. Nuclear Regulatory Commission
Washington, DC 20555

June 2, 2009

ATTENTION: Document Control Desk

SUBJECT: R.E. Ginna Nuclear Power Plant
Docket No. 50-244

Third Supplemental Response to NRC Generic Letter 2004-002, "Potential Impact of Debris Blockage on Emergency Recirculation During Design Basis Accidents at Pressurized-Water Reactors"

- REFERENCES:
- (a) Letter from John Carlin (Ginna LLC) to Document Control Desk (NRC) dated February 29, 2008, Supplementary Response to Generic Letter 2004-002, "Potential Impact of Debris Blockage on Emergency Recirculation During Design Basis Accidents at Pressurized-Water Reactors"
 - (b) Letter from John Carlin (Ginna LLC) to Document Control Desk (NRC) dated July 25, 2008, Second Supplemental Response to NRC Generic Letter 2004-002, "Potential Impact of Debris Blockage on Emergency Recirculation During Design Basis Accidents at Pressurized-Water Reactors"
 - (c) NRC Generic Letter 2004-02: "Potential Impact of Debris Blockage on Emergency Recirculation During Design Basis Accidents at Pressurized-Water Reactors"
 - (d) Letter from Douglas Pickett (NRC) to John Carlin (Ginna LLC), dated January 07, 2009, REQUEST FOR ADDITIONAL INFORMATION RE: SUPPLEMENTAL RESPONSE TO GENERIC LETTER 2004-02, "POTENTIAL IMPACT OF DEBRIS BLOCKAGE ON EMERGENCY RECIRCULATION DURING DESIGN BASIS ACCIDENTS AT PRESSURIZED WATER REACTORS" - R.E. GINNA NUCLEAR POWER PLANT

By letters dated February 29, 2008 (Reference a) and July 25, 2008 (Reference b), R.E. Ginna Nuclear Power Plant LLC (Ginna LLC) provided supplemental responses to Generic Letter 2004-02, "Potential Impact of Debris Blockage on Emergency Recirculation During Design Bases Accidents at Pressurized-Water Reactors," dated September 13, 2004 (Reference c).

Reference d requested additional information related to our supplemental responses mentioned above. Attachment (1) contains our response to the request, with the exception of an evaluation of reactor in-vessel downstream effects requested as part of Question #33. This remaining information will be provided within 90 days of the issuance of the final NRC Safety Evaluation Report on WCAP-16793-NP, Ginna's commitment for which is contained in Attachment (2). Attachment (3) provides additional supporting information for RAI Question #1.

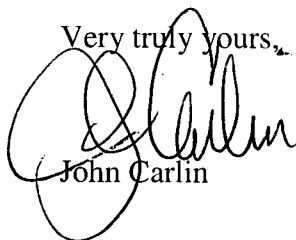
A116
NRR

WPLNRC-1002147

Document Control Desk
June 02, 2009
Page 2

If there are any questions or if additional information is required, please contact Mr. Thomas Harding at (585) 771-5219 or at Thomas.HardingJr@Constellation.com.

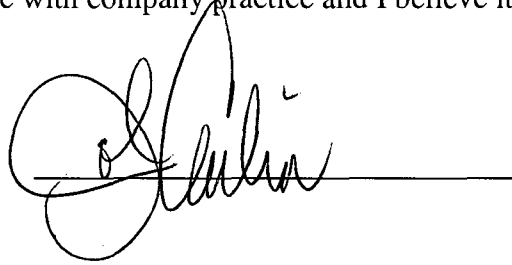
Very truly yours,

A handwritten signature in black ink, appearing to read "John Carlin". The signature is stylized with large, overlapping loops and a long horizontal stroke at the end.

John Carlin

STATE OF NEW YORK :
: TO WIT:
COUNTY OF WAYNE :

I, John Carlin, being duly sworn, state that I am Vice President, R.E. Ginna Nuclear Power Plant, LLC (Ginna LLC), and that I am duly authorized to execute and file this request on behalf of Ginna LLC. To the best of my knowledge and belief, the statements contained in this document are true and correct. To the extent that these statements are not based on my personal knowledge, they are based upon information provided by other Ginna LLC employees and/or consultants. Such information has been reviewed in accordance with company practice and I believe it to be reliable.



Subscribed and sworn before me, a Notary Public in and for the State of New York, and County of MONROE, this 2nd day of June, 2009.

WITNESS my Hand and Notarial Seal:


Notary Public
SHARON L. MILLER
Notary Public, State of New York
Registration No. 01M16017755
Monroe County
Commission Expires December 21, 2010

My Commission Expires:

12-21-10
Date

- Attachments: (1) REGNPP GL 2004-02 THIRD SUPPLEMENTAL RAI RESPONSE
(2) LIST OF REGULATORY COMMITMENTS
(3) SUMMARY OF CALCIUM SILICATE INSULATION TYPES USED INSIDE CONTAINMENT AT US NUCLEAR PLANTS

- cc: S. J. Collins, NRC
D. V. Pickett
P. D. Milano, NRC
Resident Inspector, NRC (Ginna)
P. D. Eddy, NYSDPS
A. L. Peterson, NYSERDA

ATTACHMENT 1

REGNPP GL 2004-02 THIRD SUPPLEMENTAL RAI RESPONSE

ATTACHMENT 1
REGNPP GL 2004-02 THIRD SUPPLEMENTAL RAI RESPONSE

Introduction

The complexity of the issues underlying Generic Letter (GL) 2004-02 has resulted in significant levels of margin being incorporated into the related analyses, design and testing of containment sump strainers and the impact of post-LOCA debris on plant equipment. Margin is needed to address newly discovered issues and in mitigating any potential unknowns or uncertainties; however, embedded in all supporting analyses, design and testing are layer upon layer of conservatism. In recognition of the compounding nature of these conservatisms and the need for a holistic review of compliance with GL 2004-02, the following is offered to facilitate the NRC's review and conclusion that Ginna has sufficient Emergency Core Cooling System (ECCS) pump Net Positive Suction Head (NPSH) margin available and that adequate margin exists to conclude that there is reasonable assurance that Ginna complies with GL 2004-02.

Review of Ginna Conservatisms

Strainer Head Loss Testing:

The quantity of debris used in strainer head loss testing exceeded that predicted to be generated for any given break location. The specific conservative debris quantities utilized in head loss testing are as follows:

- The largest quantity of each debris type, regardless of break location, was used in the head loss testing. This was done to ensure that the testing bounds all debris sources for all break locations. As a result, the quantity of fiber and particulate used in testing is greater than that determined to transport to the sump for any single break location.
- The maximum quantity of calcium silicate debris determined to be generated by any break location was determined to be 178.3 kg, of which 23.54 kg (~13%) is predicted to be consumed in precipitant generation. The quantity of particulate used in head loss testing was not reduced by the quantity of calcium silicate consumed in precipitant generation.
- The quantity of degraded phenolic coatings (chips) used in strainer head loss testing was increased by approximately 4 times the scaled quantity that was determined to transport to the sump. Similarly, the quantity of failed phenolic coatings (fines) was increased by approximately 1 ½ times.
- The quantity of degraded Inorganic Zinc (IOZ) coatings (fines) used in strainer head loss testing was increased by approximately 4 times the scaled quantity that was determined to transport to the sump.
- The quantity of Thermal Wrap fines used in strainer head loss testing was increased by approximately 7% above the scaled quantity that was determined to transport to the sump.
- The quantity of Temp Mat fines used in strainer head loss testing was increased by approximately 7% above the scaled quantity that was determined to transport to the sump.

ATTACHMENT 1
REGNPP GL 2004-02 THIRD SUPPLEMENTAL RAI RESPONSE

- All debris that settled on the floor of the test flume was mechanically agitated to re-suspend the debris in order to maximize the debris presented to the face of the test strainer, and therefore maximize the strainer head loss.
- The quantity of latent debris used in testing reflects an increase of 160% above the quantity determined to be in containment.
- Fibrous debris classification for intact pieces was taken as “large” pieces in the testing.
- Residual Heat Removal (RHR) pump flow rates used in testing (2300 gpm) bound all pump flow rates. Calculated flows for the case that yields the minimum NPSH for the ECCS pumps (approximately 1850 gpm) are 24% less than the flow utilized during testing. This represents additional margin for strainer head loss testing, and vortexing and flashing evaluations.

Debris Generation Analysis:

There are significant conservatisms in the performance of a debris generation calculation that comports with the NEI 04-07 Guidance Report (GR) and its associated Safety Evaluation Report (SER). The debris generation calculation provides the estimate of the quantity and characteristics of debris that could potentially be generated by a hypothetical high energy pipe break inside the Ginna reactor building [I.1]. The following layers of conservatisms are noted:

- The Zone of Influence (ZOI) radii were based on a 40% decrease of the BWROG Utility Resolution Guidance (URG) destruction pressures to conform to the NRC guidance on the SER to the GR [I.2]. The destruction pressures as endorsed by the NRC on the SER to the URG were based on conservative interpretation of the air jet blast testing that simulated a high energy steam line break [I.3]. The limiting Reactor Coolant System (RCS) line breaks are saturated water. Saturated water tests have consistently been shown to be less destructive than a steam line break as noted in the April 2008 NRC letter to the BWROG [I.4]:

Large-scale jet impact testing, such as that conducted by Swedish utilities at the Siemens - KWU facilities in Karlstein, Germany in 1994-95, has clearly demonstrated that saturated water jets are far less destructive than steam jets. This suggests that single-phase air jet tests would be conservative relative to two-phase saturated water tests (e.g., similar to steam).

Therefore, the destruction pressures should have been increased to account for the differences between steam and saturated water. The reduction of the destruction pressures by the NRC to account for undefined uncertainties added yet another layer of conservatism to an already conservatively derived destruction pressure.

- The ZOI radii derived in the SER to the GR were based on the ANS/ANSI jet model. Comparison of the Computational Fluid Dynamics (CFD) ZOI radii derived by the BWROG demonstrated that the ZOI radii for low destruction pressures such as for low density fiberglass (e.g. Nukon) are significantly lower than those derived by the ANS/ANSI jet model. This is expected since the ANS/ANSI jet model predicts an unrealistic long isobar elongation at lower pressures since the jet

ATTACHMENT 1
REGNPP GL 2004-02 THIRD SUPPLEMENTAL RAI RESPONSE

centerline pressure equation of the ANS/ANSI jet model is inherently unbounded. The use of the ANS/ANSI jet model adds another layer of conservatism to the derivation of the ZOI radii used in the Ginna calculation.

- The Ginna debris generation calculation did not employ refinements such as shadowing by large components. These refinements were not invoked in order to ensure conservatism in the calculation of debris generated in a postulated ZOI. Not implementing refinements such as shadowing adds another layer of conservatism in the calculation of the quantity of debris from a ZOI.
- The Ginna debris generation calculation adopted a four category debris size distribution for insulation debris based on the methodology provided in the SER to the GR. The implementation of the four size distribution methodology used by Ginna is conservative since the curve fits to the destruction data were conservatively performed [I.5]. The conservatism of the debris size distribution provides for another layer of conservatism in the quantification of the debris quantities reaching the ECCS sump.
- The Ginna debris generation calculation addressed the latent debris quantification by invoking the plant specific latent debris quantification performed in conjunction with the GSI-191 walkdown. This quantification employed conservatisms in the estimation of the surface areas and the measurement of the weight in the sample. The quantification of the latent debris walkdown was further increased by approximately 160% to account for uncertainties associated with latent debris on surfaces not accounted for in the walkdown. Additionally, the latent debris quantification invoked the conservative latent debris categorization provided in the SER to the GR. The use of the walkdown report to estimate the latent debris in containment, the use of the latent debris categorization of the SER to the GR and the additional 160% margin provides for another layer of conservatism in the quantification of the debris quantities reaching the ECCS sump.

Debris Transport Analysis:

Similar to the debris generation calculation, there are significant conservatisms in the performance of a debris transport calculation that comports with the NEI 04-07 GR and its associated SER. The debris transport calculation provides the estimate of the fraction of each type and size of debris that could potentially be transported to the ECCS sump strainer in the Ginna reactor building [I.6]. The following layers of conservatisms are noted:

- During the blowdown phase, significant quantities of fine and small piece debris would be blown to regions shielded from the containment sprays. The Ginna debris transport calculation conservatively neglects this phenomenon, and does not credit the retention of debris lodged in miscellaneous structures during the blowdown phase.
- Similarly, during the washdown phase, the only credit taken for debris retention is for debris washed to inactive cavities or pieces of debris held up on the concrete operating deck. Any retention of fine debris is conservatively neglected. Also, no credit was taken for the holdup of small pieces of debris on the concrete floors in upper containment.

ATTACHMENT 1
REGNPP GL 2004-02 THIRD SUPPLEMENTAL RAI RESPONSE

- The water draining from the RCS breach was assumed to do so without encountering any structures before reaching the containment pool. This is a conservative assumption since any impact with structures would dissipate the momentum of the water and decrease the turbulent energy in the pool.
- The transport analysis assumes that all transported debris would accumulate on the strainer. However, the height of the replacement strainer is such that most debris transported along the floor is not likely to lift off of the floor onto the strainer.
- No credit was taken for the unique configuration of the Ginna sump strainer location and the installed debris interceptors. The majority of the Ginna sump strainers are installed along the perimeter of the fuel transfer canal wall. Debris interceptors, constructed of the same perforated plate as used in the strainer modules, serve as a barrier to debris impacting the back side of the strainer modules. The debris that impacts the back side of the strainers would flow over the top of the strainer module. As demonstrated through strainer head loss testing, this reduces the quantity of debris that impacts approximately 40% of the installed strainer surface area.
- It was conservatively assumed that all latent debris is in the containment pool at the beginning of recirculation. This is a conservative assumption since no credit is taken for debris remaining on structures and equipment above the pool water level or transport to inactive cavities.

Head Loss and NPSH Calculations [I.7]:

- No credit for containment over-pressure has been taken, thereby, preserving additional ECCS pump NPSH margin. The additional NPSH margin that this alone provides ranges from approximately 86 ft at switchover to sump recirculation for the Large Break Loss of Coolant Accident (LBLOCA) to approximately 17 ft later in the Small Break Loss of Coolant Accident (SBLOCA), when less flow and therefore less NPSH is required.
- The strainer central duct and connecting channel head loss was taken from the most remote point from the containment sump. This value was applied to the entire sump strainer, when in reality portions of the sump strainer closer to the containment sump would experience a lower head loss than that calculated. For example, five of the sixteen strainer modules sit directly on the sump cover. These strainer modules would have no head loss due to connecting channels.
- The NPSH calculation uses strainer head loss for the LBLOCA, but recirculation pool depth for the SBLOCA, thereby conservatively bounding both breaks.
- The flow coefficient of the RHR flow control valves, HCV-624 and HCV-625, used in the NPSH calculation is conservatively applied at its upper limit based on testing, which increases the NPSH that is required.
- Values for pump Net Positive Suction Head Required (NPSHR) are taken for cold water conditions (<100 °F). This results in larger NPSHR values than that for actual water

ATTACHMENT 1
REGNPP GL 2004-02 THIRD SUPPLEMENTAL RAI RESPONSE

temperatures. However, the vapor pressure is taken at the saturation temperature (212 °F) of a depressurized containment. These assumptions maximize NPSHR while minimizing Net Positive Suction Head Available (NPSHA).

- The RCS was assumed to be fully depressurized for LBLOCA cases resulting in the highest possible RHR flow rate.
- For SBLOCA cases, when the RHR system is incapable of providing adequate flow to the RCS, the minimum pressure allowable for the restarting of high head Safety Injection (SI) pumps following sump switchover is assumed. These assumptions allow for the minimum back pressure during both the LBLOCA and SBLOCA scenarios resulting in maximum flow.
- The original vendor non-degraded pump head curve was used. This is conservative, because degraded pump head results in a drop in flow rate.
- By maximizing the RHR pump flow rate, the NPSH required is maximized. The maximum flow rate from the ProtoFlo analysis is less than the 2300 gpm used in testing, which ensures that the flow related losses due to a clogged strainer are conservative.
- The NPSH margin was determined to be 1.92 ft WC for the LBLOCA, and 1.57 ft WC for the SBLOCA.

Introduction References:

- I.1 Calculation ALION-CAL-CONS-3237-02, "Ginna Reactor Building GSI-191 Debris Generation Calculation", Revision 1.
- I.2 NEI 04-07 Volume 2, "Pressurized Water Reactor Sump Performance Evaluation Methodology", Revision 0.
- I.3 NEDO-32686-A Volumes 1 and 3, "Utility Resolution Guide for ECCS Suction Strainer Blockage", October 1998.
- I.4 Letter from John A. Grobe (NRC) to Richard Anderson (BWROG), ADAMS Accession Number ML080500540, "Subject: Potential Issues related to Emergency Core Cooling Systems (ECCS) Strainer Performance at Boiling Water Reactors", April 10, 2008.
- I.5 Alion Document ALION-REP-ALION-2806-01, "Insulation Debris Size Distribution for use in GSI-191 Resolution", Revision 3.
- I.6 Calculation ALION-CAL-GINNA-4376-03, "Ginna GSI-191 Debris Transport Calculation", Revision 2.
- I.7 DA-ME-2005-085, "NPSH for ECCS Pumps During Injection and Sump Recirculation," Revision 2.

ATTACHMENT 1
REGNPP GL 2004-02 THIRD SUPPLEMENTAL RAI RESPONSE

RESPONSES TO NRC RAIS CONTAINED IN JANUARY 7, 2009 LETTER

Preface:

Since the previous Ginna GL 2004-02 submittals, some analysis refinements, as well as, additional strainer testing have been completed. As a result, the following RAI responses reflect the most current basis for demonstrating compliance with the GL. Some details of previous submittals are superseded by the following.

RAI-1: *Please identify the source of the test data used to support the debris size distribution assumed for calcium silicate. Please compare the banding method, jacketing properties, and manufacturing process for the calcium silicate insulation material installed at Ginna versus the material and jacketing system or systems used for destruction testing.*

RAI-1 Response: The source data used to support the debris size distribution for calcium silicate (Cal-Sil) was from the Ontario Power Generation (OPG) Tests as documented in NUREG/CR-6808 [1.1].

A comparison of the Cal-Sil types is shown below in Table 1.1. The exact type of Cal-Sil used for the OPG testing was not documented. Note, however, that this test data is used as the basis for the 5.5D ZOI size that was accepted in the SER as well as the data set used in the SER (Appendix ii) Confirmatory Debris Generation Analyses to determine and confirm the destruction pressure/ZOI size.

The same approach recommended in the SER appendix was used to determine the size distribution in the Ginna debris generation calculation [1.2] based on the Alion size distribution methodology report [1.3]. This included conservatively increasing the accepted ZOI size of 5.5D to 6.4D for Cal-Sil. Table 1.2 shows a comparison of the Alion size distribution to the average OPG size distribution [1.3]. This table shows that the Alion size distribution is more conservative than the average OPG size distribution.

Since the Thermo-12 Gold Cal-Sil at Ginna uses a similar banding system and more robust cladding (Stainless Steel (SS) vs. aluminum), there is no reason to suspect that the Cal-Sil would be generated at a lower destruction pressure or a smaller size distribution than the OPG values used in the SER.

ATTACHMENT 1
REGNPP GL 2004-02 THIRD SUPPLEMENTAL RAI RESPONSE

Table 1.1 – Comparison of Ginna and OPG Cal-Sil

	Ginna Cal-Sil	OPG Cal-Sil
Name	Thermo-12 Gold	Not provided
Manufacturer	Johns Manville	Not provided
Banding	SS bands on 8” to 12” centers, with a band at each circumferential overlap [1.4]	SS bands on 8” centers where the jet was centered, varied between 3” and 8 ¼” elsewhere
Jacketing	Type 301 or 304 SS, with thickness of 0.01” for piping and 0.016 for equipment [1.4]	Aluminum with a thickness of 0.016”.
Manufacturing	Molded Cal-Sil conforming to ASTM C 533 Type 1 [1.4]	Not provided

Table 1.2 – Cal-Sil debris size distribution within each zone compared to average OPG size distribution

Size	Alion Size Distribution 70.0 psi ZOI (2.7D)	Alion Size Distribution 20.0 – 70.0 psi ZOI (6.4D – 2.7D)	Average OPG Size Distribution 20.0 psi ZOI (6.4D)
Fines (Particulate)	50%	23%	20%
Small Pieces (Under 1” to Over 3”)	50%	15%	13%
Remains on Target	0%	62%	67%

The other type of Cal-Sil installed at Ginna is Cal-Sil with amosite asbestos fibers. In his document, *Summary of Calcium Silicate Insulation Types Used inside Containment at US Nuclear Plants*, [Attachment 3] Gordon H. Hart, P.E., describes that over the past 50 years or so of nuclear power plant construction and operation, several different types of Cal-Sil pipe and block insulation have been used. The summary prepared by Hart was based upon information provided by Tom Whitaker (800-866-3234 x. 5101, whitakert@iig-llc.com) of Technical Support at Industrial Insulation Group, LLC, (IIG), currently the only North American manufacturer of Cal-Sil.

Hart categorizes Cal-Sil with asbestos fiber as Type 1 Cal-Sil created with a post-autoclave process that was discontinued in the early 1970’s due to asbestos’ carcinogenic attributes. Type 2 is free of asbestos fibers and is made by a filter press pre-autoclave process (also called the Johns-Manville Process, which is the method that is used to produce the Thermo-12 Gold at Ginna). Type 3 is also free of asbestos fiber and is made in a pour and mold process known as the Pabco Process, also a Post Autoclave process.

Further, according to IIG [Attachment 3], Type 3 Cal-Sil is more friable than Type 2 Cal-Sil. Type 3 Cal-Sil is softer and will most likely erode faster in a moving fluid than Type 2 Cal-Sil. Further according to IIG, “To my (Whitaker’s) knowledge, there is no published information related to erosion rates of any of these products. The comparison of the erosion rates is based on personal experience in the Calcium Silicate business since 1972.”

ATTACHMENT 1
REGNPP GL 2004-02 THIRD SUPPLEMENTAL RAI RESPONSE

Also according to IIG, Whitaker indicates that, "My opinion is that the asbestos-based Cal-Sil would have less erosion due to moving fluids than the non-asbestos based insulation products."

In summary, based upon the above information,

- Type 1, asbestos fiber-reinforced, Post Autoclave process, Cal-Sil is the least susceptible to erosion of the three Cal-Sil types described by Hart,
- Type II, non-asbestos, Johns-Manville Process Cal-Sil is less susceptible to erosion than the Type III Cal-Sil, and
- Type III, Pabco/Post Autoclave Process Cal-Sil is the most susceptible Cal-Sil of the three Cal-Sil types described by Hart.

The technical specification that calls for the use of asbestos laden Cal-Sil [1.5] was written in 1968 and it is reasonable to assume that this type of Cal-Sil at Ginna can be categorized as Type 1.

Table 6.4 in the Debris Generation Calculation uses a bulk density of 15 lb/ft³ for both Cal-Sil and asbestos Cal-Sil, which is higher than the density of 14.5 as reported in the GR [1.6]. The higher density used results in a conservative and greater quantity of destroyed insulation.

Both Cal-Sil insulation types use stainless steel jacketing with the same banding [1.4, 1.5]. Both Cal-Sil insulation types use a ZOI size of 6.4D (with the aforementioned stainless steel jacketing) in comparison to the aluminum jacketing reported in the SER [1.7] with a ZOI size of 5.5D.

Since the material types are similar, the asbestos Cal-Sil is considered to be more robust, both types have the same jacketing/banding system (which is more robust than aluminum jacketing from the SER and OPG testing), and a more conservative ZOI size is used than the size suggested in the SER, the debris generation calculation has treated both the Cal-Sil and asbestos Cal-Sil in a conservative and reasonable manner.

RAI-1 References:

- 1.1 D. V. Rao, C. J. Schafer, M. T. Leonard, K. W. Ross, "Knowledge Base for the Effect of Debris on Pressurized Water Reactor Emergency Core Cooling Sump Performance", NUREG/CR-6808, February 2003.
- 1.2 Calculation ALION-CAL-CONS-3237-02, "Ginna Reactor Building GSI-191 Debris Generation Calculation", Revision 1.
- 1.3 Alion Document ALION-REP-ALION-2806-01, "Insulation Debris Size Distribution for use in GSI-191 Resolution", Revision 3.
- 1.4 Engineering Specification ME-269, "Fabrication and Installation of Pipe, Duct and Equipment Insulation", June 15, 1994.
- 1.5 Engineering Specification SP-5401, "Pipe, Duct, and Equipment Insulation", August 22, 1967
- 1.6 NEI PWR Sump Performance Task Force Report NEI 04-07, "Pressurized Water Reactor Sump Performance Evaluation Methodology", Revision 0.
- 1.7 NRC Safety Evaluation Report, "Safety Evaluation by the Office of Nuclear Reactor Regulation Related to NRC Generic Letter 2004-02, Nuclear Energy Institute Guidance Report 'Pressurized Water Reactor Sump Performance Evaluation Methodology'", Revision 0, December 2004.

ATTACHMENT 1
REGNPP GL 2004-02 THIRD SUPPLEMENTAL RAI RESPONSE

RAI-2: *Please justify the treatment of the Asbestos insulation debris as though it was Thermo-12 Gold (surrogate) debris by either providing the comparative evaluation, or showing the transport, erosion, and head loss characteristics of the Thermo-12 Gold are conservative with respect to the corresponding characteristics for Asbestos.*

RAI-2 Response: As a point of clarification, the debris type “asbestos” that is listed in the debris generation and debris transport calculations is Cal-Sil with asbestos fibers, not asbestos blankets.

For debris transport purposes, the Cal-Sil with asbestos fines were treated similarly to the other fine debris generated, and the debris transport fraction was determined to be 83% [2.1].

The small pieces of Cal-Sil/asbestos (which have similar densities) were all assumed to remain in lower containment and reach the active pool. The relative quietness and lack of turbulence in the Ginna containment pool resulted in low transport fractions within the pool; 0% for Case 1 (break far from the sump) and 33% for Case 2 (break close to the sump).

As stated in the response to RAI-1, Type 1 Cal-Sil (which is the only type containing asbestos) is the least susceptible to erosion in the containment pool. Thus, any erosion of this type of Cal-Sil would be conservatively bounded by the erosion fraction used for the Thermo-12 Gold Cal-Sil.

For head loss purposes, the debris types were given the same density (higher than what was recommended in the GR, which results in more debris generated) and the debris types were given the same size distribution and erosion fractions (even though the asbestos Cal-Sil is considered more robust).

For both the fines and small pieces of Cal-Sil generated, the quantity of asbestos fiber within the Cal-Sil was conservatively ignored. If the fiber portion of the Cal-Sil was accounted for, even assuming a high percentage per unit volume, the quantity of fiber is insignificant in comparison to the overall quantity of fiber generated. The fraction of a percent increase in fiber generated would not be as detrimental to head loss as treating the asbestos Cal-Sil as 100% Cal-Sil particulate.

RAI-2 References:

- 2.1 Calculation ALION-CAL-GINNA-4376-03, “Ginna GSI-191 Debris Transport Calculation”, Revision 2.

RAI-3: *The supplemental responses did not provide sufficient information for the NRC staff to verify that transport had been adequately evaluated. The licensee should re-submit a transport evaluation in accordance with the revised content guide (ADAMS Accession No. ML073110389). The licensee should refer to previous adequate transport supplemental responses, such as the one provided for Crystal River (ADAMS Accession Number ML080640544). In developing a revised transport response, the licensee should specifically consider the following non-exhaustive list of subject areas:*

- a) *A description of the assumed behavior of each type of debris during blowdown, washdown, pool fill and recirculation transport.*

ATTACHMENT 1
REGNPP GL 2004-02 THIRD SUPPLEMENTAL RAI RESPONSE

- b) *A washdown discussion describing the spray distribution model with specific focus on the credit taken and basis for retention of debris in upper containment.*
- c) *For pool fill transport, addressal of any direct transport to the sump strainers, any credit for debris washed into inactive volumes, and the accompanying technical bases.*
- d) *A description of the deviations and refinements from the staff SE-approved transport methodology (SE Section 3.6), with the technical basis for these items.*
- e) *A statement as to the CFD code used for the transport evaluation and a description of specific aspects of the model and assumptions used (e.g., pool height, sump flow and pump configuration, turbulence modeling, number of cells used in the analysis, and the pipe breaks for which simulations were performed).*
- f) *A listing of the debris transport metrics that were used for all types of debris, including degraded coating chips.*
- g) *A description of the assumptions and technical basis that support the credit for settling and/or hold-up of fine debris that resulted in a 66% transport percentage.*
- h) *A description of the methodology used to estimate the erosion of fibrous and calcium silicate insulation in the containment pool (and any other insulation types for which erosion was assumed).*
- i) *A statement of the height of the debris interceptors, a description of their modeling in the CFD, a summary of the transport metrics used for debris that is assumed to climb over the interceptors, and a description of the credit that was taken for debris capture at the debris interceptors.*
- j) *A discussion as to why the transport fractions for Temp-Mat are higher than for Thermal Wrap. Presumably, the denser fiberglass (Temp-Mat) would be less transportable for equivalent sizes of debris than the less dense fiberglass (Thermal Wrap). However, the results presented in the supplemental response show the opposite behavior.*

RAI-3 Response: In order to completely respond to this RAI, the following information is presented in a manner which is intended to supersede the previously submitted Section 3.e of the Supplemental Response to Generic Letter 2004-02. For completeness, the information contained in the guidance document is presented as part of the introduction. The following information is taken from the Ginna debris transport calculation [3.1].

The objective of the debris transport evaluation process is to estimate the fraction of debris that would be transported from debris sources within containment to the sump suction strainers.

1. *Describe the methodology used to analyze debris transport during the blowdown, wash-down, pool-fill-up, and recirculation phases of an accident.*
2. *Provide the technical basis for assumptions and methods used in the analysis that deviate from the approved guidance.*
3. *Identify any computational fluid dynamics codes used to compute debris transport fractions during recirculation and summarize the methodology, modeling assumptions, and results.*
4. *Provide a summary of, and supporting basis for, any credit taken for debris interceptors.*
5. *State whether fine debris was assumed to settle and provide basis for any settling credited.*
6. *Provide the calculated debris transport fractions and the total quantities of each type of debris transported to the strainers.*

ATTACHMENT 1
REGNPP GL 2004-02 THIRD SUPPLEMENTAL RAI RESPONSE

Description of Methodology

The methodology used in the transport analysis is based on the NEI 04-07 guidance report (GR) for refined analyses as modified by the NRC's safety evaluation report (SER), as well as the refined methodologies suggested by the SER in Appendices III, IV, and VI. The specific effect of each of four modes of transport was analyzed for each type of debris generated. These modes of transport are:

- *Blowdown transport* – the vertical and horizontal transport of debris to all areas of containment by the break jet.
- *Wash-down transport* – the vertical (downward) transport of debris by the containment sprays and break flow.
- *Pool fill-up transport* – the transport of debris by break and containment spray flows from the Refueling Water Storage Tank (RWST) to regions that may be active or inactive during recirculation.
- *Recirculation transport* – the horizontal transport of debris from the active portions of the recirculation pool to the sump screens by the flow through the emergency core coolant system (ECCS).

The logic tree approach was then applied for each type of debris determined from the debris generation calculation. The logic tree shown in Figure 3.1 is somewhat different than the baseline logic tree provided in the GR. This departure was made to account for certain non-conservative assumptions identified by the SER including the transport of large pieces, erosion of small and large pieces, the potential for wash-down debris to enter the pool after inactive areas have been filled, and the direct transport of debris to the sump screens during pool fill-up. Also, the generic logic tree was expanded to account for a more refined debris size distribution. (Note that some branches of the logic tree were not required for certain debris types).

ATTACHMENT 1
REGNPP GL 2004-02 THIRD SUPPLEMENTAL RAI RESPONSE

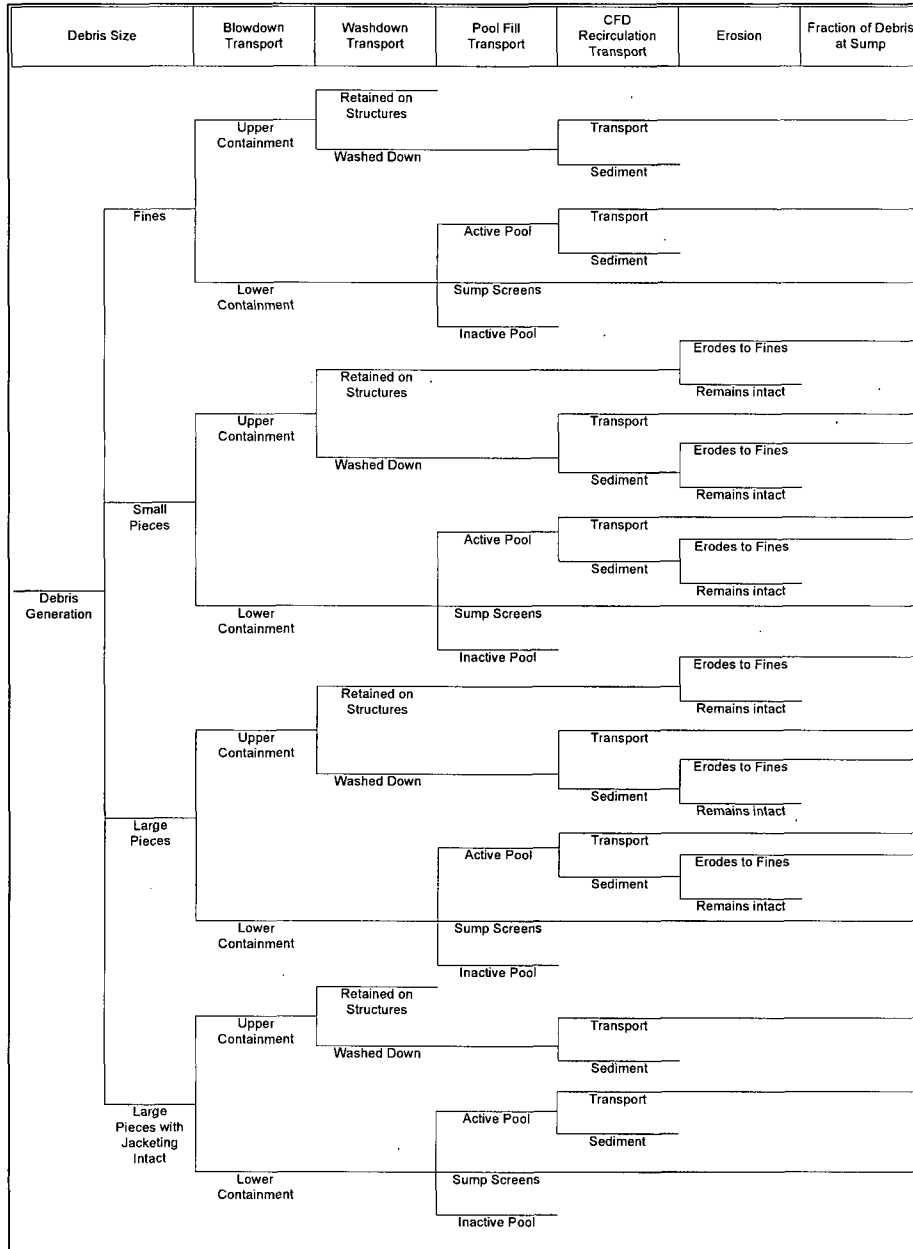


Figure 3.1 – Generic Debris Transport Logic Tree

The basic methodology used for the Ginna transport analyses is shown below:

1. Based on many of the containment building drawings, a three-dimensional model was built using Computer Aided Drafting (CAD) software.
2. Debris types and size distributions were gathered from the debris generation calculation for each postulated break location.
3. The fraction of debris blown into upper containment was determined based on the flow of steam during the blowdown.
4. The quantity of debris washed down by spray flow was conservatively determined based on relevant test data and the spray flow split in upper containment.

ATTACHMENT 1
REGNPP GL 2004-02 THIRD SUPPLEMENTAL RAI RESPONSE

5. The quantity of debris transported to inactive areas or directly to the sump strainer was calculated based on the volume of the inactive and sump cavities proportional to the water volume at the time these cavities are filled.
6. Using conservative assumptions, the locations of each type/size of debris at the beginning of recirculation was determined.
7. A CFD model was developed to simulate the flow patterns that would develop in the pool during recirculation.
8. A graphical determination of the transport fraction of each type of debris was made using the velocity and Turbulent Kinetic Energy (TKE) profiles from the CFD model output, along with the determined initial distribution of debris.
9. The recirculation transport fractions from the CFD analysis were gathered to input into the logic trees.
10. The quantity of debris that could experience erosion due to the break flow or spray flow was determined.
11. The overall transport fraction for each type of debris was determined by combining each of the previous steps in logic trees.

Blowdown Transport

The fraction of blowdown flow to various regions was estimated using the relative volumes of containment. Fine debris can be easily suspended and carried by the blowdown flow. Small and large piece debris can also be easily carried by the high velocity blowdown flow in the vicinity of the break. However, in areas farther away from the break that are not directly affected by the blowdown, this debris would likely fall to the floor.

The volumes for the upper containment (areas above the operating deck, including the refueling canal) and for lower containment were determined from the CAD model. Because the debris was assumed to be carried with the blowdown flow, the flow split is proportional to the containment volumes. This results in a transport fraction for the fine debris to upper containment of 89%.

The Drywell Debris Transport Study (DDTS) [3.2] testing provides debris holdup values for blowdown occurring in a wetted and highly congested area. Values associated with grating being present in the blowdown flowpath were utilized in the Ginna blowdown analysis. The DDTS also presents values for holdup when blowdown travels a flow path with 90° turns. Although 90° turns might not have to be negotiated by debris blown to upper containment at Ginna, significant bends would have to be made. Therefore, it was estimated that 5% (versus the 17% value in the study) of the small fiberglass debris blown upward would be trapped due to changes in flow direction.

Grated platforms exist low in the steam generator compartments at Ginna covering approximately 50% of the compartment area [3.3]. The grating was credited with capturing some of the small and large debris not blown to upper containment.

The following tables (Table 3.1 and Table 3.2) show the transport fractions for each type/size of debris to upper containment and containment pool due to the blowdown forces for the LBLOCA breaks. Note that debris outside the ZOI (including latent dirt/dust and fibers) is not affected by the blowdown, and therefore the blowdown transport fraction for this debris is not analyzed.

ATTACHMENT 1
REGNPP GL 2004-02 THIRD SUPPLEMENTAL RAI RESPONSE

Table 3.1 – Blowdown Transport Fractions of Debris to Upper Containment

Debris Type	Fines	Small Pieces	Unjacketed Large Pieces	Jacketed Large Pieces
RMI	NA	0%	0%	NA
Cal-Sil with Asbestos	89%	0%	NA	NA
Temp-Mat	89%	76%	25%	25%
Thermal-Wrap	89%	76%	25%	25%
Phenolic Paint (inside ZOI)	89%	NA	NA	NA
IOZ Paint (inside ZOI)	89%	NA	NA	NA
Phenolic Paint (outside ZOI)	NA	NA	NA	NA
IOZ Paint (outside ZOI)	NA	NA	NA	NA
Dirt/Dust	NA	NA	NA	NA
Latent Fiber	NA	NA	NA	NA

Table 3.2 – Blowdown Transport Fractions of Debris to Containment Pool

Debris Type	Fines	Small Pieces	Unjacketed Large Pieces	Jacketed Large Pieces
RMI	NA	100%	100%	NA
Cal-Sil with Asbestos	11%	100%	NA	NA
Temp-Mat	11%	21%	38%	38%
Thermal-Wrap	11%	21%	38%	38%
Phenolic Paint (inside ZOI)	11%	NA	NA	NA
IOZ Paint (inside ZOI)	11%	NA	NA	NA
Phenolic Paint (outside ZOI)	NA	NA	NA	NA
IOZ Paint (outside ZOI)	NA	NA	NA	NA
Dirt/Dust	NA	NA	NA	NA
Latent Fiber	NA	NA	NA	NA

Washdown Transport

During the washdown phase of a LOCA, debris would be transported down to the containment pool by operation of the containment spray system. Significant amounts of debris could, however, be captured on the concrete floors and grated areas above the containment floor as containment spray water transporting the debris drains through grating to reach the pool.

The containment sprays would drain to the pool consecutively through two levels of the containment building (the operating deck and the intermediate floor). The flow split through the operating deck

ATTACHMENT 1
REGNPP GL 2004-02 THIRD SUPPLEMENTAL RAI RESPONSE

elevation would be 13.8% to the refueling cavity, 84.4% off of the concrete operating deck through the stairwells or grated openings, and 1.8% directly through an opening without grating.

Since the refueling cavity drains to the inactive reactor cavity, any debris washed into the refueling cavity would be held up (either in the refueling cavity or the reactor cavity) and would not be in the active pool during recirculation.

Of the overall 2,600 gpm spray flow, 26.4% would run off into the stairwell and the two grated areas on Elevation 278'-4" (686 gpm), and 58.0% would runoff into the stairwell at Elevation 274'-6" (1,508 gpm) [3.1].

The height of water on the operating deck floor can be approximated as weir flow over a weir opening where the opening length is equal to the open perimeters. The following equation describes the weir flow [3.4]:

$$Q = 3.33 \cdot L \cdot H^{1.5} \quad \text{Equation 1}$$

As shown in Appendix 1 of the debris transport calculation [3.1], the total perimeter around the two hatches and the stairwell at the 278'-4" elevation is 102.0 ft. Since the total runoff flow to these regions is 686 gpm (1.50 ft³/s), the water height can be calculated as follows:

$$H = \left(\frac{Q}{3.33 \cdot L} \right)^{\frac{2}{3}} = \left(\frac{1.50 \text{ ft}^3/\text{s}}{3.33 \cdot 102.0 \text{ ft}} \right)^{\frac{2}{3}} = 0.027 \text{ ft} = 0.32 \text{ in} \quad \text{Equation 2}$$

Taking the flow rate, water depth, and flow perimeters, the average velocity on the 278'-4" floor would be approximately 0.5 ft/s.

As shown in Appendix 1 of the debris transport calculation [3.1], the perimeter around the stairwell on the 274'-6" floor is 5.3 ft. Since the total flow to this stairwell is 1,508 gpm (3.36 ft³/s), the water height can be calculated as follows:

$$H = \left(\frac{Q}{3.33 \cdot L} \right)^{\frac{2}{3}} = \left(\frac{3.36 \text{ ft}^3/\text{s}}{3.33 \cdot 5.3 \text{ ft}} \right)^{\frac{2}{3}} = 0.331 \text{ ft} = 3.97 \text{ in} \quad \text{Equation 3}$$

Again, taking the flow rate, water depth, and flow perimeters, the average velocity on the 274'-6" floor would be approximately 1.9 ft/s.

The incipient tumbling velocity for small pieces of fiberglass is 0.12 ft/s [3.5]. However, since this tumbling velocity is for 1 inch clumps of fiberglass completely submerged in water, the velocity required to tumble clumps of fiberglass sitting on the higher portion of the operating deck at Ginna would be somewhat different since the pieces would not be fully submerged. Assuming that the small pieces of fiberglass on the operating deck are 1 inch clumps with dimensions of approximately 1" × 1" × ½", the clumps would be approximately two-thirds submerged in the 0.32" water level on the operating deck. As

ATTACHMENT 1
REGNPP GL 2004-02 THIRD SUPPLEMENTAL RAI RESPONSE

shown in the following calculations, the difference in the submergence level has a significant impact on the transportability of the fiberglass pieces.

The bulk density of Temp-Mat fiberglass is $9.0 \text{ lb}_m/\text{ft}^3$ and that for Thermal Wrap is $2.4 \text{ lb}_m/\text{ft}^3$; and the material density is $162 \text{ lb}_m/\text{ft}^3$ for Temp-Mat and is $159 \text{ lb}_m/\text{ft}^3$ for Thermal Wrap [3.6]. Using the following porosity equation [3.6], along with an air density of $0.075 \text{ lb}_m/\text{ft}^3$ [3.6] gives the following porosity for Temp-Mat and Thermal Wrap:

$$\phi = \frac{159 \text{ lb}_m/\text{ft}^3 - 2.4 \text{ lb}_m/\text{ft}^3}{159 \text{ lb}_m/\text{ft}^3 - 0.075 \text{ lb}_m/\text{ft}^3} = 0.985 \quad \text{Equation 4}$$

$$\phi = \frac{162 \text{ lb}_m/\text{ft}^3 - 9.0 \text{ lb}_m/\text{ft}^3}{162 \text{ lb}_m/\text{ft}^3 - 0.075 \text{ lb}_m/\text{ft}^3} = 0.945$$

When saturated with water at 272 °F (density of $58.2 \text{ lb}_m/\text{ft}^3$), the bulk density of the fiberglass would be:

$$\rho_b = 159 \text{ lb}_m/\text{ft}^3 - 0.985 \cdot (159 \text{ lb}_m/\text{ft}^3 - 58.2 \text{ lb}_m/\text{ft}^3) = 59.7 \text{ lb}_m/\text{ft}^3 \quad \text{Equation 5}$$

$$\rho_b = 162 \text{ lb}_m/\text{ft}^3 - 0.945 \cdot (162 \text{ lb}_m/\text{ft}^3 - 58.2 \text{ lb}_m/\text{ft}^3) = 63.9 \text{ lb}_m/\text{ft}^3$$

The horizontal forces acting on the piece of fiberglass include the drag from the water flow (a function of the water velocity and the cross sectional area of fiberglass), and the friction force between the fiberglass and concrete. The friction force is directly proportional to the normal force which is equal to the weight of the piece of fiberglass minus the buoyancy.

$$\sum F_{\text{horizontal}} = F\{\text{velocity, area}\} - \text{Friction} = 0 \quad \text{Equation 6}$$

$$\text{Friction} = \mu \cdot N \quad \text{Equation 7}$$

$$N = \text{Weight} - \text{Buoyancy} \quad \text{Equation 8}$$

$$\text{Weight} = V \cdot \rho_b \cdot g \quad \text{Equation 9}$$

$$\text{Buoyancy} = V_{\text{submerged}} \cdot \rho_{\text{water}} \cdot g \quad \text{Equation 10}$$

Since the pieces of fiberglass on the operating deck at Ginna would only be two-thirds submerged:

$$V_{\text{submerged}} = 2/3 \cdot V \quad \text{Equation 11}$$

$$N_{\text{Partially Submerged}} = V \cdot \rho_b \cdot g - 2/3 \cdot V \cdot \rho_{\text{water}} \cdot g = V \cdot (\rho_b - 2/3 \cdot \rho_{\text{water}}) \cdot g \quad \text{Equation 12}$$

And the ratio of the normal forces on a two-thirds submerged piece of fiberglass versus a fully submerged piece would be:

$$\frac{N_{\text{Half Submerged}}}{N_{\text{Fully Submerged}}} = \frac{V \cdot (\rho_b - 2/3 \cdot \rho_{\text{water}}) \cdot g}{V \cdot (\rho_b - \rho_{\text{water}}) \cdot g} = \frac{59.7 \text{ lb}_m/\text{ft}^3 - 2/3 \cdot 58.2 \text{ lb}_m/\text{ft}^3}{59.7 \text{ lb}_m/\text{ft}^3 - 58.2 \text{ lb}_m/\text{ft}^3}$$

ATTACHMENT 1
REGNPP GL 2004-02 THIRD SUPPLEMENTAL RAI RESPONSE

$$\frac{N_{Half\ Submerged}}{N_{Fully\ Submerged}} = \frac{V \cdot (\rho_b - 2/3 \cdot \rho_{water}) \cdot g}{V \cdot (\rho_b - \rho_{water}) \cdot g} = \frac{60.5 lb_m / ft^3 - 2/3 \cdot 59.0 lb_m / ft^3}{60.5 lb_m / ft^3 - 59.0 lb_m / ft^3}$$

= 14

Equation 13

Therefore, since the coefficient of friction between fiberglass and concrete would be constant, and the reduced cross-sectional area for a partially submerged piece of fiberglass can be conservatively neglected, a 14 times higher flow velocity would be required to tumble a piece of fiberglass that is two-thirds submerged compared to a piece of fiberglass that is fully submerged. Since the incipient tumbling velocity for a fully submerged piece of fiberglass is 0.12 ft/s, a velocity of approximately 1.7 ft/s would be required to tumble the small pieces of fiberglass on the higher elevation of the operating deck at Ginna. Since this is significantly higher than the actual water velocity on the operating deck, the small fiberglass debris would not transport to the grated openings.

For fiberglass pieces on the lower operating deck elevation, the water level is high enough to completely submerge the pieces, and the water velocity is high enough to tumble the debris along the floor. However, since the flow would approach the stairwell on the 274'-6" elevation in a roughly uniform radial fashion, the velocity would be lower farther from the stairwell. The velocity can be approximated by using the flow rate to the stairwell, the water depth, and the perimeter of a semi-circle around the stairwell. The following equation can be used to calculate the distance from the strainer where the water velocity would be less than the tumbling velocity for small fiberglass:

$$L_{Perimeter} = \frac{Q}{H \cdot V_{tumbling}} = \frac{3.36 ft^3/s}{0.331 ft \cdot 0.12 ft/s} = 85 ft$$

Equation 14

$$R_{semi-circle} = \frac{L_{Perimeter}}{\pi} = \frac{85 ft}{\pi} = 27 ft$$

Equation 15

Therefore, within a radius of 27 ft around the stairwell, the velocity would be high enough to tumble the small pieces of fiberglass. This is equivalent to a semi-circular area of approximately 1,150 ft². Since the overall area of the operating deck floor at Elevation 274'-6" is 2,847 ft² (Appendix 1 of the debris transport calculation [3.1]), approximately 40% of the fiberglass on this floor would transport to the stairwell.

Based on the relative containment areas, 14% of the debris blown to upper containment would transport to the refueling canal. The remaining debris could washdown through the various hatches and stairwells. Taking the overall operating deck floor areas from Appendix 1 [3.1], and the corresponding transport fractions for each region yields the following washdown fraction for small pieces of fiberglass from the operating deck:

$$F_{washdown(small\ fiber)} = \frac{F_{278'-4"} \cdot A_{278'-4"} + F_{DS} \cdot A_{DS} + F_{274'-6"} \cdot A_{274'-6"}}{A_{Total} - A_{RFC}}$$

Equation 16

ATTACHMENT 1
REGNPP GL 2004-02 THIRD SUPPLEMENTAL RAI RESPONSE

$$F_{washdown (small\ fiber)} = \frac{0.00 \cdot 4461 ft^2 + 1.00 \cdot 153 ft^2 + 0.40 \cdot 2847 ft^2}{8659 ft^2 - 1198 ft^2} = 0.17 \quad \text{Equation 17}$$

Since the large piece debris blown to upper containment would not transport easily due to the containment sprays and would be held up on grating, the washdown fraction for this debris was assumed to be negligible.

The following tables (Table 3.3 and Table 3.4) provide the washdown fractions of debris for Ginna.

Table 3.3 – Washdown Transport Fractions to Lower Containment

Debris Type	Fines	Small Pieces	Unjacketed Large Pieces	Jacketed Large Pieces
RMI	NA	NA	NA	NA
Cal-Sil with Asbestos	86%	NA	NA	NA
Temp-Mat	86%	17%	0%	0%
Thermal-Wrap	86%	17%	0%	0%
Phenolic Paint (inside ZOI)	86%	NA	NA	NA
IOZ Paint (inside ZOI)	86%	NA	NA	NA
Phenolic Paint (outside ZOI)	NA	NA	NA	NA
IOZ Paint (outside ZOI)	NA	NA	NA	NA
Dirt/Dust	NA	NA	NA	NA
Latent Fiber	NA	NA	NA	NA

Table 3.4 – Washdown Transport Fractions of Debris to the Refueling Cavity/Reactor Cavity

Debris Type	Fines	Small Pieces	Unjacketed Large Pieces	Jacketed Large Pieces
RMI	NA	NA	NA	NA
Cal-Sil with Asbestos	14%	NA	NA	NA
Temp-Mat	14%	14%	14%	14%
Thermal-Wrap	14%	14%	14%	14%
Phenolic Paint (inside ZOI)	14%	NA	NA	NA
IOZ Paint (inside ZOI)	14%	NA	NA	NA
Phenolic Paint (outside ZOI)	NA	NA	NA	NA
IOZ Paint (outside ZOI)	NA	NA	NA	NA
Dirt/Dust	NA	NA	NA	NA
Latent Fiber	NA	NA	NA	NA

ATTACHMENT 1
REGNPP GL 2004-02 THIRD SUPPLEMENTAL RAI RESPONSE

Pool Fill Transport

The only significant inactive cavity volume at Ginna is the reactor cavity. This cavity is filled by containment sprays draining from the refueling canal as well as water from the containment pool via the non-emergency containment sump (Sump A). Sump A has a 6" curb around it. The total volume of the reactor cavity is 6,020 ft³ [3.7]. Since 1,650 ft³ of water would fill the cavity via the refueling canal [3.7], the volume of the cavity that would be filled via Sump A is 4,370 ft³.

The recirculation sump pit (Sump B) at Ginna also has a 6" curb around it, which is covered by a solid diamond plate. A portion of the strainer also sits on top of the sump pit. The volume of Sump B is 992 ft³ [3.7]. Since both Sump A and Sump B have a 6" curb around them, these cavities would start to fill simultaneously as soon as the water level reaches 6". Using the CAD model, the 6" pool volume was calculated to be 3,094 ft³ (Appendix 4 of the debris transport calculation [3.1]).

As described in the debris transport calculation, the fraction of debris washed to the inactive cavity during pool fill-up is:

$$F_{fill-up} = 1 - e^{-\frac{V_{Cavity}}{V_{Pool}}} \quad \text{Equation 18}$$

Since the Sump A and Sump B cavities would start filling simultaneously, and Sump B would finish filling first, the debris split to each cavity can be calculated using the following equations (modified from Equation 18):

$$F_{SumpB} = \frac{1 - e^{-\frac{2 \cdot V_{SumpB}}{V_{Pool}}}}{2} = \frac{1 - e^{-\frac{2 \cdot 992 \text{ ft}^3}{3094 \text{ ft}^3}}}{2} = 0.24 \quad \text{Equation 19}$$

$$F_{SumpA} = 1 - 2 \cdot F_{SumpB} - e^{-\frac{V_{SumpA} - V_{RFC Sprays} - V_{SumpB}}{V_{Pool}}} + F_{SumpB}$$

$$= 1 - 2 \cdot 0.24 - e^{-\frac{6020 \text{ ft}^3 - 1650 \text{ ft}^3 - 992 \text{ ft}^3}{3094 \text{ ft}^3}} + 0.24 = 0.42 \quad \text{Equation 20}$$

Since the curb around the sump would stop sunken debris from washing over during the fill-up phase (only a thin sheet of water would be flowing over the top of the curbs as the cavity fills), this transport fraction was only applied for the fine debris that is likely to be suspended. After the sump cavity and reactor cavity have been filled there would be no preferential direction to the pool flow until recirculation is initiated.

Although the transport fraction to each sump is higher than the 15% limit specified in the SER, these transport fractions are considered to be reasonable since the Sump B transport represents transport to the sump strainer, and the Sump A transport is only applied to fine debris in the containment pool at the end of the blowdown phase. Since almost 90% of the fine debris is blown to upper containment, 42% transport of the fines in lower containment to the reactor cavity represents much less than 15% of the overall debris generated.

ATTACHMENT 1
REGNPP GL 2004-02 THIRD SUPPLEMENTAL RAI RESPONSE

Table 3.5 and Table show the fractions of debris that would transport directly to the sump strainer or to the inactive reactor cavity during pool fill-up. Note that qualified degraded coatings outside the paint ZOI are assumed to fail after pool fill-up has occurred, so the transport fraction for this debris during fill-up is 0%. The latent debris was conservatively assumed not to transport to inactive cavities.

Table 3.5 – Pool Fill-up Transport Fractions of Debris to Sump Strainer

Debris Type	Fines	Small Pieces	Unjacketed Large Pieces	Jacketed Large Pieces
RMI	NA	0%	0%	NA
Cal-Sil with Asbestos	24%	NA	NA	NA
Temp-Mat	24%	0%	0%	0%
Thermal-Wrap	24%	0%	0%	0%
Phenolic Paint (inside ZOI)	24%	NA	NA	NA
IOZ Paint (inside ZOI)	24%	NA	NA	NA
Phenolic Paint (outside ZOI)	NA	NA	NA	NA
IOZ Paint (outside ZOI)	NA	NA	NA	NA
Dirt/Dust	NA	NA	NA	NA
Latent Fiber	NA	NA	NA	NA

Table 3.6 – Pool Fill-up Transport Fractions of Debris to Inactive Reactor Cavity

Debris Type	Fines	Small Pieces	Unjacketed Large Pieces	Intact Blankets
Stainless Steel RMI	NA	0%	0%	NA
Cal-Sil with Asbestos	42%	NA	NA	NA
Temp-Mat	42%	0%	0%	0%
Thermal-Wrap	42%	0%	0%	0%
Phenolic Paint (inside ZOI)	42%	NA	NA	NA
IOZ Paint (inside ZOI)	42%	NA	NA	NA
Phenolic Paint (outside ZOI)	NA	NA	NA	NA
IOZ (outside ZOI)	NA	NA	NA	NA
Dirt/Dust	NA	NA	NA	NA
Latent Fiber	NA	NA	NA	NA

Recirculation Transport Using CFD

The recirculation pool debris transport fractions were determined through CFD modeling. To accomplish this, a three dimensional CAD model was imported into the CFD model, flows into and out of the pool were defined, and the CFD simulation was run until steady-state conditions were reached. The result of the CFD analysis is a three-dimensional model showing the turbulence and fluid velocities within the pool. By comparing the direction of pool flow, the magnitude of the turbulence and velocity, the initial location of debris, and the specific debris transport metrics (i.e. the minimum velocity or turbulence

ATTACHMENT 1
REGNPP GL 2004-02 THIRD SUPPLEMENTAL RAI RESPONSE

required to transport a particular type/size of debris), the recirculation transport of each type/size of debris to the sump screens was determined.

Flow-3D[®] Version 9.0 developed by Flow Science Incorporated was used for the CFD modeling. The key CFD modeling attributes/considerations included the following:

Computational Mesh:

A rectangular mesh was defined in the CFD model that was fine enough to resolve important features, but not so fine that the simulation would take prohibitively long to run. A 6" by 6" cell was chosen as the largest cell size that could reasonably resolve obstacles in the lower containment. For the cells right above the containment floor, the mesh was set to 3" tall in order to closely resolve the vicinity of settled debris.

Modeling of Break Flow:

The water stream falling from the postulated break would introduce momentum into the containment pool that would influence the flow dynamics. This break stream momentum is accounted for by introducing the break flow to the pool at the velocity a freefalling object would have if it fell the vertical distance from the location of the break to the surface of the pool.

The break stream was introduced in the CFD model by defining a flow region populated with mass source particles and setting the flow rate and velocity using mass source particles. The break source was situated near the postulated break location, below the surface of the pool. This was done to avoid the splashing (which would drastically increase the calculation run time) that would occur if the source was above the pool surface

Containment Sump:

The mass sink used to pull flow from the CFD model was defined within the sump. A negative flow rate was set for the sump mass sink, which tells the CFD model to draw the specified amount of water from the pool over the entire exposed surface area of the mass sink obstacle.

Turbulence Modeling:

Several different turbulence modeling approaches can be selected for a Flow-3D[®] calculation. The approaches are (ranging from least to most sophisticated):

- Prandtl mixing length
- Turbulent energy model
- Two-equation k- ϵ model
- Renormalized Group Theory (RNG) model
- Large eddy simulation model

The RNG turbulence model was judged to be the most appropriate for this CFD analysis due to the large spectrum of length scales that would likely exist in a containment pool during emergency recirculation. The RNG approach applies statistical methods in a derivation of the averaged equations for turbulence quantities (such as turbulent kinetic energy and its dissipation rate). RNG-based turbulence schemes rely less on empirical constants while setting a framework for the derivation of a range of models at different scales.

ATTACHMENT 1
REGNPP GL 2004-02 THIRD SUPPLEMENTAL RAI RESPONSE

Steady State Metrics:

The CFD model was started from a stagnant state at the pool depth at the time of recirculation, and run for a total of 4 to 5 minutes simulated time. A plot of mean kinetic energy was used to determine when steady-state conditions were reached. Checks were also made of the velocity and turbulent energy patterns in the pool to verify that steady-state conditions were reached.

Debris Transport Metrics:

- 1) Metrics for predicting debris transport have been adopted or derived from data. The specific metrics are the TKE necessary to keep debris suspended, and the flow velocity necessary to tumble sunken debris along a floor. The metrics utilized in the Ginna transport analysis are found in Table 3.7 as follows:

Table 3.7 – Debris Transport Metrics

Debris Type	Size	Terminal Settling Velocity	Reference	Calculated Minimum TKE Required to Suspend (ft ² /sec ²)	Flow Velocity Associated with Incipient Tumbling (ft/s)	Reference
Stainless Steel RMI	Small Pieces (<4")	0.37	NUREG/CR-6772 Table 3.5 [3.5]	0.21	0.28	NUREG/CR-6772 Table 3.5 [3.5]
	Large Pieces (>4")	0.48	NUREG/CR-6772 Table 3.5 [3.5]	0.35	0.28	NUREG/CR-6772 Table 3.5 [3.5]
Thermal-Wrap™	Individual Fibers	0.0074	NUREG/CR-6808 Fig 5-2 [3.5]	8.2E-05	NA	-
	Small Pieces (<6")	0.15	NUREG/CR-6772 Table 3.1 [3.5]	3.4E-02	0.12	NUREG/CR-6772 Table 3.2 [3.5]
	Large Pieces (>6")	0.41	NUREG/CR-6772 Table 3.1 [3.5]	0.25	0.37	NUREG/CR-6808 Table 5-3 [3.8]
Cal-Sil and Asbestos	5-micron (144 lb _m /ft ³)	1.1E-04	Calculated per Stokes' law	1.78E-08	NA	-
	Small Pieces (1" chunks)	1.0	Calculated using Flow-3D	1.5	0.25	NUREG/CR-6772 Table C.19a [3.5]
Paint Debris	10-micron particulate (94 lb _m /ft ³)	1.7E-04	Calculated per Stokes' law	4.1E-08	NA	-
	10-micron particulate (457 lb _m /ft ³)	2.0E-03	Calculated per Stokes' law	6.1E-06	NA	-
	Phenolic paint chips	0.13	NUREG/CR-6916 [3.9]	2.5E-02	0.27	NUREG/CR-6916 [3.9]
Dirt/Dust	17.3-micron particulate (169 lb _m /ft ³)	1.7E-03	Calculated per Stokes' law	4.1E-06	NA	-

Graphical Determination of Debris Transport Fractions:

The following steps were taken to determine what percentage of a particular type of debris could be expected to transport through the containment pool to the emergency sump screens.

ATTACHMENT 1

REGNPP GL 2004-02 THIRD SUPPLEMENTAL RAI RESPONSE

- Colored contour velocity and TKE maps indicating regions of the pool through which a particular type of debris could be expected to transport were generated from the Flow-3D[®] results in the form of bitmap files.
- The bitmap files were overlaid on the initial debris distribution plots and imported into AutoCAD[®] with the appropriate scaling factor to convert the length scale of the color maps to feet.
- For the uniformly distributed debris, closed polylines were drawn around the contiguous areas where velocity or TKE was high enough that debris could be carried in suspension or tumbled along the floor to the sump screens.
- The areas within the closed polylines were determined utilizing an AutoCAD[®] querying feature.
- The combined area within the polylines was compared to the debris distribution area.
- The percentage of a particular debris type that would transport to the sump screens was estimated based on the above comparison.

Plots showing the TKE and the velocity magnitude in the pool were generated for each case to determine areas where specific types of debris would be transported. The limits on the plots were set according to the minimum TKE or velocity metrics necessary to move each type of debris. Regions where the debris would be suspended were specifically identified in the plots as well as regions where the debris would be tumbled along the floor. Color coding TKE portions of the plots is a three-dimensional representation of the TKE. The velocity portion of the plots represents the velocity magnitude just above the floor level (1.5”), where tumbling of sunken debris could occur. Directional flow vectors were also included in the plots to determine whether debris in certain areas would be transported to the sump screens or transported to quieter regions of the pool where it could settle to the floor.

It was also necessary to determine the distribution of debris prior to the event as well as prior to the beginning of recirculation. Since the various types and sizes of debris transport differently during the blowdown, washdown, and pool fill-up phases, the initial distribution of this debris at the start of recirculation can vary widely. Insulation debris on the pool floor would be scattered around by the break flow as the pool fills, and debris in upper containment would be washed down at various locations by the spray flow. It was assumed that the debris washed down by containment sprays would remain in the general vicinity of the washdown locations until recirculation starts. Other key considerations for the debris types include:

- Latent debris in containment (dirt/dust and fibers) was assumed to be uniformly distributed on the containment floor at the beginning of recirculation.
- Unqualified coatings in lower containment were assumed to be uniformly distributed in the recirculation pool.
- It was assumed that the fine debris in lower containment at the end of the blow-down would be uniformly distributed in the pool at the beginning of recirculation.
- Small and large pieces of insulation debris not blown to upper containment were conservatively assumed to be distributed between the locations where it would be destroyed and the sump screens.

The following figures and discussions are presented as an example of how the recirculation transport fraction determination was performed for a single debris type at Ginna (small pieces of Reflective Metal Insulation (RMI)). This same approach was utilized for the other debris types analyzed at Ginna.

ATTACHMENT 1
REGNPP GL 2004-02 THIRD SUPPLEMENTAL RAI RESPONSE

Figure shows that the turbulence in the pool is only high enough to suspend small pieces of RMI in the vicinity of the break. Since the small pieces of RMI would settle in most of the pool, the tumbling velocity is the predominant means of transport.

The small RMI debris was assumed to be distributed as shown in Figure 3.33.3. This area was overlaid on top of the plot showing tumbling velocity and flow vectors to determine the recirculation transport fraction.

The area where small pieces of RMI would transport within the initial distribution area is 506 ft² as shown in Figure 3.43.4. Since the initial distribution area was determined to be 1,305 ft², the recirculation transport fraction for small pieces of RMI is 39%.



Figure 3.2 –TKE and Velocity with Limits Set at Suspension/Tumbling of Small Pieces of RMI

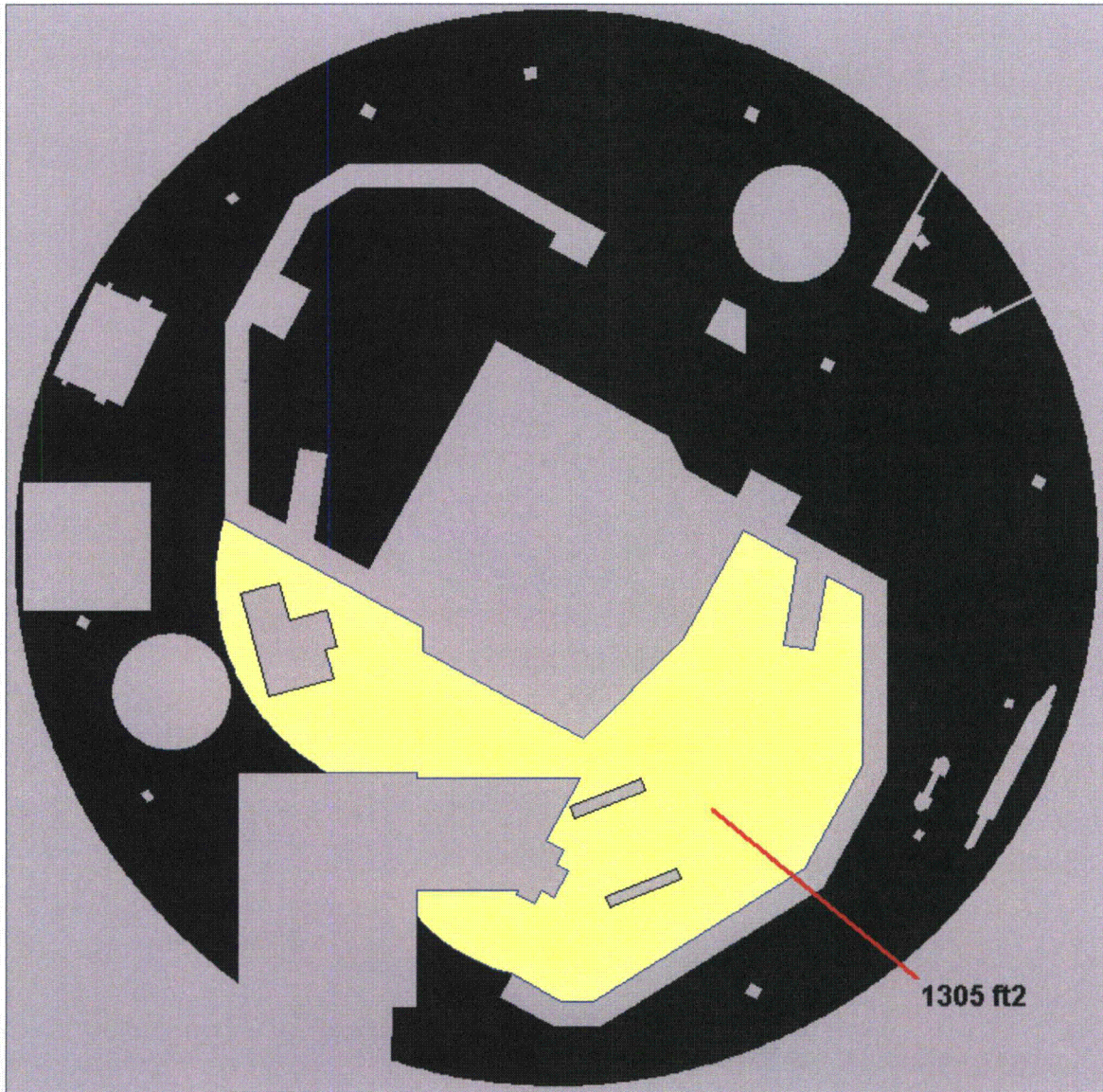


Figure 3.3 – Distribution of Small and Large Pieces of Debris in Lower Containment



Figure 3.4 – Floor Area Where Small RMI Would Transport to the Sump

Deviations From Regulatory Guidance

The only deviations where the debris transport analysis deviates from the regulatory guidance are in the pool fill and debris erosion.

Pool Fill:

The guidance specifies that the pool fill transport should be limited to 15% for transport to an inactive cavity. Although the transport fraction to each sump is higher than the 15% limit specified in the SER, these transport fractions are considered to be reasonable since the Sump B transport represents transport to the sump strainer, and the Sump A transport is only applied to fine debris in the containment pool at the end of the blowdown phase. Since almost 90% of the fine debris is blown to upper containment, 42% transport of the fines in lower containment to the reactor cavity represents much less than 15% of the overall debris generated.

ATTACHMENT 1
REGNPP GL 2004-02 THIRD SUPPLEMENTAL RAI RESPONSE

Debris Erosion:

The guidance specifies that an erosion fraction of 90% should be used for fiberglass debris. The SER states that with such limited data, the use of the 90% value is necessary to ensure conservatism. The SER also states that this number can possibly be reduced, once better erosion data are available.

The insulation debris type(s) with the potential for erosion at Ginna are Temp-Mat, Thermal-Wrap, Cal-Sil, and Asbestos. The individual fibers and Cal-Sil/asbestos fines would not be subject to further erosion, and by definition, intact blankets are still covered by the original jacketing and therefore would also not be subject to erosion. This leaves the small and large pieces of fiberglass (Temp-Mat and Thermal-Wrap).

Tests performed as a part of the DDTS have indicated that the erosion of fibrous debris is significantly different for debris directly impacted by containment sprays versus debris directly impacted by break flow. The erosion of large pieces of fibrous debris by containment sprays was found to be less than 1%, whereas the erosion due to the break flow was much higher. Due to differences in the design of Pressurized Water Reactor (PWR) nuclear plants compared to the Boiling Water Reactor (BWR) nuclear plants, the results of the erosion testing in the DDTS are only partially applicable. In a BWR plant, a LOCA accident would generate debris that would be held up below the break location on grating above the suppression pool. In the Ginna plant, however, the break would generate debris that would either be blown to upper containment or blown out away from the break. Most of the debris would not be hung up directly below the break flow where it would undergo the high erosion rates suggested by the DDTS. Any debris blown to upper containment that is not washed back down, however, could be subject to erosion by the sprays. However, since the containment sprays at Ginna are secured prior to recirculation, spray erosion would be negligible.

Since the SER test data showed in general that the erosion consisted primarily of small, loosely attached pieces of fiber breaking off from larger pieces, it is considered reasonable to assume that erosion would taper off after 24 hours. To be conservative, however, the 24 hour erosion determined in the Ginna analysis was rounded up to 10%. This erosion fraction was applied for both small and unjacketed large pieces of fiberglass in the containment pool.

It was assumed that the erosion of the Cal-Sil and Asbestos Cal-Sil chunks debris in the recirculation pool would be 50%. Given the low flow rates and velocities in the recirculation pool at Ginna, it is likely that the actual erosion fraction would be significantly less than this (approximately 10% to 20% based on engineering judgment).

Use of Debris Interceptors

Debris interceptors are not integrated into the Ginna debris transport analyses and no credit was taken for them holding up debris.

Credit for Settling

Settling of large and small pieces is credited in areas of the pool where the TKE and tumbling velocities are low enough not to move the debris with respect to the debris transport metric from Table .

ATTACHMENT 1
REGNPP GL 2004-02 THIRD SUPPLEMENTAL RAI RESPONSE

Settling was also credited for fiberglass and IOZ fines. Based on the settling velocity for this debris (see Table 3.7), the TKE in the Ginna containment pool would only be high enough to suspend the fiberglass and IOZ fines in regions between the break location and the sump strainer (see Figure 5 and Figure 3.). Since containment spray is not used during recirculation at Ginna, the pool is essentially stagnant in regions of the pool that are outside the primary flow path from the break to the sump. No credit was taken for settling of other fine debris including Cal-Sil, phenolic coatings, dirt/dust, and latent fiber.

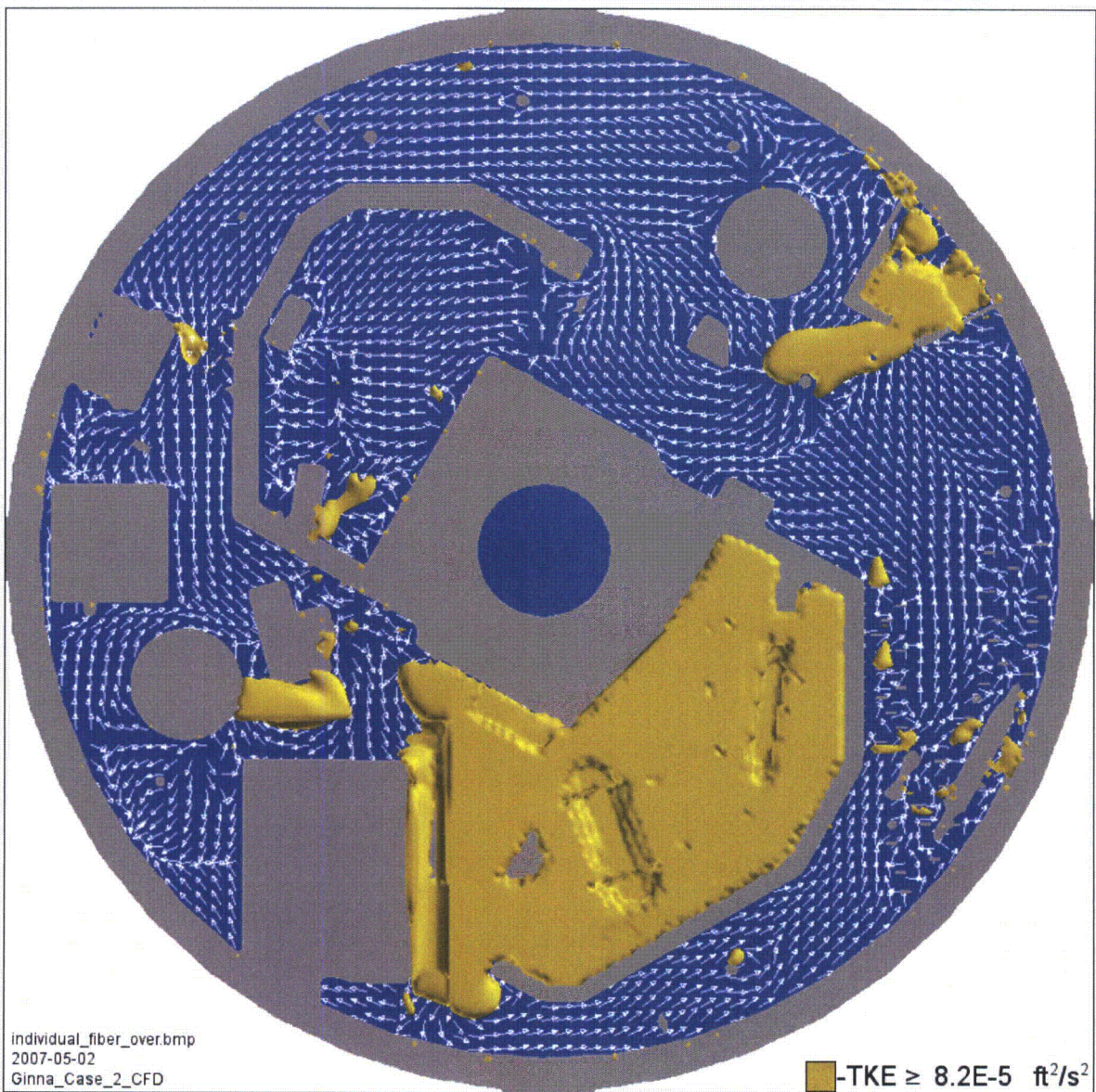


Figure 3.5 – TKE with Limits Set at Suspension of Individual Fibers (Compartment B Break)

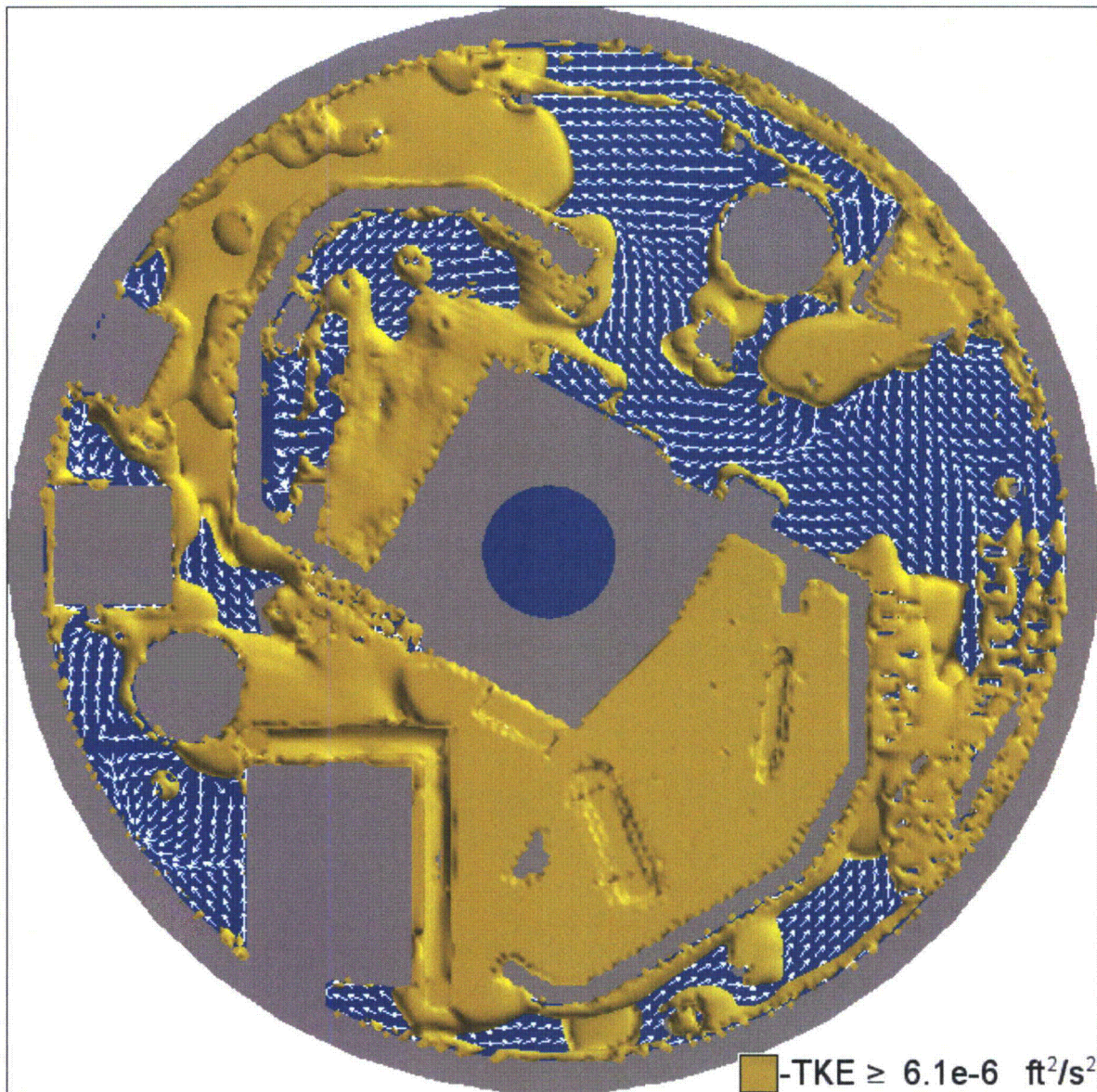


Figure 3.6 – TKE with Limits Set at Suspension of Inorganic Zinc Particulate (Compartment B Break)

Final Debris Transport Data

Transport logic trees were developed for each size and type of debris generated. These trees were used to determine the total fraction of debris that would reach the sump screen in each of the postulated cases. The postulated cases for Ginna include the LBLOCA in Compartments A and B (Table 3.8 and Table) and the results for an SBLOCA in the pressurizer spray line (Table).

ATTACHMENT 1
REGNPP GL 2004-02 THIRD SUPPLEMENTAL RAI RESPONSE

Table 3.8 – Overall Debris Transport (Case 1)

Debris Type	Debris Size	Debris Quantity Generated	Debris Transport Fraction	Debris Quantity at Sump
Stainless Steel RMI	Small Pieces (<4")	1,656 ft ²	0%	0 ft ²
	Large Pieces (>4")	552 ft ²	0%	0 ft ²
	Total	2,208 ft²	0%	0 ft²
Thermal-Wrap	Fines	90.2 ft ³	62%	55.9 ft ³
	Small Pieces (<6")	316.4 ft ³	4%	12.7 ft ³
	Large Pieces (>6")	107.8 ft ³	4%	4.3 ft ³
	Intact Pieces (>6")	115.4 ft ³	0%	0 ft ³
	Total	629.8 ft³	12%	72.9 ft³
Temp-Mat	Fines	9.5 ft ³	62%	5.9 ft ³
	Small Pieces (<6")	37.7 ft ³	34%	12.8 ft ³
	Large Pieces (>6")	5.6 ft ³	38%	2.1 ft ³
	Intact Pieces (>6")	6.0 ft ³	38%	2.3 ft ³
	Total	58.8 ft³	39%	23.1 ft³
Cal-Sil with Asbestos	Fines	8.7 ft ³	83%	7.2 ft ³
	Small Pieces (>1")	6.9 ft ³	50%	3.5 ft ³
	Total	15.6 ft³	69%	10.7 ft³
Qualified Phenolic (10D)	Total (fines)	757 lb	83%	628 lb
Qualified IOZ (10D)	Total (fines)	94 lb	76%	71 lb
Qualified Phenolic (5D)	Total (fines)	130 lb	83%	108 lb
Qualified IOZ (5D)	Total (fines)	29 lb	76%	22 lb
Qualified Degraded Phenolic	Total (chips)	199 lb	0%	0 lb
Qualified Degraded IOZ	Total (fines)	88 lb	91%	80 lb
Dirt/Dust	Total (fines)	85 lb	100%	85 lb
Latent Fiber	Total (fines)	15 lb	100%	15 lb

ATTACHMENT 1
REGNPP GL 2004-02 THIRD SUPPLEMENTAL RAI RESPONSE

Table 3.9 – Overall Debris Transport (Case 2)

Debris Type	Debris Size	Debris Quantity Generated	Debris Transport Fraction	Debris Quantity at Sump
Stainless Steel RMI	Small Pieces (<4")	1,656 ft ²	39%	646 ft ²
	Large Pieces (>4")	552 ft ²	39%	215 ft ²
	Total	2,208 ft²	39%	861 ft²
Thermal-Wrap	Fines	90.7 ft ³	24%	21.8 ft ³
	Small Pieces (<6")	318.6 ft ³	26%	82.8 ft ³
	Large Pieces (>6")	108.1 ft ³	15%	16.2 ft ³
	Intact Pieces (>6")	115.7 ft ³	13%	15.0 ft ³
	Total	633.2 ft³	21%	135.8 ft³
Temp-Mat	Fines	7.7 ft ³	24%	1.8 ft ³
	Small Pieces (<6")	30.6 ft ³	34%	10.4 ft ³
	Large Pieces (>6")	13.3 ft ³	38%	5.1 ft ³
	Intact Pieces (>6")	14.1 ft ³	38%	5.4 ft ³
	Total	65.7 ft³	35%	22.7 ft³
Cal-Sil with Asbestos	Fines	14.7 ft ³	83%	12.2 ft ³
	Small Pieces (>1")	11.5 ft ³	67%	7.7 ft ³
	Total	26.2 ft³	76%	19.9 ft³
Qualified Phenolic (10D)	Total (fines)	869 lb	83%	721 lb
Qualified IOZ (10D)	Total (fines)	122 lb	36%	44 lb
Qualified Phenolic (5D)	Total (fines)	116 lb	83%	96 lb
Qualified IOZ (5D)	Total (fines)	28 lb	36%	10 lb
Qualified Degraded Phenolic	Total (chips)	199 lb	13%	26 lb
Qualified Degraded IOZ	Total (fines)	88 lb	42%	37 lb
Dirt/Dust	Total (fines)	85 lb	100%	85 lb
Latent Fiber	Total (fines)	15 lb	100%	15 lb

ATTACHMENT 1
REGNPP GL 2004-02 THIRD SUPPLEMENTAL RAI RESPONSE

Table 3.10 – Overall Debris Transport for a Break in the Pressurizer Spray Line (Case 3)

Debris Type	Debris Size	Debris Quantity Generated	Debris Transport Fraction	Debris Quantity at Sump
Temp-Mat	Fines	0.9 ft ³	100%	0.9 ft ³
	Small Pieces (<6")	3.5 ft ³	100%	3.5 ft ³
	Total	4.4 ft³	100%	4.4 ft³
Cal-Sil with Asbestos	Fines	1.4 ft ³	100%	1.4 ft ³
	Small Pieces (>1")	1.4 ft ³	100%	1.4 ft ³
	Total	2.9 ft³	100%	2.9 ft³
Qualified Phenolic (10D)	Total (fines)	10 lb	100%	10 lb
Qualified IOZ (10D)	Total (fines)	4 lb	100%	4 lb
Qualified Phenolic (5D)	Total (fines)	2.5 lb	100%	2.5 lb
Qualified IOZ (5D)	Total (fines)	1.1 lb	100%	1.1 lb
Qualified Degraded Phenolic	Total (chips)	199 lb	100%	199 lb
Qualified Degraded IOZ	Total (fines)	88 lb	100%	88 lb
Dirt/Dust	Total (fines)	85 lb	100%	85 lb
Latent Fiber	Total (fines)	15 lb	100%	15 lb

Temp-Mat (Higher Density Fiber Glass) High Transport Fraction vs Thermal Wrap (Lower Density Fiber Glass) Low Transport Fraction

Based on fibrous debris testing, it was assumed that the Thermal-Wrap debris would not float in the containment pool. Test data has shown that fiberglass insulation sinks more readily in hotter water [3.6]. Given the high initial temperature of the Ginna containment pool, this is a reasonable assumption.

However, due to concerns that the higher density fiberglass (Temp-Mat) may not become saturated with water as easily as low density fiberglass, it was conservatively assumed that small and large pieces of Temp-Mat would float for an extended period of time, and therefore would readily transport in the recirculation pool.

Within the small and large piece Thermal-Wrap logic trees, the calculated recirculation transport fractions were used. However, for Temp-Mat small and large pieces, the logic trees conservatively assumed that all small and large pieces of Temp-Mat in the containment pool transport to the sump (a recirculation transport fraction of 100%). Using two example logic trees from a single case and debris size (Figure 3.73.7 and Figure 3.8), it can be seen that using the actual transport fraction for Thermal-Wrap and an overly-conservative 100% transport fraction for Temp-Mat accounts for this difference.

ATTACHMENT 1
 REGNPP GL 2004-02 THIRD SUPPLEMENTAL RAI RESPONSE

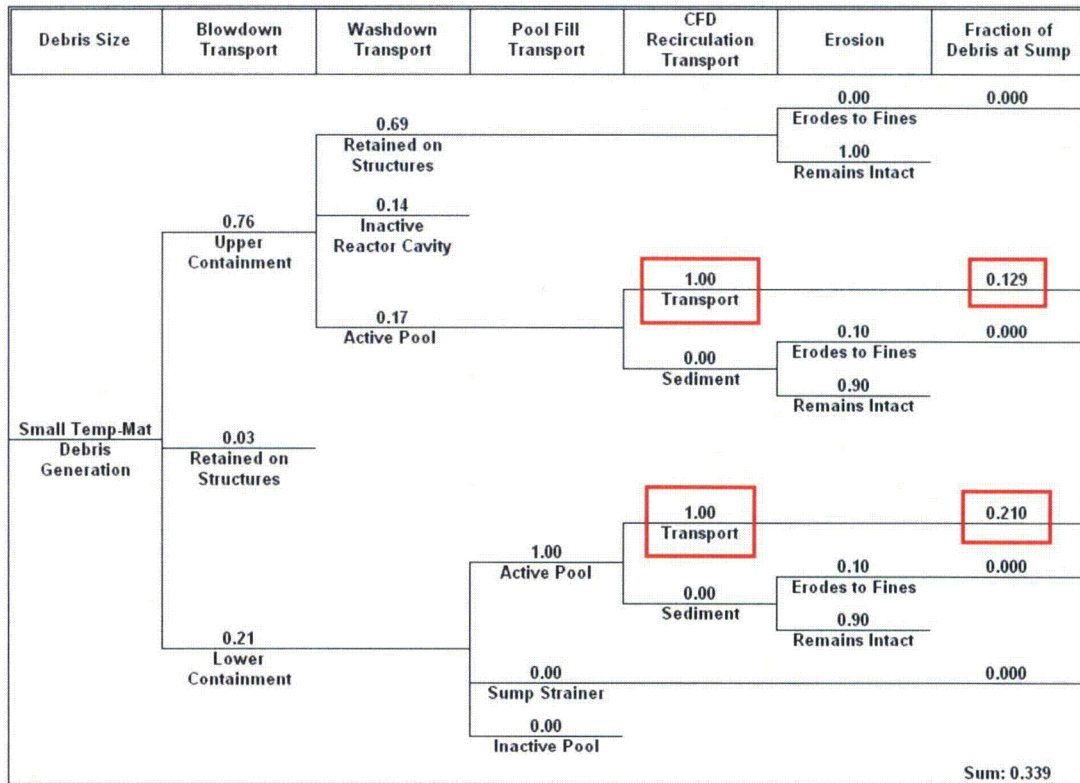


Figure 3.7 – Temp-Mat Small Pieces Debris Transport Logic Tree (Case 1)

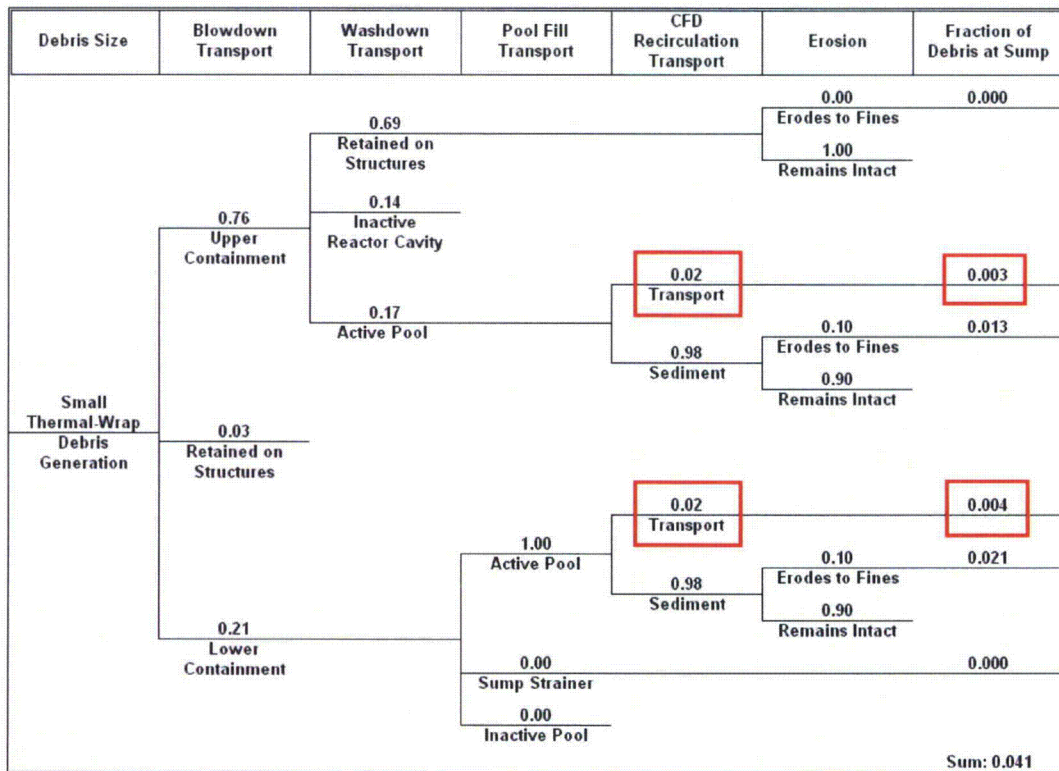


Figure 3.8 – Thermal-Wrap Small Pieces Debris Transport Logic Tree (Case 1)

ATTACHMENT 1
REGNPP GL 2004-02 THIRD SUPPLEMENTAL RAI RESPONSE

RAI-3 References:

- 3.1 Calculation ALION-CAL-GINNA-4376-03, "Ginna GSI-191 Debris Transport Calculation", Revision 2.
- 3.2 D. V. Rao, et al., "Drywell Debris Transport Study: Experimental Work", NUREG/CR-6369, Volume 2, 1999.
- 3.3 Drawing 33013-2101, "Plant Arrangement Cont. Struct. & Intermediate Bldg. Plan – Basement Floor El. 235' – 8'''", Revision 3.
- 3.4 Adrien, Nicolas G., "Computational Hydraulics and Hydrology, An Illustrated Dictionary", CRC Press, 2004, p. 134.
- 3.5 D. V. Rao and B.C. Letellier, A.K. Maji, B. Marshall, "GSI-191: Separate-Effects Characterization of Debris Transport in Water," NUREG/CR-6772, 2002.
- 3.6 Calculation ALION-CAL-CONS-3237-02, "Ginna Reactor Building GSI-191 Debris Generation Calculation", Revision 1.
- 3.7 Calculation DA-ME-2005-085, "NPSH for ECCS Pumps During Injection and Sump Recirculation", Revision 2.
- 3.8 D. V. Rao, C.J. Schafer, M.T. Leonard, K.W. Ross, "Knowledge Base for the Effect of Debris on Pressurized Water Reactor Emergency Core Cooling Sump Performance", NUREG/CR-6808, 2003.
- 3.9 A. Fullerton, T. Fu, D. Walker, and J. Carneal, "Hydraulic Transport of Coating Debris", NUREG/CR-6916, 2006.

RAI-4: *Please provide verification that the fibrous size distribution used during testing was prototypical or conservative compared to the size distribution predicted by the transport evaluation.*

RAI-4 Response: Table 4.1, below, provides the calculated quantities and size distribution of fibrous debris generated and transported to the sump strainers. For some size classifications, the quantity of fibrous debris used in strainer testing was increased. The quantities used in testing were determined by applying a scaling factor of 51.02 to the size classification quantity. The method of calculating the scaling factor is provided below. For each fibrous debris type, the worst case quantity of debris transported was used, irrespective of the postulated break location. This is conservative, since it maximizes the fibrous debris used in strainer testing and therefore bounds all break locations.

The strainer head loss testing specification [4.3] identified the quantities of fibrous debris to be used during testing. The preparation of the fibrous debris used in the head loss tests conformed to the debris size distribution specified in the debris transport analysis. Fibrous debris was prepared in four debris size categories: fines, small pieces, large pieces, and intact pieces.

Fines were prepared by chopping and shredding the prescribed quantity of fibrous debris. The chopped and shredded fibrous debris was baked at high temperature overnight to assist in the release of the individual fibers. The chopped, shredded, and baked fibrous debris was placed in a large barrel and pummeled with the jet-like force from a pressure washer nozzle until a slurry of fiber fines suspended in water resulted. Fibrous debris size distribution analyses were performed that verify the debris preparation techniques used. The photo that follows (Figure 4.1) shows the initial fiber fines addition. It can be seen that the fines are fully suspended in cloud-like form with no large clumps or fiber clusters.

ATTACHMENT 1
 REGNPP GL 2004-02 THIRD SUPPLEMENTAL RAI RESPONSE

Small fiber pieces (<6”) were prepared by chopping the specified quantity of fibrous insulation in approximately 1” x 1” squares and shredding the pieces. Large and intact fiber insulation (>6”) were conservatively combined as a single debris size class. The specified quantities were prepared by chopping the insulation in approximately 6” x 6” squares. Water was added to the barrels of fibrous debris several hours before addition to the test loop to allow sufficient soaking time for the fiber. Photos of the prepared fibrous debris follow (Figure 4.2).

Table 4.1: Fibrous Debris Quantities for Strainer Head Loss Testing

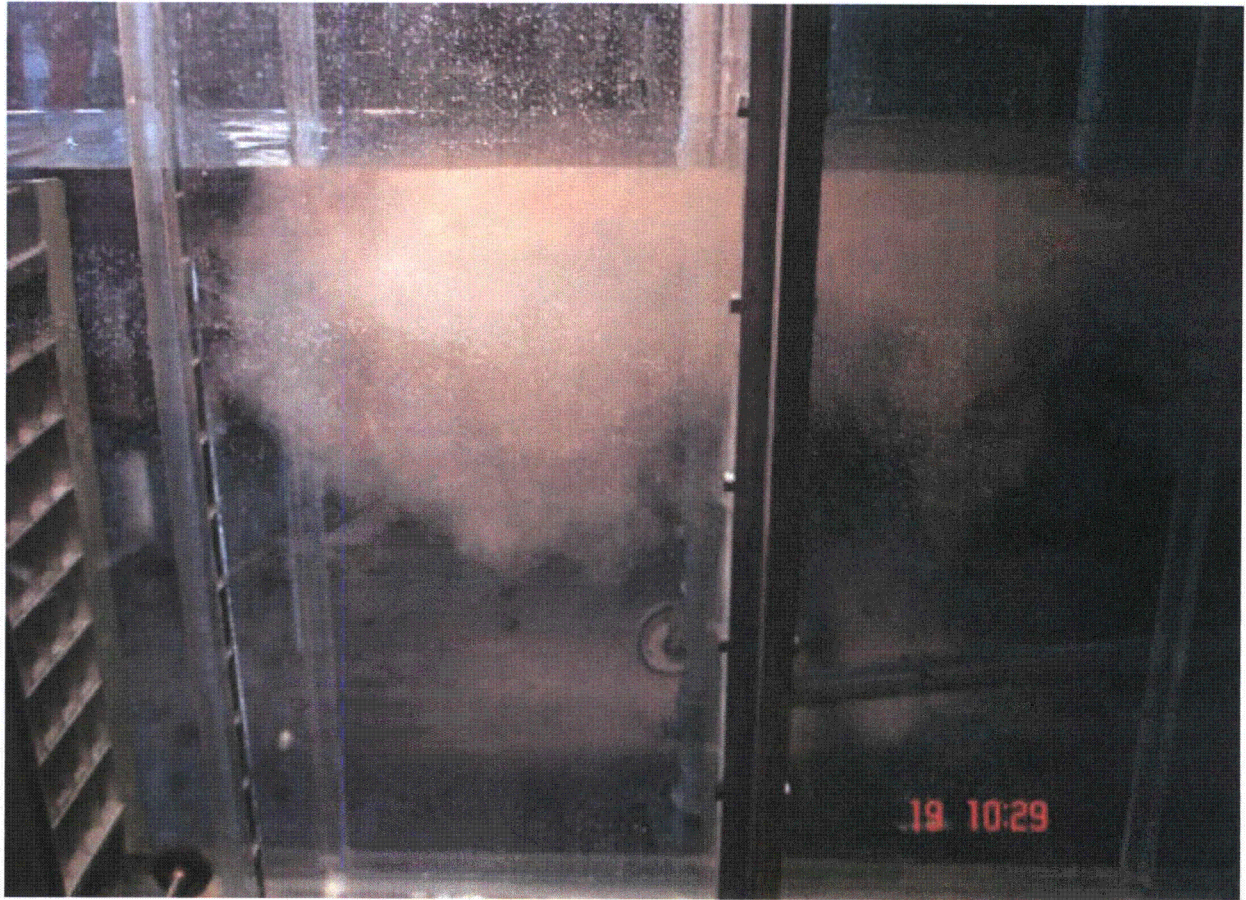
Fiber Material	Quantity Generated [4.1] (ft ³)	Transport Fraction [4.2] (%)	Quantity at Sump [4.2] (ft ³)	Density (lb/ ft ³)	Mass at Sump (lbm)	Mass at Sump (kg)	Scaling Factor [4.3]	Quantity Required for Test (kg)	Quantity Used During Testing [4.4] (kg)
Thermal Wrap									
Fines	90.2	62	55.9	2.4	134.2	60.872	51.02	1.193	1.411
Small Pieces (<6”)	318.6	26	82.8	2.4	198.7	90.138	51.02	1.767	1.767
Large Pieces (>6”)	108.1	15	16.2	2.4	38.9	17.636	51.02	0.666	0.666
Intact Pieces (>6”)	115.7	13	15.0	2.4	36.0	16.329	51.02		
TempMat									
Fines	9.5	62	5.9	9.0	53.1	24.086	51.02	0.472	0.504
Small Pieces (<6”)	37.7	34	12.8	9.0	115.2	52.254	51.02	1.024	1.024
Large Pieces (>6”)	13.3	38	5.1	9.0	45.9	20.820	51.02	0.840	0.840
Intact Pieces (>6”)	14.1	38	5.4	9.0	48.6	22.045	51.02		
Latent Fiber									
Fines*	6.25	100	6.25	2.4	15.0	6.804	51.02	0.133	0.133

* Modeled as Thermal Wrap

Calculation of Scaling Factor:

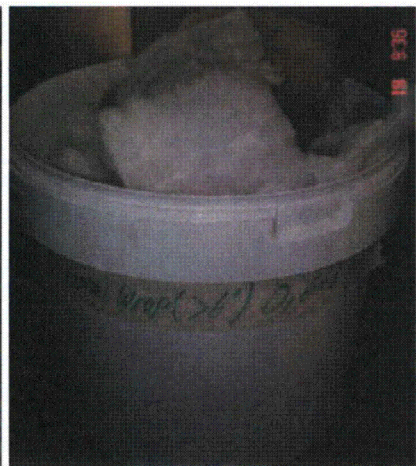
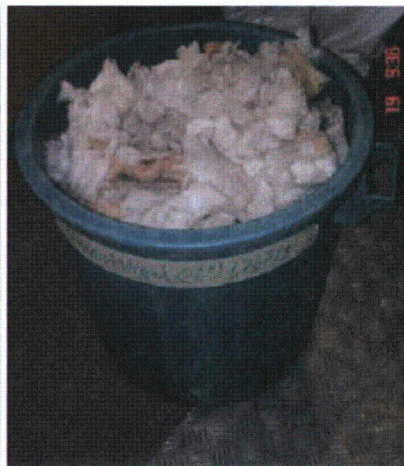
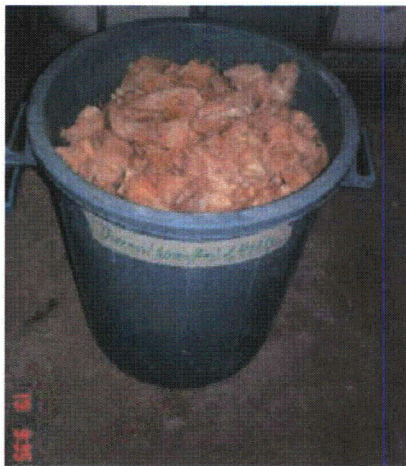
$$\text{Scaling Factor} = \frac{\text{Plant Strainer Surface Area (4089 ft}^2\text{)} - \text{Sacrificial Surface Area (118 ft}^2\text{)}}{\text{Test Strainer Surface Area (77.823 ft}^2\text{)}} = 51.02$$

Figure 4.1: Ginna Strainer Testing – Fiber Fines Debris Addition to the Test Loop



ATTACHMENT 1
REGNPP GL 2004-02 THIRD SUPPLEMENTAL RAI RESPONSE

Figure 4.2: Ginna Strainer Testing Debris Preparation



ATTACHMENT 1
REGNPP GL 2004-02 THIRD SUPPLEMENTAL RAI RESPONSE

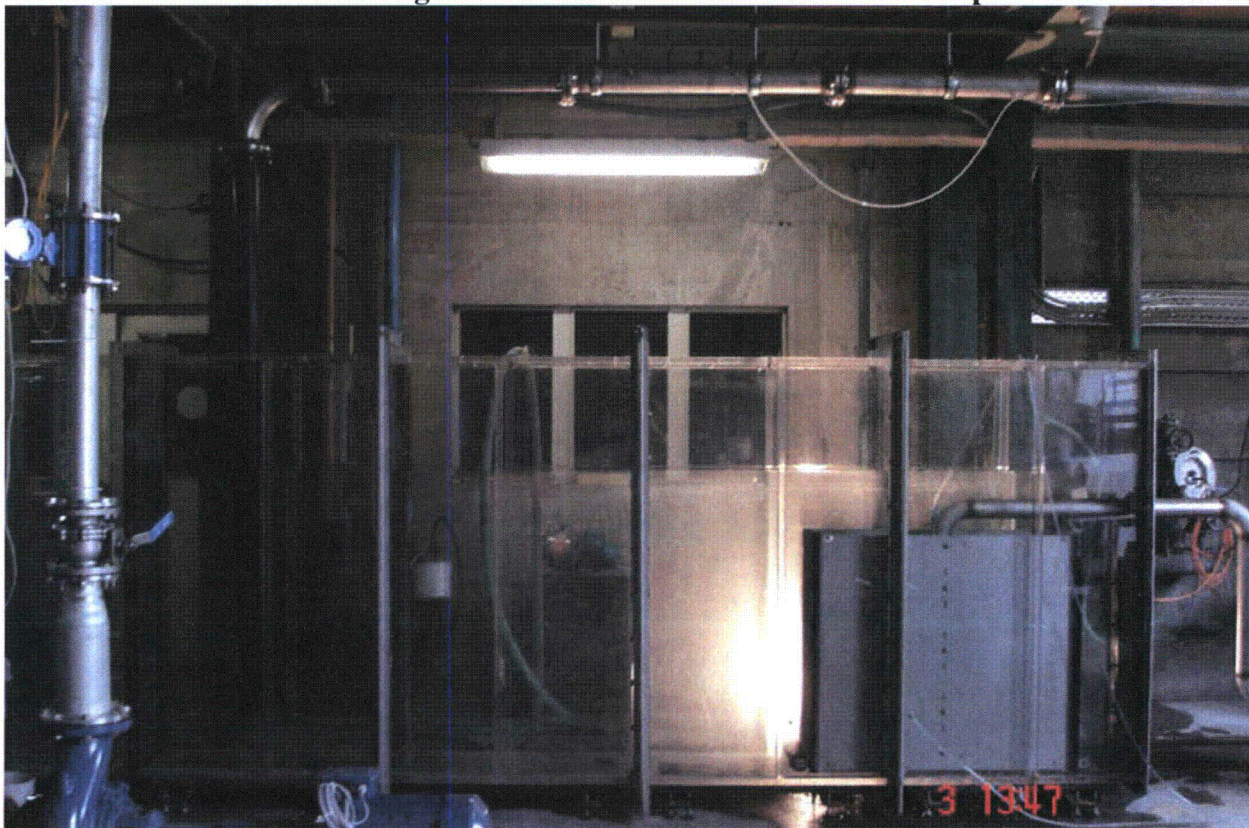
RAI-4 References:

- 4.1 ALION-CAL-CONS-3237-02, "Ginna Reactor Building GSI-191 Debris Generation Calculation," Rev. 1.
- 4.2 ALION-CAL-GINNA-4376-03, "Ginna GSI-191 Debris Transport Calculation," Rev. 2.
- 4.3 Q.003.84809, "Double Sided Chemical Effect Head Loss Test Specification," Rev. 0.
- 4.4 680/41439, "Chemical Effects Test," Rev. 1.

RAI-5: *Please provide details of the debris addition procedures used. Please include a description of fibrous concentration during debris addition, the debris addition location, and the method of adding fibrous debris to the test tank. Please provide verification that the debris introduction processes did not result in non-prototypical settling, agglomeration, or deposition of debris.*

RAI-5 Response: The test loop in which strainer head loss testing was conducted consists of a tank approximately 12 m long x 0.5 m wide x 2 m high. A double sided strainer segment is positioned at one end of the test tank. Pump suction is taken from the center channel of the strainer and circulated to the opposite end of the test tank, through a submerged sparger. Test debris is added to the test tank near the surface of the tank water above the sparger location (Figure 5.1).

Figure 5.1: CCI Multi-functional Test Loop



ATTACHMENT 1
REGNPP GL 2004-02 THIRD SUPPLEMENTAL RAI RESPONSE

Fibrous debris was prepared in individual preparation buckets for each fiber type and debris size classification. Following baking of the fiber for 24 hours at 250 °C, fibrous fines were prepared in batches by breaking down approximately 0.5 kg of fibers with a pressure washer using 30-45 liters of water, until the proper size was achieved. Samples of the fiber fines were taken for size characterization. Other fiber size classification preparation buckets were filled with water and allowed to soak for several hours before addition to the test loop.

The fiber slurry batches were added to the test loop at the water surface above the sparger location, approximately 2.5 m from the face of the strainer. Approximately 4 liters of fiber slurry from the preparation bucket was filled into a 5 liter dip bucket used to transfer the fiber from the preparation buckets to the test loop. The dip bucket was placed into the test loop at the water surface to allow loop water to enter and further agitate/dilute the fiber fines. The dip bucket was then slowly picked up and lowered down to allow the fines to “waft” into the test loop (Figure 5.2). All fiber batches were added very slowly into the test loop to prevent a jet of water from the sparger forcing the debris to the bottom. During the addition, water from the loop was used to help dilute/agitate the debris in the addition bucket with care taken to not create waves or turbulence in the loop. Periodic mixing of the preparation bucket was accomplished by a drill with a propeller style bit. Similarly, the propeller was used to agitate the test loop and re-suspend any fibers which may have settled, again taking care not to create turbulence that would impact the debris layer on the strainers.

During testing, it was observed that the fiber fines readily transported to the strainer surface without any agglomeration or settling (Figure 5.3). Only after the larger debris size classifications were introduced did any significant pile begin to build immediately in front of the strainer face (Figure 5.4).

Figure 5.2: Dip Bucket Adding Fiber in the Test Loop



Figure 5.3: Fiber Fines Distributed in the Test Loop

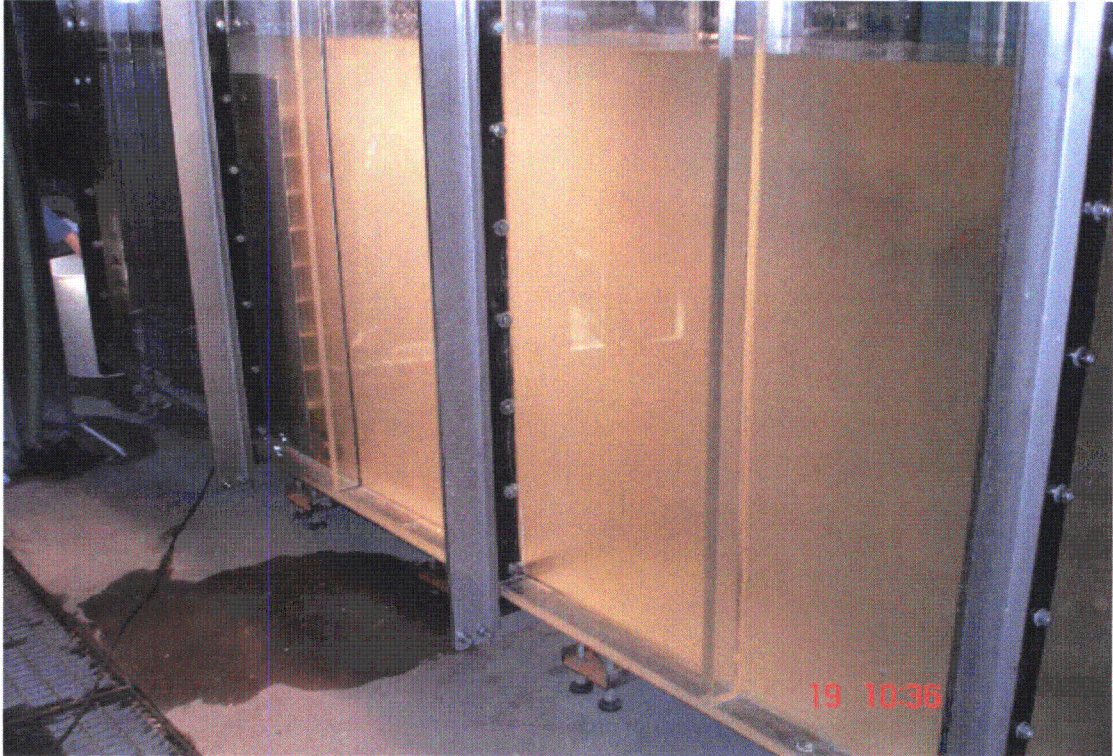


Figure 5.4: Debris Pile



ATTACHMENT 1
REGNPP GL 2004-02 THIRD SUPPLEMENTAL RAI RESPONSE

RAI-6: *If the test(s) allowed near-field settling, please provide a comparison of the flows predicted around the strainer in the plant versus the flows present in the test flume. Please show that the test velocities and turbulence levels were prototypical or conservative compared to the plant. If the test(s) allowed settling, please provide the amount (percentage by type) of debris that settled in the test tank.*

RAI-6 Response: The strainer head loss test specification [6.1] defined the strainer head loss test loop flow rate to be used during the Ginna testing as 10.24 m³/h. This value was derived from the maximum containment recirculation flow rate of 2300 gpm [6.2] with a scaling factor and SI units conversion applied, as follows:

$$\text{Scaling Factor} = \frac{\text{Plant Strainer Surface Area (4089 ft}^2\text{)} - \text{Sacrificial Surface Area (118 ft}^2\text{)}}{\text{Test Strainer Surface Area (77.823 ft}^2\text{)}} = 51.02$$

$$\text{Test Flow Rate} = \frac{2300 \text{ gpm} * 3.785 * 10^{-3} \text{ m}^3/\text{gal} * 60 \text{ min/hr}}{51.02} = 10.24 \text{ m}^3/\text{h}$$

During the strainer head loss testing, test flow rate measurements were electronically taken every 30 seconds. Data from the Ginna strainer head loss test report [6.3] confirms that the test loop flow rate was maintained between 10.2 and 10.3 m³/h. Since the test pump flow was scaled from the maximum expected ECCS pump flow corresponding to the test strainer surface area, the flow approach velocity of the test strainer is identical to that which would be seen in containment.

The results of the debris transport analysis show that the Total Kinetic Energy (TKE) of the recirculation pool in the area of the sump strainers does not exceed the value below which all debris types would settle except for fiber fines and particulate. Since fiber fines and particulate were added to the test loop first, for thin bed testing, and essentially no near-field settling was observed during the tests, the near field settling that did occur was predominately large pieces of debris. As a result, the quantity of debris presented to the face of the strainer, which settled in the area directly in front of the strainer during testing, is considered prototypical.

The test loop was of adequate size that there were no visible signs of flow turbulence near the test pump return sparger or near the test strainer. On occasion, during the initial stages of the head loss testing, debris that had settled to the bottom of the test loop was manually agitated with a propeller drill bit to re-suspend the debris. This was done to maximize the debris presented to the face of the strainer. Great care was taken not to disturb the debris layer that had accumulated on the strainer. As a result, the propeller was never allowed to get any closer than 2 meters from the face of the strainer, and only used in short bursts.

ATTACHMENT 1
REGNPP GL 2004-02 THIRD SUPPLEMENTAL RAI RESPONSE

The fiber fines transported easily while the larger size category fiber debris and RMI tended to settle. This debris was agitated until it was determined the debris would not transport substantially closer to the strainer.

Test 1 settled quantities and locations:

Sedimentation in front of the strainer test module =	61%
Sedimentation behind the strainer test module =	5%
Debris in the pockets, front side =	20%
Debris in the pockets, back side =	14%

Test 1 Repeat settled quantities and locations:

Sedimentation in front of the strainer test module =	54%
Sedimentation behind the strainer test module =	7%
Debris in the pockets, front side =	19%
Debris in the pockets, back side =	20%

No statement can be made to the actual percentages by type of debris which settled immediately in front of the strainer. The over-whelming majority of the fiber fines transported into the strainer pockets. The majority of the near field settling on the bottom of the test loop was made up of larger fiber pieces, paint chips and RMI (Figure 6.1).

Figure 6.1: Full Debris Load, Including Chemical Precipitate



ATTACHMENT 1
REGNPP GL 2004-02 THIRD SUPPLEMENTAL RAI RESPONSE

RAI-6 References:

- 6.1 Q.003.84809, "Double Sided Chemical Effect Head Loss Test Specification," Rev. 0.
- 6.2 DA-ME-2005-085, "NPSH for ECCS Pumps During Injection and Sump Recirculation," Rev. 2.
- 6.3 680/41439, "Chemical Effect Test," Rev. 1.

RAI-7: *If agitation was utilized to prevent debris settling, please discuss the methods by which the strainer debris bed was not non-conservatively disturbed by the agitation and that non-prototypical transport did not result.*

RAI-7 Response: On occasion, during the initial stages of the head loss testing, debris that had settled to the bottom of the test loop was manually agitated with a drill equipped with a propeller-style drill bit to re-suspend the debris. This was done to maximize the debris presented to the face of the strainer. Great care was taken not to disturb the debris layer that had accumulated on the strainer. As a result, the propeller was never allowed to get any closer than 2 meters from the face of the strainer, and only used in short bursts. During or after debris agitations there were no visual signs or pressure drop indications that the debris bed was adversely or non-conservatively affected. Each agitation re-suspended the targeted fiber fines and particulate evenly throughout the height and width of the test flume. Agitating the flume resulted in a conservatively even debris distribution as it provided more opportunity for fiber fines to remain as single fibers and maximize the potential to distribute along the filtering area with highest penetration velocity. The slow addition of debris along with agitation effectively prevents non-prototypical sedimentation, agglomeration and deposition of debris during debris addition.

RAI-8: *Please provide the test termination criteria and the methodology by which the final head loss values were extrapolated to the ECCS mission time or some predicted steady state value. Please include enough test data to allow the extrapolation results to be verified.*

RAI-8 Response: As provided in the strainer head loss test specification [8.1], the test termination criteria is less than a 1% change in strainer head loss over two consecutive 30 minute periods. This criterion was met. However, as an added measure to ensure that the maximum possible strainer head loss had been achieved, the test was allowed to continue to run until sufficient test tank turnovers, equivalent to the containment recirculation pool volume turnovers for a 30 day mission time, had been achieved. The first strainer head loss test, Test 1, was run for approximately 6.5 days (see Figure 8.1, below, from [8.2]). For the test tank fluid volume and pump flow rate, the test tank fluid turnover rate was 10.8 minutes per turnover [8.1]. Therefore, the total number of test tank fluid volume turnovers during Test 1 was approximately 867. The Ginna containment recirculation pool volume at the minimum recirculation pool level is 176,833 gal. [8.3]. The bounding maximum recirculation pool flow rate is 2300 gpm [8.3]. Therefore, the maximum number of containment recirculation pool turnovers during a 30 day mission time is approximately 562. Hence, the number of test tank fluid volume turnovers exceeded the expected containment recirculation pool turnovers by 54%.

A verification of Test 1 was conducted to ensure repeatability of test results. Test 1 Rep was conducted immediately following the conclusion of Test 1. All test conditions with respect to debris loading, flow rates, strainer surface area, etc. were the same as Test 1. Test 1 Rep was run for approximately 5 days

ATTACHMENT 1

REGNPP GL 2004-02 THIRD SUPPLEMENTAL RAI RESPONSE

(see Figure 8.2, below, from [8.2]). This corresponds to approximately 667 test tank turnovers, again, exceeding the number of containment recirculation pool turnovers.

During strainer head loss testing, head loss values were taken every 30 seconds. As can be seen in the Test 1 plot of strainer head loss values (Figure 8.1), the head loss was stable for nearly 2 days prior to the termination of the test. The head loss during this time had minimal variation (+/- 2 mbar) and the overall trend was steady, to trending down. As a result, it was determined that the maximum strainer head loss had been achieved and no extrapolation of head loss data was performed. The maximum head loss achieved during the test, adjusted for test tank fluid temperature variations and normalized to 20 °C, was 95.2 mbar [8.4]. Since this head loss was the maximum achieved and since subsequent head loss measurements were lower and stable, to trending down, 95.2 mbar at 20 °C was taken as the maximum sump strainer head loss due to debris on the strainer. This value is equivalent to 29.7 mbar (0.99 ft WC) corrected to the minimum containment recirculation pool design temperature of 195 °F.

As can be seen in the Test 1 Rep plot of strainer head loss values (Figure 8.2), the head loss was stable for nearly 1 1/2 days prior to the termination of the test. The head loss during this time had minimal variation (+/- 2 mbar) and the overall trend was steady. As a result, it was determined that the head loss values achieved in Test 1 were valid and bounded the maximum strainer head loss that would be seen in the Ginna containment. The maximum head loss achieved during the Test 1 Rep, adjusted for test tank fluid temperature variations and normalized to 20 °C, was 87.7 mbar [8.4].

Figure 8.1: Ginna Strainer Head Loss Test 1 Results

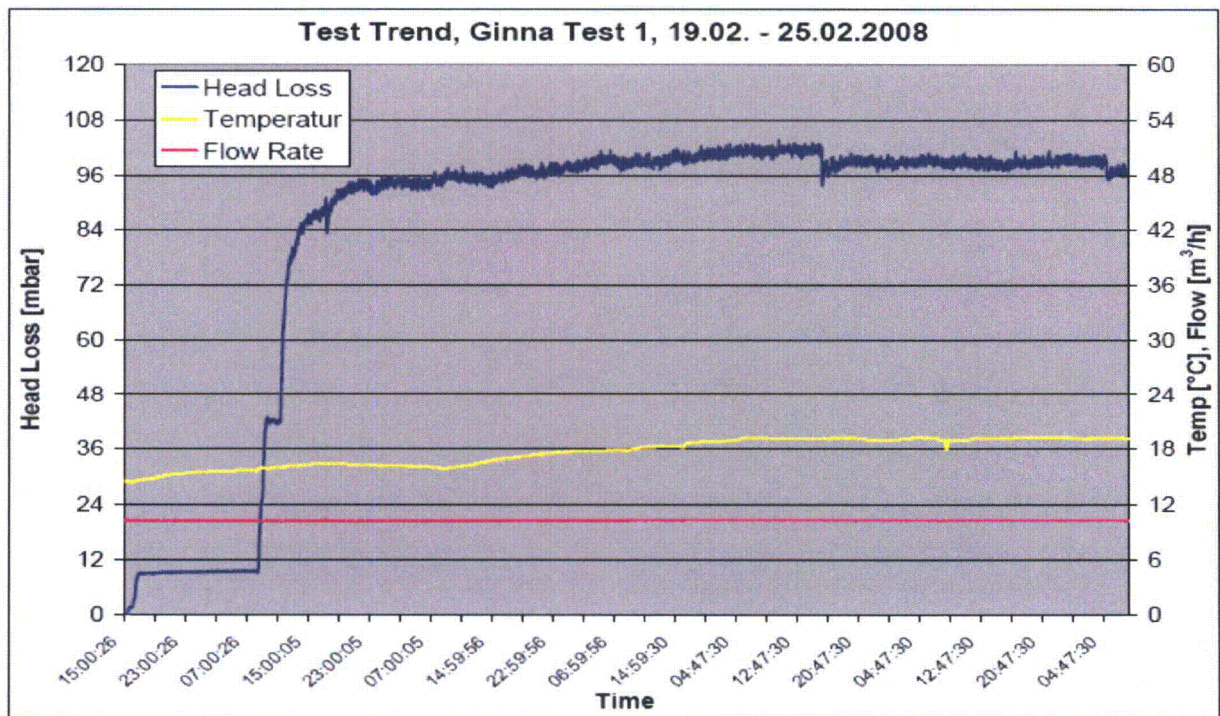
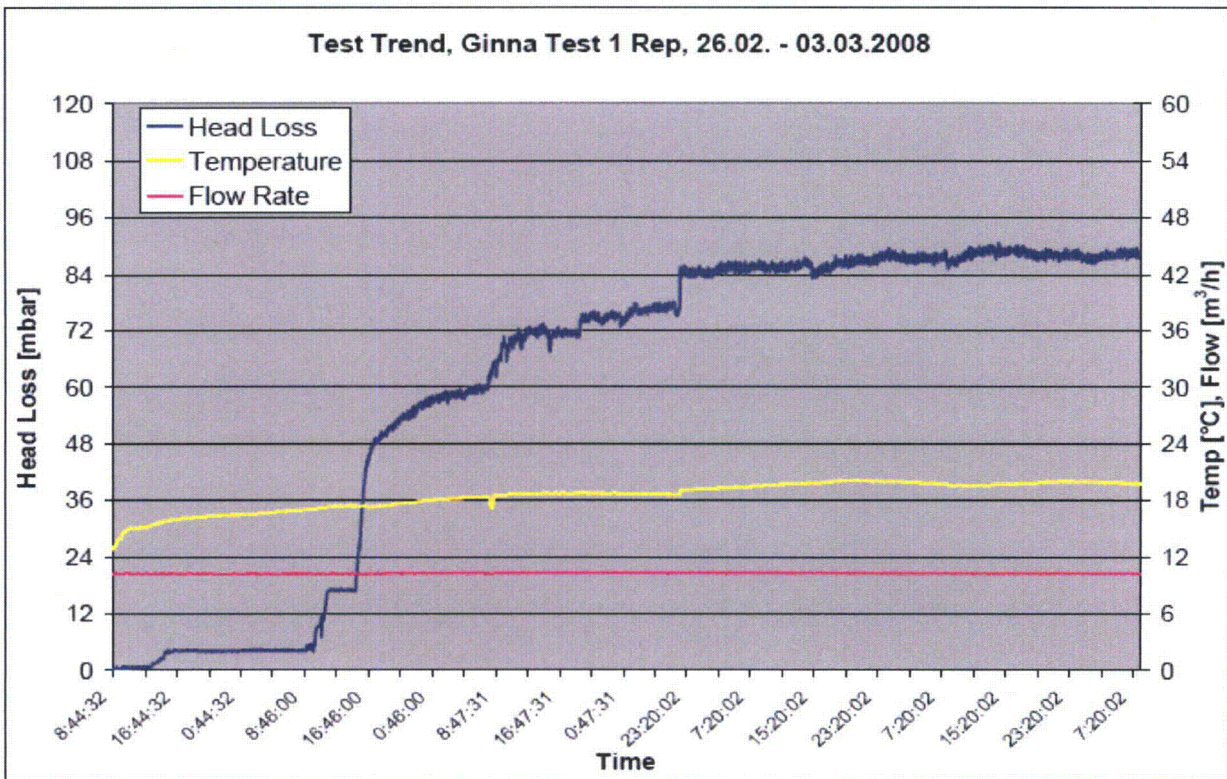


Figure 8.2: Ginna Strainer Head Loss Test 1 Rep Results



RAI-8 References:

- 8.1 Q.003.84809, "Double Sided Chemical Effect Head Loss Test Specification," Rev. 0.
- 8.2 680/41439, "Chemical Effect Test," Rev. 1.
- 8.3 DA-ME-2005-085, "NPSH for ECCS Pumps During Injection and Sump Recirculation," Rev. 2.
- 8.4 3SA-096.077, "Head Loss Calculation Including Chemical Effects," Rev. 1.

RAI-9: Please provide information that verifies that the thin bed testing was conducted in a manner that would result in prototypical or conservative head loss values. Please see the "Revised Review Guidance for Strainer Head Loss and Vortexing (ADAMS Accession No. ML080230038). The second supplemental response indicated that small amounts of fibrous debris were added to the test followed by small amounts of particulate. However, the intent of thin bed testing is to determine if the limiting particulate load, combined with gradually increasing amounts of fiber, will result in greater head losses than the full debris load. In addition, the staff believes that it is most conservative to ensure that fine (easily suspendable) fibers are used in thin bed testing until the amount of fine fiber predicted to reach the strainer has been added to the test flume.

ATTACHMENT 1
REGNPP GL 2004-02 THIRD SUPPLEMENTAL RAI RESPONSE

RAI-9 Response: Thin bed testing was performed in February/March 2008. The testing introduced four small batches of fiber fines, each equivalent to approximately 1/16" debris layer across the strainer surface. Each batch of fiber fines was added and the head loss allowed to stabilize prior to the addition of the subsequent batch. Following the addition of the four batches of fiber fines, approximately one quarter of the total particulate load (Cal-Sil fines, coatings fines, and latent dirt), was introduced into the test loop. No thin bed effect was observed, as the head loss for the two tests run was approximately 1 mbar.

Because the NRC Guidance Report, which provided expectations on thin bed testing, was issued in March 2008, after the Ginna 2008 testing was complete, the above referenced testing did not strictly adhere to the latest guidance. So, additional thin bed testing was performed at the Control Components Incorporated (CCI) test facility in Switzerland in March 2009. The thin bed testing performed strictly adhered to the protocol laid out in the March 2008 NRC Guidance Report. All particulate (Cal-Sil fines, coatings fines, and latent dirt/dust) was added to the test loop and allowed to circulate, followed by gradually increasing quantities of fiber fines. All fiber fines from the Temp-Mat, and thermal wrap insulation, as well as latent fiber were added to the test loop in four batches. All thermal wrap was added to the test loop prior to any addition of Temp-Mat. Each of the four batches contained sufficient fiber fines to cover the strainer surface with a layer approximately 1/16" thick. The head loss was allowed to stabilize between batches. The maximum head loss achieved during the 2009 thin bed testing was approximately 1 mbar. Again, no thin bed effect was observed, reinforcing testing performed in 2008.

RAI-10: *Please provide flow rates used during testing.*

RAI-10 Response: The strainer head loss test specification [10.1] defined the strainer head loss test loop flow rate to be used during the Ginna testing as 10.24 m³/h. This value was derived from the maximum containment recirculation flow rate of 2300 gpm [10.2] with a scaling factor and SI units conversion applied, as follows:

$$\text{Scaling Factor} = \frac{\text{Plant Strainer Surface Area (4089 ft}^2\text{)} - \text{Sacrificial Surface Area (118 ft}^2\text{)}}{\text{Test Strainer Surface Area (77.823 ft}^2\text{)}} = 51.02$$

$$\text{Test Flow Rate} = \frac{2300 \text{ gpm} * 3.785 * 10^{-3} \text{ m}^3/\text{gal} * 60 \text{ min/hr}}{51.02} = 10.24 \text{ m}^3/\text{h}$$

During the strainer head loss testing, test flow rate measurements were electronically taken every 30 seconds. Data from the Ginna strainer head loss test report [10.3] confirms that the test loop flow rate was maintained between 10.2 and 10.3 m³/h.

RHR pump flow rates used in testing (2300 gpm) bound all pump flow rates. Calculated flows for the case that yields the minimum NPSH for the ECCS pumps (approximately 1850 gpm) are 24% less than the flow utilized during testing. This represents additional margin for strainer head loss testing, and vortexing and flashing evaluations.

ATTACHMENT 1
REGNPP GL 2004-02 THIRD SUPPLEMENTAL RAI RESPONSE

RAI-10 References:

- 10.1 Q.003.84809, "Double Sided Chemical Effect Head Loss Test Specification," Rev. 0.
- 10.2 DA-ME-2005-085, "NPSH for ECCS Pumps During Injection and Sump Recirculation," Rev. 2.
- 10.3 680/41439, "Chemical Effect Test," Rev. 1.

RAI-11: *Please provide information that verifies that the amounts of debris added to the test flume were scaled correctly.*

RAI-11 Response: Table 11.1 provides the details of the containment debris quantities generated and transported to the sump, and therefore the minimum quantities required for testing. These values originate from the debris generation and debris transport analyses [11.1 and 11.2]. The calculated quantity of debris expected at the containment sump is the product of the quantity generated and the transport fraction. The mass of material required for testing is determined by applying a scaling factor and SI unit conversion.

Table 11.2 provides the specific quantities of debris materials used during testing. These values originate from the strainer head loss testing specification and head loss report [11.3 and 11.4]. The debris quantities used during testing meet or exceed the calculated quantities required for testing, as they appear in Table 11.1. The following details the debris quantities used during testing.

- 1) TempMat and Thermal Wrap large (>6") and intact piece (>6") quantities were combined as a single debris category in which the debris was prepared as 6" by 6" squares. This is deemed conservative.
- 2) The quantity of latent fiber was modeled as Thermal Wrap fines and added to the total quantity of Thermal Wrap fines.
- 3) RMI small (<4") and large (>4") piece quantities were combined as a single debris category in which all RMI was modeled as small pieces (<4"). This is deemed conservative.
- 4) The quantity of degraded phenolic coatings (chips) used in strainer head loss testing was taken as approximately four times the scaled quantity that was determined to transport to the sump. This is deemed conservative.
- 5) Stone flour was used as a surrogate for phenolic coating fines. This is valid since the particle size of the surrogate is smaller than that specified for phenolic coating fines. Therefore, this yields more conservative test results.
- 6) Zinc dust was used as a surrogate for IOZ fines. Zinc dust is the raw material of IOZ. The quantity of degraded IOZ coatings (fines) used in strainer head loss testing was taken as four times the scaled quantity that was determined to transport to the sump. This quantity was added to the quantity of non-degraded IOZ (fines) within the zone of influence. This is deemed conservative.
- 7) Cal-Sil dust and zinc dust was used as a surrogate for Cal-Sil fines. This is valid since the particle size of the surrogates is the same as that specified for Cal-Sil fines.
- 8) Stone flour was used as a surrogate for latent debris particulate (dirt/dust). This is valid since the particle size of the surrogate is smaller than that specified for latent dust/dirt. Therefore, this yields more conservative test results.

ATTACHMENT 1
REGNPP GL 2004-02 THIRD SUPPLEMENTAL RAI RESPONSE

Table 11.1: Debris Quantities Required for Strainer Head Loss Testing

Debris Type	Quantity Generated [11.1]	Transport Fraction [11.2] (%)	Quantity at Sump [11.2]	Density (lb/ ft ³)	Mass at Sump (lbm)	Mass at Sump (kg)	Scaling Factor [11.3]	Quantity Required for Test (kg)
INSULATION								
RMI (0.002")								
Small Pieces (<4")	1.656 ft ²	39	646 ft ²	493.2	53.1	24.078	51.02	0.472
Large Pieces (>4")	552 ft ²	39	215 ft ²	493.2	17.7	8.023	51.02	0.157
Thermal Wrap								
Fines	90.2	62	55.9	2.4	134.2	60.872	51.02	1.193
Small Pieces (<6")	318.6	26	82.8	2.4	198.7	90.138	51.02	1.767
Large Pieces (>6")	108.1 ft ³	15	16.2 ft ³	2.4	38.9	17.636	51.02	0.346
Intact Pieces (>6")	115.7 ft ³	13	15.0 ft ³	2.4	36.0	16.329	51.02	0.320
TempMat								
Fines	9.5	62	5.9	9.0	53.1	24.086	51.02	0.472
Small Pieces (<6")	37.7	34	12.8	9.0	115.2	52.254	51.02	1.024
Large Pieces (>6")	13.3 ft ³	38	5.1 ft ³	9.0	45.9	20.820	51.02	0.408
Intact Pieces (>6")	14.1 ft ³	38	5.4 ft ³	9.0	48.6	22.045	51.02	0.432
Cal-Sil								
Fines	14.7 ft ³	83	12.2 ft ³	15.0	183.0	83.008	51.02	1.627
Small Pieces (>1")	11.5 ft ³	67	7.7 ft ³	15.0	115.5	52.390	51.02	1.027
COATINGS								
Qualified Phenolic								
Fines	869 lb	83	721 lb	-	721	327.040	51.02	6.410
Chips (degraded)	199 lb	13	26 lb	-	26	11.793	51.02	0.231
Qualified IOZ								
Fines	122 lb	58	71 lb	-	71	32.205	51.02	0.631
Fines (degraded)	88 lb	100	80 lb	-	80	36.287	51.02	0.711
LATENT DEBRIS								
Dust/Dirt Fines	85 lb	100	85 lb	-	85	38.555	51.02	0.756
Fiber Fines	15 lb	100	15 lb	2.4	15.0	6.804	51.02	0.133

ATTACHMENT 1
REGNPP GL 2004-02 THIRD SUPPLEMENTAL RAI RESPONSE

Table 11.2: Debris Quantities Used in Strainer Head Loss Testing

Debris Type	Mass (kg)	Comment
Fibrous Debris		
TempMat Fines	0.504	The quantity used during testing exceeds the quantity required by 0.032 kg (~7%).
TempMat Small Pieces (<6")	1.024	Conforms to analysis required quantity.
TempMat Large Pieces (>6")	0.840	Conforms to analysis required quantity. Large piece and intact piece totals combined (0.408 + 0.432 kg)
Thermal Wrap Fines	1.411	The quantity used during testing exceeds the quantity required by 0.085 kg (~7%). Additionally, the quantity includes latent fiber (0.133 kg), which is modeled as Thermal Wrap.
Thermal Wrap Small Pieces (<6")	1.767	Conforms to analysis required quantity.
Thermal Wrap Large Pieces (>6")	0.666	Conforms to analysis required quantity. Large piece and intact piece totals combined (0.346 + 0.320 kg).
Particulate Debris		
RMI (0.002") (<4")	0.629	Conforms to analysis required quantity. Small piece and large piece totals combined (0.472 + 0.157 kg)
Cal Sil Fines	1.627	Conforms to analysis required quantity. Testing quantities of Cal-Sil fines was achieved by using 1.293 kg of Cal-Sil dust and 0.334 kg of zinc dust.
Cal Sil (<1")	1.027	Conforms to analysis required quantity.
Phenolic Paint (chips)	0.853	The quantity used during testing exceeds the quantity required by approximately 3 times.
Zinc Dust	3.849	Zinc dust was used as a surrogate for IOZ fines. The quantity used during testing exceeds the quantity required for degraded IOZ coatings by 3 times. Zinc dust was, in part, used as a surrogate for Cal-Sil fines. The testing quantities of zinc dust are proportioned as follows: Qualified IOZ Coatings = 0.631 kg Qualified Degraded IOZ Coatings = 2.884 kg Cal-Sil fines = 0.334 kg
Stone Flour	10.925	Stone flour was used as a surrogate for phenolic coatings fines and latent debris particulate (dirt/dust). The quantity used during testing exceeds the quantity required for phenolic coatings by approximately 1 ½ times. The testing quantities of stone flour are proportioned as follows: Latent Dust/Dirt = 0.756 kg Phenolic Coatings = 10.168 kg

RAI-11 References:

- 11.1 ALION-CAL-CONS-3237-02, "Ginna Reactor Building GSI-191 Debris Generation Calculation," Rev. 1.
- 11.2 ALION-CAL-GINNA-4376-03, "Ginna GSI-191 Debris Transport Calculation," Rev. 2.
- 11.3 Q.003.84809, "Double Sided Chemical Effect Head Loss Test Specification," Rev. 0.
- 11.4 680/41439, "Chemical Effect Test," Rev. 1.

ATTACHMENT 1
REGNPP GL 2004-02 THIRD SUPPLEMENTAL RAI RESPONSE

RAI-12: Please provide information that shows that pressure-related phenomena (e.g., boreholes or channeling) did not occur during testing. A description of flow sweeps conducted following testing that shows a head loss change is approximately proportional to flow change is acceptable for this purpose.

RAI-12 Response: The results of the Ginna head loss testing with full debris load, including chemical precipitants, (Figure 12.1 and 12.2) showed no evidence of bore holes or channeling. The strainer head loss over the 4 days of testing, following the introduction of debris, showed minimal variation of head loss and no open strainer surface area. The variation of head loss, from peak to trough, was approximately 6 mbar, with no sudden change of head loss that could be attributed to any pressure related phenomena. This conclusion was further supported by direct observation of the debris bed (Figure 12.3). Two separate tests were conducted with very similar results. Had any pressure related phenomena existed, the results of these tests would not have so closely resembled each other. The strainer head loss, for which temperature/viscosity correction was applied, was taken as the most conservative value for the head loss and test pool water temperature.

Figure 12.1: Ginna Strainer Head Loss Test 1 Results

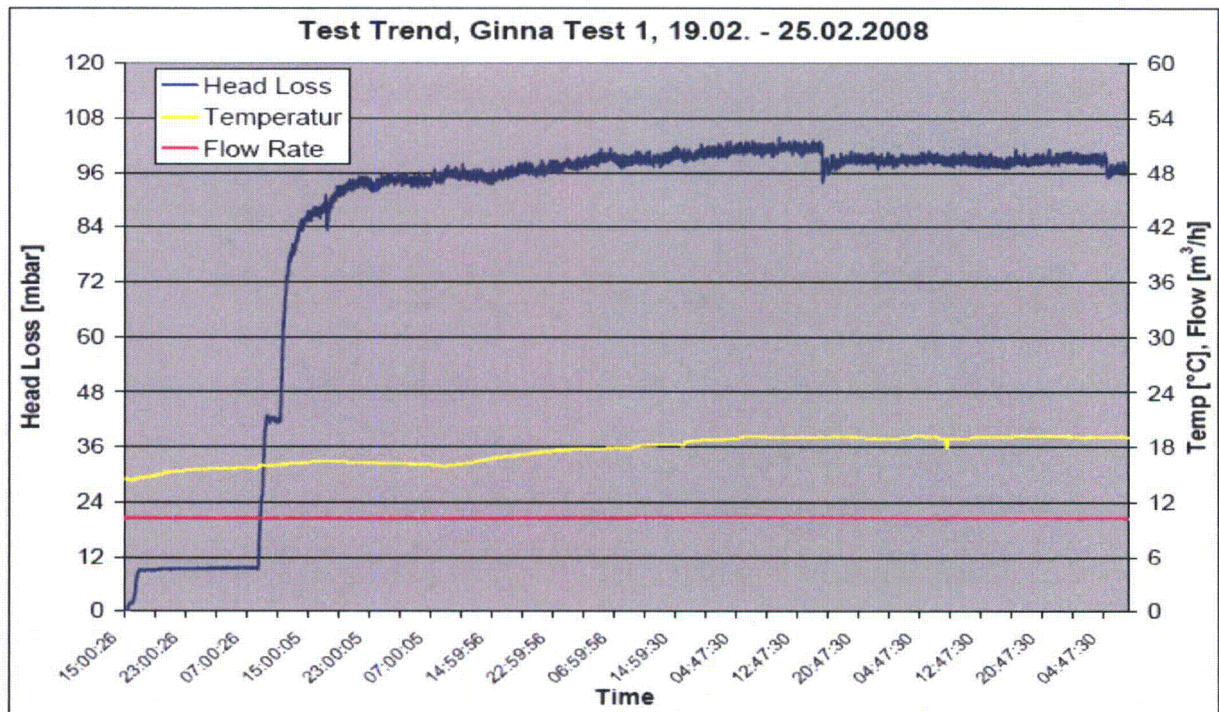


Figure 12.2: Ginna Strainer Head Loss Test 1 Rep Results

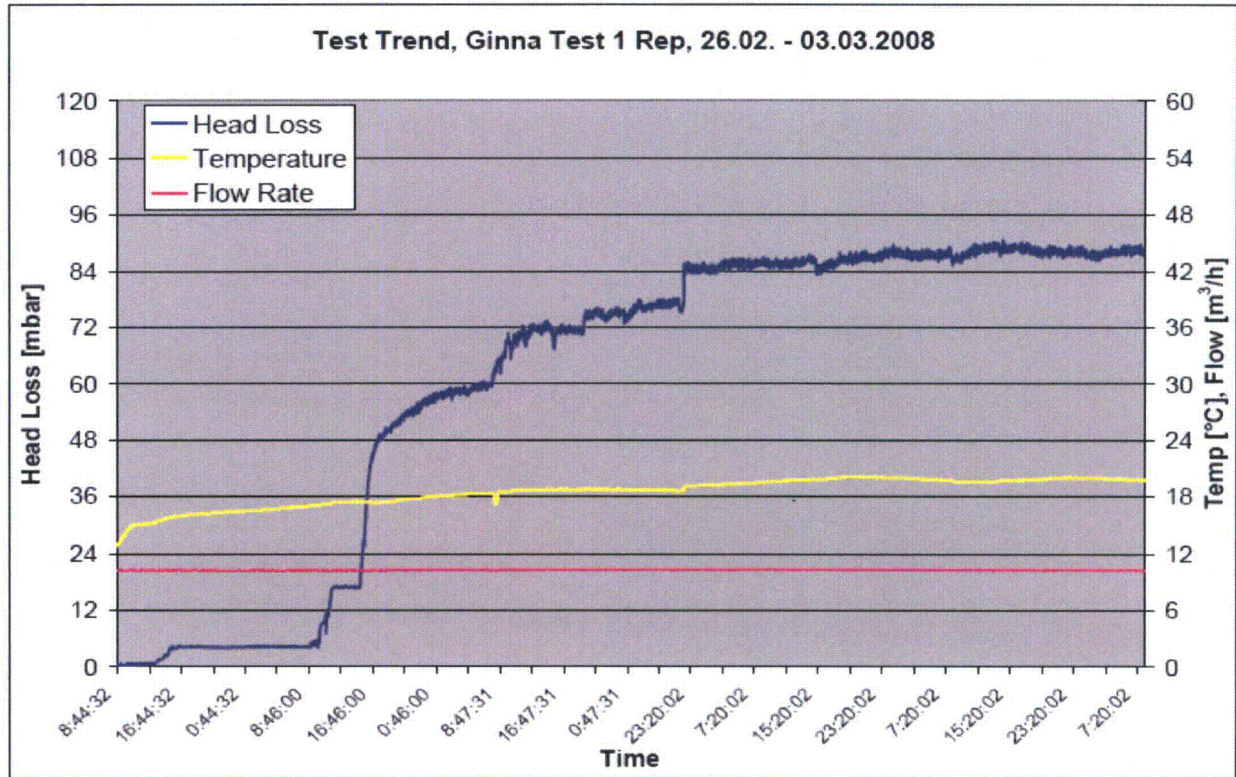
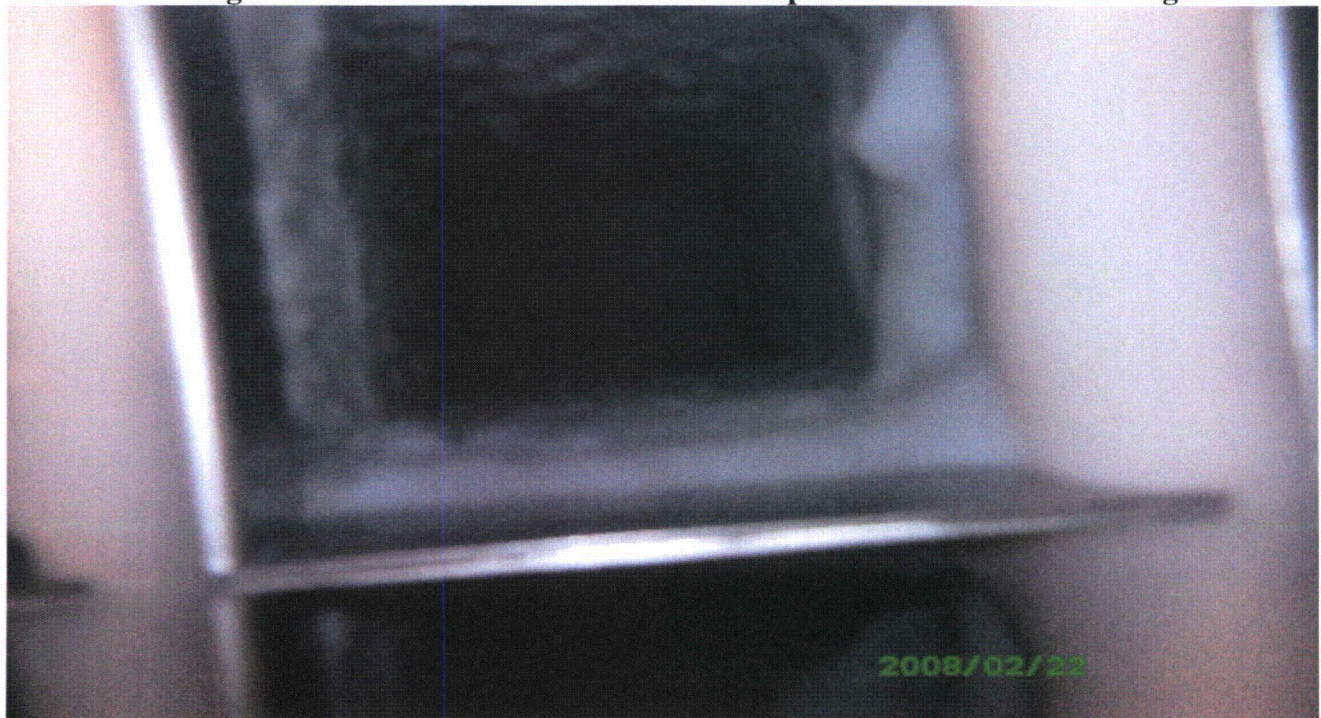


Figure 12.3: Ginna Strainer Pocket at Completion of Head Loss Testing



ATTACHMENT 1
REGNPP GL 2004-02 THIRD SUPPLEMENTAL RAI RESPONSE

RAI-13: *Please provide any conservatisms that were used during the strainer final head loss testing.*

RAI-13 Response: The following are conservatisms applied during final head loss testing:

- 1) The largest quantity of each debris type, regardless of break location, was used in the head loss testing. This was done to ensure that the testing bounds all debris sources for all break locations. As a result, the quantity of fiber and particulate used in testing is greater than that determined to transport to the sump for any single break location.
- 2) The quantity of latent debris used in testing reflects an increase of 160% above the quantity determined to be in containment.
- 3) The maximum quantity of calcium silicate debris determined to be generated by any break location was determined to be 178.3 kg, of which 23.54 kg (~13%) is predicted to be consumed in precipitant generation. The quantity of particulate used in head loss testing was not reduced by the quantity of calcium silicate consumed in precipitant generation.
- 4) Large (>6") and intact piece (>6") quantities of TempMat and Thermal Wrap were combined as a single debris category in which the debris was prepared as 6" by 6" squares.
- 5) RMI small (<4") and large (>4") piece quantities were combined as a single debris category in which all RMI was modeled as small pieces (<4").
- 6) The quantity of degraded phenolic coatings (chips) used in strainer head loss testing was increased by approximately 4 times the scaled quantity that was determined to transport to the sump. Similarly, the quantity of phenolic coatings (fines) was increased by approximately 1 ½ times.
- 7) The quantity of degraded IOZ coatings (fines) used in strainer head loss testing was increased by approximately 4 times the scaled quantity that was determined to transport to the sump.
- 8) The quantity of Thermal Wrap fines used in strainer head loss testing was increased by approximately 7% above the scaled quantity that was determined to transport to the sump.
- 9) The quantity of Temp Mat fines used in strainer head loss testing was increased by approximately 7% above the scaled quantity that was determined to transport to the sump.
- 10) All debris that settled on the floor of the test flume was mechanically agitated to re-suspend the debris in order to maximize the debris presented to the face of the test strainer, and therefore maximize the strainer head loss.
- 11) RHR pump flow rates used in testing (2300 gpm) bound all pump flow rates. Calculated flows for the case that yields the minimum NPSH for the ECCS pumps (approximately 1850 gpm) are 24% less than the flow utilized during testing. This represents additional margin for strainer head loss testing, and vortexing and flashing evaluations.

ATTACHMENT 1
REGNPP GL 2004-02 THIRD SUPPLEMENTAL RAI RESPONSE

RAI-14: *Please provide the methodology used for calculation of clean strainer head loss.*

RAI-14 Response: The clean strainer head loss was determined through testing and calculation. Head loss of the clean strainer filtering screen was determined in the test loop preceding the debris load testing. The strainer surface area, flow rate, scaling factor, etc. were the same as those for the debris load testing. No measurable head loss of the clean strainer surface area was recorded. Therefore, no temperature / density scaling was required. The strainer module connecting channel and duct head loss was determined by calculation [14.1]. The strainer train of the longest length was selected for the calculation, since its head loss would bound that from the other trains with shorter or no connecting channels and ducts. The strainer surface area was determined for each of the strainer trains in order to determine the proportionate flow through the train for which head loss was determined. With the dimensions of the various channels and ducts known, the flow velocities and hydraulic diameters were determined. The hydraulic resistances of the curved connecting ducts were determined using Reference 14.2. The total clean strainer head loss was calculated as the sum of the individual head losses through the clean strainer, connecting channels, center flow plenum, connecting ducts, and sump entrance. The total clean strainer head loss is 3.91 mbar or 0.131 ft WC at the containment sump minimum temperature of 195 °F and 2300 gpm.

RAI-14 References:

- 14.1 3SA-096.077, "Head Loss Calculation Including Chemical Effects," Rev. 1.
- 14.2 E. Fried, I. E. Idelchik, Flow Resistance, A Design Guide for Engineers, Hemisphere Publishing Corporation, 1989.

RAI-15: *Please provide the following information as discussed in Enclosure 3 to a letter from the NRC to NEI dated March 28, 2008 (ADAMS Accession No. ML080380214). Specifically, please provide the information requested by item 16.d on page 20 (termination criteria) and items 17.d.i and 17.d.ii on page 21 (test pressure drop curve and an explanation of any extrapolation of data).*

RAI-15 Response: As stated in the strainer head loss test specification [15.1], the test termination criteria is less than a 1% change in strainer head loss over two consecutive 30 minute periods. This criterion was met. However, as an added measure to ensure that the maximum possible strainer head loss had been achieved, the test was allowed to continue to run until sufficient test tank turnovers, equivalent to the containment recirculation pool volume turnovers for a 30 day mission time, had been achieved. The first strainer head loss test, Test 1, was run for approximately 6 ½ days (see Figure 15.1, below, from Ref. 15.2). For the test tank fluid volume and pump flow rate, the test tank fluid turnover rate was 10.8 minutes per turnover [15.1]. Therefore, the total number of test tank fluid volume turnovers during Test 1 was approximately 867. The Ginna containment recirculation pool volume at the minimum recirculation pool level is 176,833 gal. [15.3]. The bounding maximum recirculation pool flow rate is 2300 gpm [15.3]. Therefore, the maximum number of containment recirculation pool turnovers during a 30 day mission time is approximately 562. Hence, the number of test tank fluid volume turnovers exceeded the expected containment recirculation pool turnovers by 54%.

A verification of Test 1 was conducted to ensure repeatability of test results. Test 1 Rep was conducted immediately following the conclusion of Test 1. All test conditions with respect to debris loading, flow rates, strainer surface area, etc. were the same as Test 1. Test 1 Rep was run for approximately 5 days

ATTACHMENT 1
REGNPP GL 2004-02 THIRD SUPPLEMENTAL RAI RESPONSE

(see Figure 15.2, below, from Ref. 15.2). This corresponds to approximately 667 test tank turnovers, again, exceeding the number of containment recirculation pool turnovers.

During strainer head loss testing, head loss values were taken every 30 seconds. As can be seen in the Test 1 plot of strainer head loss values (Figure 15.1), the head loss was stable for nearly 2 days prior to the termination of the test. The head loss during this time had minimal variation (± 2 mbar) and the overall trend was steady, to trending down. As a result, it was determined that the maximum strainer head loss had been achieved and no extrapolation of head loss data was performed. The maximum head loss achieved during the test, adjusted for test tank fluid temperature variations and normalized to 20 °C, was 95.2 mbar [15.4]. Since this head loss was the maximum achieved and since subsequent head loss measurements were lower and stable, to trending down, 95.2 mbar at 20 °C was taken as the maximum sump strainer head loss due to debris on the strainer. This value is equivalent to 29.7 mbar (0.99 ft WC) corrected to the minimum containment recirculation pool design temperature of 195 °F.

As can be seen in the Test 1 Rep plot of strainer head loss values (Figure 15.2), the head loss was stable for nearly 1 1/2 days prior to the termination of the test. The head loss during this time had minimal variation (± 2 mbar) and the overall trend was steady. As a result, it was determined that the head loss values achieved in Test 1 were valid and bounded the maximum strainer head loss that would be seen in the Ginna containment. The maximum head loss achieved during the Test 1 Rep, adjusted for test tank fluid temperature variations and normalized to 20 °C, was 87.7 mbar [15.4].

Figure 15.1: Ginna Strainer Head Loss Test 1 Results

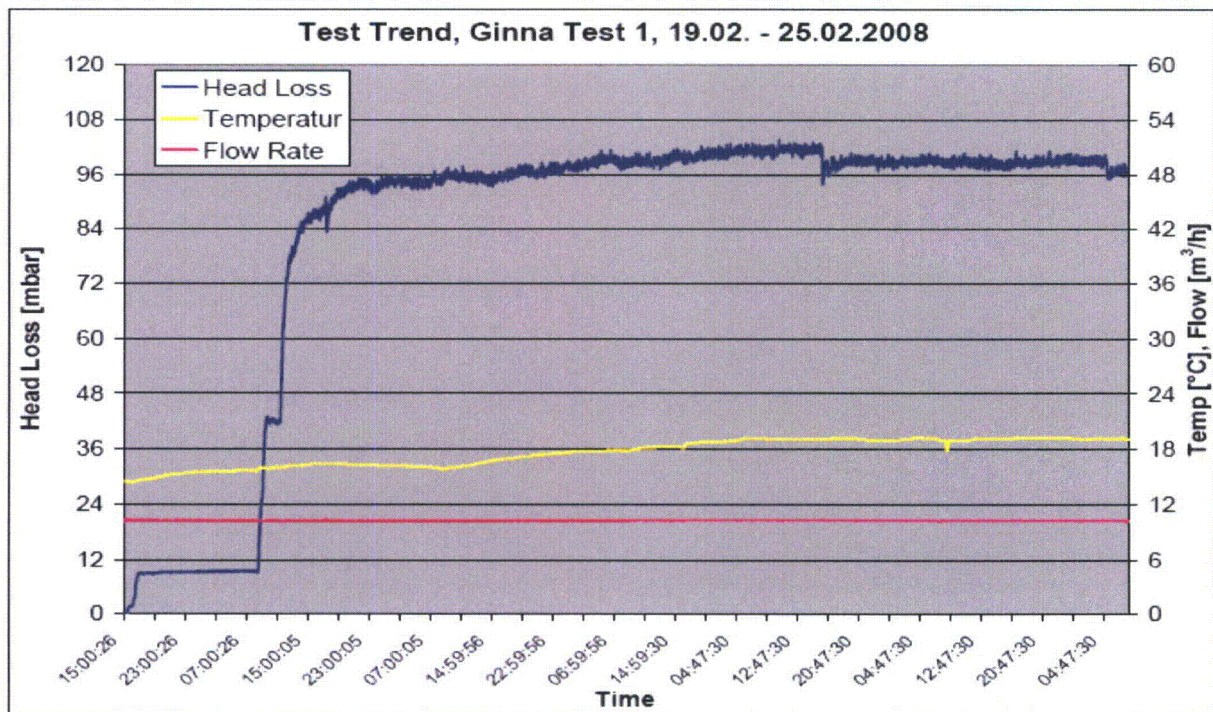
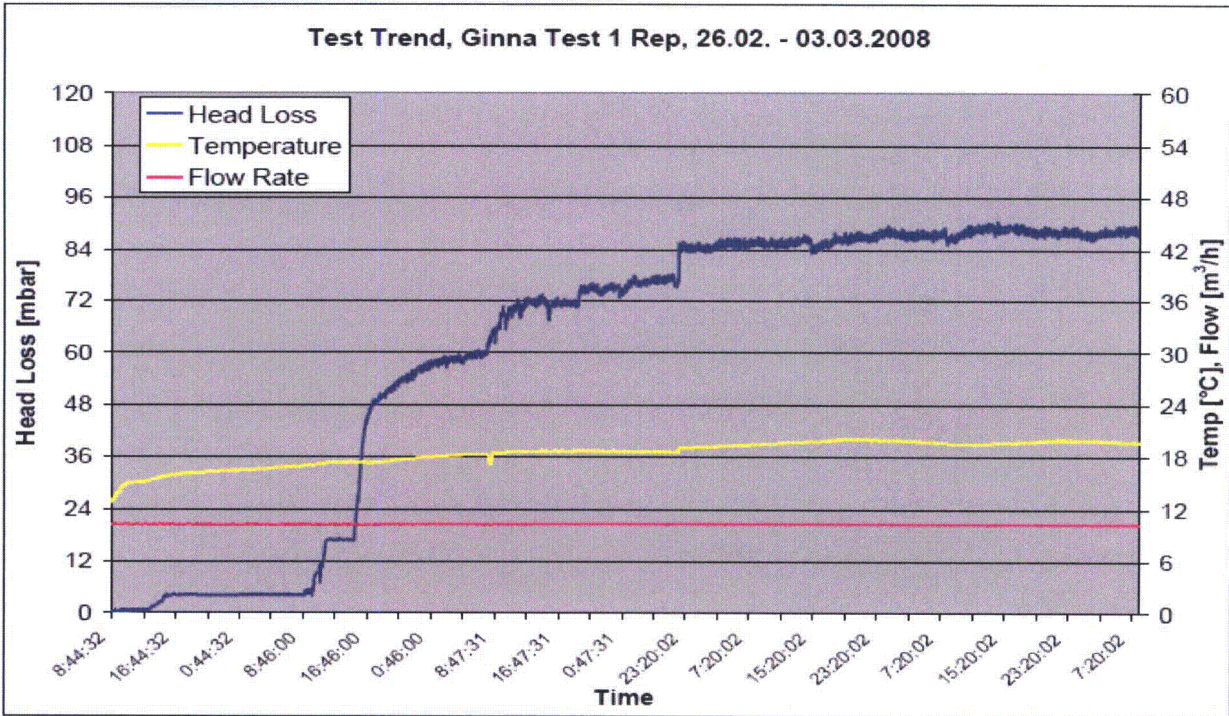


Figure 15.2: Ginna Strainer Head Loss Test 1 Rep Results



RAI-15 References:

- 15.1 Q.003.84809, “Double Sided Chemical Effect Head Loss Test Specification,” Rev. 0.
- 15.2 680/41439, “Chemical Effect Test,” Rev. 1.
- 15.3 DA-ME-2005-085, “NPSH for ECCS Pumps During Injection and Sump Recirculation,” Rev. 2.
- 15.4 3SA-096.077, “Head Loss Calculation Including Chemical Effects,” Rev. 1.

RAI-16: *Please provide a basis for the assertion that strainer submergence is greater than debris bed head loss. The strainer head loss, as determined by testing, appears to exceed the strainer submergence of 7 inches. Please provide a flashing evaluation considering the calculated head loss value for debris and the clean strainer.*

RAI-16 Response: The worst case full debris load sump strainer head loss was determined through testing to be 0.99 ft WC [16.1]. This represents the head loss across the debris bed and the clean strainer. The minimum water level in containment upon completion of the switchover to recirculation is 3.39 ft [16.2]. The top of the sump strainer pockets is 33.63 inches (2.80 ft) above the containment basement floor [16.3]. Therefore, the minimum strainer submergence is 0.59 ft (3.39 ft – 2.80 ft) or 7.08 inches. At the containment minimum design pressure of -2 psig [16.6] and the maximum normal containment temperature of 120 F [16.7], the partial pressure of dry air in containment at the start of the event is 11.0 psia or 25.4 ft.

ATTACHMENT 1
REGNPP GL 2004-02 THIRD SUPPLEMENTAL RAI RESPONSE

The minimum pressure behind the strainer is 25 ft (25.4 ft + 0.59 ft - 0.99 ft) above saturation pressure. The water will be maintained above the saturation pressure behind the strainer debris bed, and flashing will not occur.

Additionally, although Ginna does not credit containment over-pressure, evaluations which do credit containment over-pressure help to provide a sense of the likely margin that will exist. Evaluations show that the pressure downstream of the sump strainer is always much higher than the vapor pressure at the containment recirculation pool temperature. The following table contains the values of the pressure difference between containment pressure and the containment recirculation pool vapor pressure starting at 45 minutes (2700 seconds) into the event.

Time (sec.)	Containment Pressure (psia) [16.4]	Containment Sump Temperature (F) [16.5]	Saturation Pressure (psia)	Pressure Difference (psi)
2700	53	247	28	25
6000	45	234	22	23
10000	37	214	15	22
30000	26	168	5.6	20.4
100000	22	141	2.9	19.1
300000	21	128	2.0	19
1000000	19	115	1.4	17.6
3000000	18	108	1.2	16.8

As shown above, the minimum pressure difference between containment pressure and the containment recirculation pool vapor pressure is 16.8 psi. This equates to 39 ft WC, significantly greater than the debris bed head loss. Therefore, no flashing will occur inside the strainer.

RAI-16 References:

- 16.1 3SA-096.077, "Head Loss Calculation Including Chemical Effects," Rev. 1.
- 16.2 DA-ME-2005-085, "NPSH for ECCS Pumps During Injection and Sump Recirculation," Rev. 2.
- 16.3 103.134.547.500, "Ginna Layout," Rev. A001.
- 16.4 Ginna UFSAR Figure 6.2-4, Rev. 21.
- 16.5 Ginna UFSAR Figure 6.2-6, Rev. 21.
- 16.6 Ginna Technical Specification 3.6.4.
- 16.7 Ginna Technical Specification 3.6.5.

ATTACHMENT 1
REGNPP GL 2004-02 THIRD SUPPLEMENTAL RAI RESPONSE

RAI-17: *Please clarify the basis for determining the limiting pump flow rates used in the net positive suction head (NPSH) calculation. How were these pump and sump flow rates determined? Are the assumed pump flows 1) “runout” (pump tested maximum) flow values, 2) preset maximum flow values, or 3) manually controlled flow rates? If runout flow values are not used, how is the flow controlled so as not to exceed the value assumed in the NPSH calculation?*

RAI-17 Response: The flow rates in the NPSH calculation [17.1] were determined from a 10 CFR 50 Appendix B approved ProtoFlo software model. The software model developed precisely reflects the Emergency Core Cooling (ECCS), Containment Spray (CSS), and Component Cooling Water (CCW) Systems at Ginna by inclusion of every line, valve, fitting, and elevation change to an as-built configuration. The RHR pump flow to the reactor is controlled in the software model via RHR pump discharge control valves, HCV-624 and HCV-625. The position of these valves is prevented from being opened beyond 30° open via a hard stop [17.2]. Testing was performed on these valves in order to develop accurate performance curves through the full range of valve position [17.3 and 17.4]. Based on the results of the testing the most conservative resistance has been assigned to the valves in the software model. During testing a range of K values were determined for each valve position, and the minimum K value at the open position of 30° was used in the model to allow for the maximum amount of flow. Several cases were run using this flow resistance for valves HCV-624 and HCV-625 to determine the limiting flow rates.

The case that produced the maximum flow rate using the ProtoFlo software resulted in 2287 gpm with an NPSH margin of 5.12 feet. This case uses the RHR pumps in series with the high head SI pumps. Assumptions consisted of a depressurized RCS and containment. The SI pumps only operate at this low of a RCS pressure for long term post LOCA boron precipitation. This case is based on the most conservative maximum sump water temperature at this point following a LOCA of 182.35°F. The results are from Case 22 of [17.1].

The most limiting case for low head recirculation, i.e. RHR, results in a NPSH margin of 2.99 feet. This case assumed that one of the two suction valves from the containment sump to the RHR pumps fails to open. The single operating RHR pump was determined to have a flow rate of 1835 gpm. The high head SI pumps are not operating in this case, because this case was run to postulate the most limiting conditions following a large break LOCA. After switchover to sump recirculation following a large break, the high head SI pumps would not be restarted for design bases scenarios. The containment and RCS were both assumed to be depressurized to maximize RHR flow. Containment sump water temperature was assumed equal to the saturation temperature for 14.7 psia, or 212°F. Results are from Case 8 of [17.1].

The most limiting scenario for high head recirculation with the SI pumps in series with the RHR pumps, results in a NPSH margin of 2.64 feet. This case corresponds to the limiting SBLOCA. The RHR pump flow for this case is 1850 gpm. The RCS pressure was assumed to be 61.33 psia. The higher RCS pressure limits both the low and high head pump flow rates. The RCS pressure was determined to be the minimum pressure allowable for the high head SI pumps to be restarted following the switch over to the containment sump. The containment was assumed to be depressurized to 14.7 psia, and the sump water temperature was assumed equal to the saturation temperature of 14.7 psia, or 212°F. Results are from Case 20 of [17.1].

ATTACHMENT 1
REGNPP GL 2004-02 THIRD SUPPLEMENTAL RAI RESPONSE

Other NPSH calculation conservatisms to maximize flow and NPSH include:

- The RCS was assumed to be fully depressurized for LBLOCA cases resulting in the highest possible RHR flow rate.
- For SBLOCA cases, when the RHR system is incapable of providing adequate flow to the RCS, the minimum pressure allowable for the restarting of high head SI pumps following sump switchover is assumed. These assumptions allow for the minimum back pressure during both the LBLOCA and SBLOCA scenarios resulting in maximum flow.
- The original vendor non-degraded pump head curve was used. This is conservative, because degraded pump head results in a drop in flow rate.
- By maximizing the RHR pump flow rate, the NPSH required is maximized. The maximum flow rate from the ProtoFlo analysis is less than the 2300 gpm used in testing, which ensures that the flow related losses due to a clogged strainer is conservative.

RAI-17 References:

- 17.1 DA-ME-2005-085, "NPSH for ECCS Pumps During Injection and Sump Recirculation," Rev. 2.
- 17.2 Setpoint Change Request (SPCR) 2006-0001 and Setpoint SP-3816.
- 17.3 2420C, Specification, "Inspection And Flow Loop Test Procedure For 8 Inch Butterfly Valve," Rev. 1.
- 17.4 2442C, Analysis, "Results From Discrete Angle Flow Coefficient Testing And Cavitation Analysis Of 8 Inch Butterfly Valve," Rev. 0.

RAI-18: *Please provide the methodology for determining pump suction and other flow-related head losses. Please provide the assumptions and bases for the application of this methodology.*

RAI-18 Response: Flow-related head losses in the NPSH calculation [18.1] for the recirculation phase of ECCS operation were determined using the Appendix B approved ProtoFlo software. The software uses the Darcy-Weisbach Equation for calculating flow losses. The ECCS, Containment Spray (CSS), and Component Cooling Water (CCW) Systems are modeled in the ProtoFlo software. The entire system is modeled for piping lengths, fittings, valves, and elevations to an as-built configuration. This ensures the accuracy of the model, and therefore assumptions are not used in the determination of flow-related head losses.

RAI-18 References:

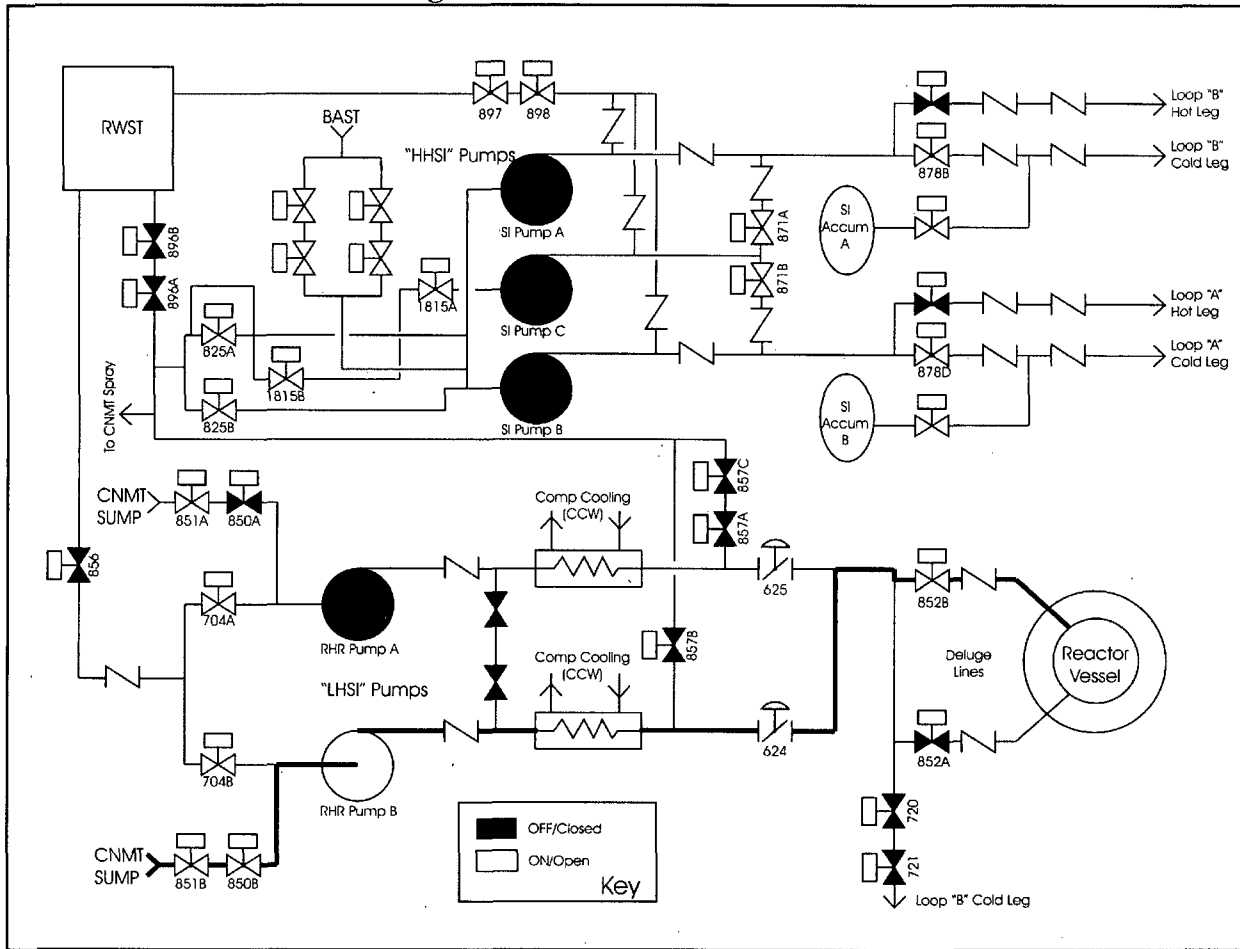
- 18.1 DA-ME-2005-085, "NPSH for ECCS Pumps During Injection and Sump Recirculation," Rev. 2.

ATTACHMENT 1
 REGNPP GL 2004-02 THIRD SUPPLEMENTAL RAI RESPONSE

RAI-19: Please provide information that illustrates why there is a difference in the NPSH margin results for the case where “B” RHR pump is operating with a suction line failure (“Suction Line Fails to Open” case) and the case where the “B” RHR pump is operating with a failure of Train A (“Train A Failure” case).

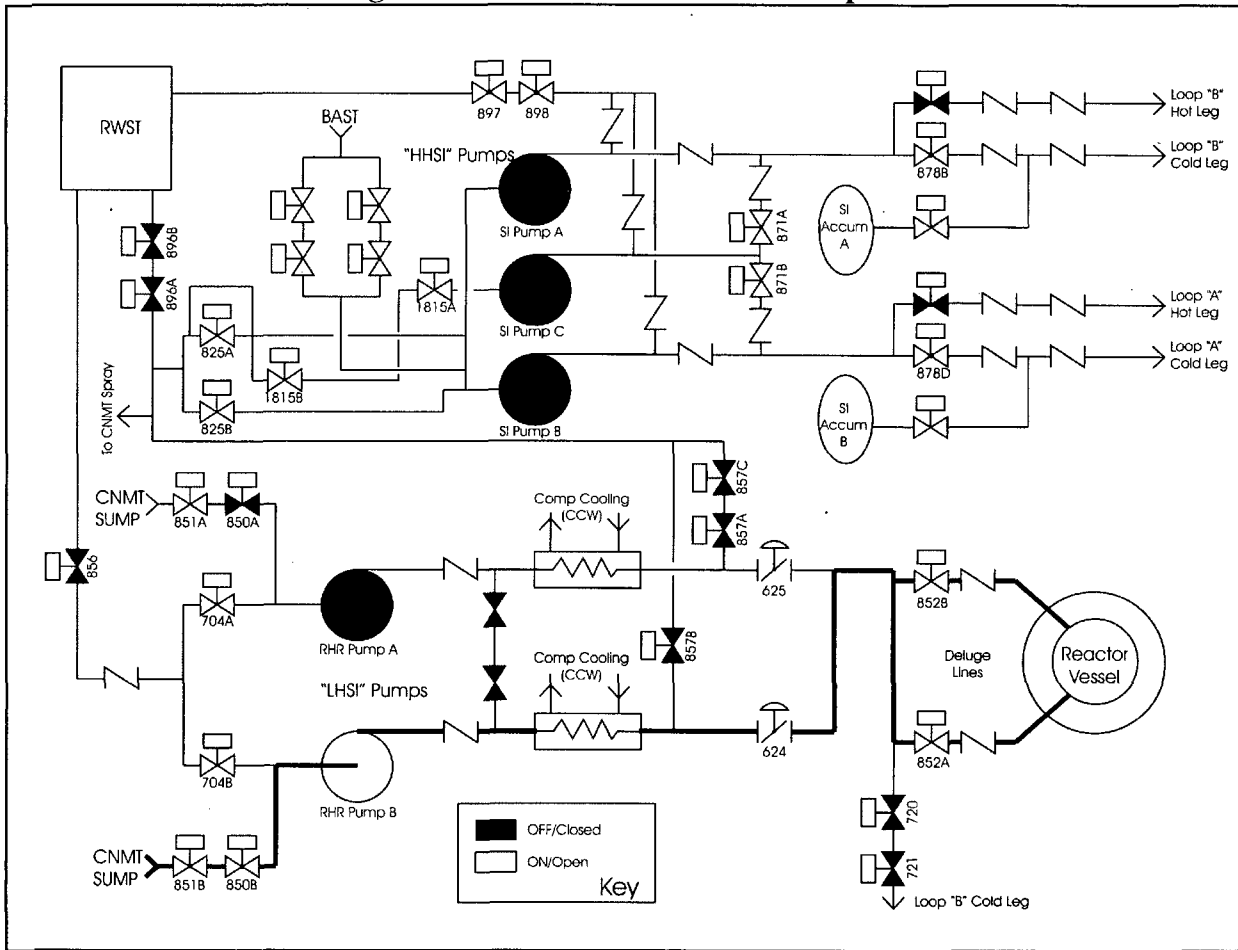
RAI-19 Response: The difference in the NPSH margin between the “Suction Line Failure” case and the “Train “A” Failure” case lies in the difference in system configuration. The “Train “A” Failure” case has a system configuration that provides more flow resistance to the operation of the “B” RHR pump than the “Suction Line Failure” case. Figure 19.1 shows the configuration for the “Train “A” Failure” case. The “Train “A” Failure” case results in the failure of the RHR “A” sump valve (850A) to open, the “A” RHR pump to start, and the “A” deluge valve to open. For the “Suction Line Failure” case, only the RHR “A” sump valve (850A) will fail to open.

Figure 19.1: “Train “A” Failure”



From Figure 19.1, it can be seen that the “B” RHR pump provides flow through only one of the deluge lines when Train “A” fails. However, for the case in which one suction line valve (from the sump) fails to open, the operating RHR pump is providing flow through both deluge lines (see Figure 19.2 below).

Figure 19.2: "Suction Line Fails to Open"



Therefore, the "B" RHR pump flow rate will be less in the "Train "A" Failure" case than the "Suction Line Failure" case. From the NPSH calculation [19.1], the flow rate for the "B" RHR pump for the "Suction Line Failure" case is 1671 gpm, whereas, the flow rate for the "B" RHR pump for the "Train "A" Failure" case is 1343 gpm. Since the flow rate is less, the NPSHR will be less resulting in more NPSH margin in the "Train "A" Failure" case than in the "Suction Line Failure" case.

RAI-19 References:

- 19.1 DA-ME-2005-085, "NPSH for ECCS Pumps During Injection and Sump Recirculation," Rev. 2

ATTACHMENT 1
REGNPP GL 2004-02 THIRD SUPPLEMENTAL RAI RESPONSE

RAI-20: *Please provide the NPSH margin results for the hot-leg injection case wherein two safety injection (SI) pumps are operated in series with a single RHR pump for a sump flow rate of 2200 gpm. This configuration is described at the top of page 50 in the supplemental response.*

RAI-20 Response: From the Ginna NPSH calculation [20.1], the NPSH margin for the case with a single residual heat removal (RHR) pump providing flow to a single deluge line and two of the high head safety injection (HHSI) pumps is 8.79 feet (Case 22). The NPSH margin with two deluge lines open with two HHSI pumps in series with an RHR pump is 5.12 feet (Case 23). The additional margin between these two cases and the most limiting case, with respect to NPSH, can be attributed to Sump "B" temperature differences. At the time these cases are postulated (> 4 hours), the Sump "B" temperature is significantly lower, thereby providing approximately 7 psid benefit to NPSH available from vapor pressure differences.

RAI-20 References:

20.1 DA-ME-2005-085, "NPSH for ECCS Pumps During Injection and Sump Recirculation," Rev. 2.

RAI-21: *Please provide the methodology for determining $NPSH_R$ (NPSH required) for the ECCS and CSS pumps.*

RAI-21 Response: A fourth-order polynomial curve was overlaid on the as-tested manufacturer's pump curve [21.1] for NPSHR. Two sets of data for NPSHR were compared; one for cold water and one for water at a temperature of 212°F. Since the data for cold water required more NPSH, this data was used for creating the polynomial curve. The 10 CFR 50 Appendix B approved ProtoFlo software package was then used to determine the flow rate for several limiting cases. The flows in the model are controlled via flow control valves (HCV-624 and HCV-625) that were set to their maximum open position of 30° to allow for the highest flow rate for the RHR pumps. NPSHR was then calculated using the flow rates generated by the ProtoFlo software in the fourth order polynomial equation for NPSHR.

Similarly, the NPSHR for the SI and CS pumps was taken from the manufacturer's test curves [21.2] and [21.3]. Similar criteria, with respect to water temperature, apply to the SI and CS pumps as listed above for the RHR pumps. NPSHR values were determined for the flows rates determined by the model for each case by linearly interpolating between test points from the curves. This is conservative since the NPSHR values will actually be lower than that determined, based on the parabolic nature of these curves.

RAI-21 References:

- 21.1 Pacific Pump Curves 33250 (A/B) Dated 3-4-68.
- 21.2 Ingersoll-Rand Correspondence Dated 6-16-97 (I-R-LTR-6/16/97).
- 21.3 Ingersoll-Rand Correspondence Dated 1-14-82.

ATTACHMENT 1
REGNPP GL 2004-02 THIRD SUPPLEMENTAL RAI RESPONSE

RAI-22: *Please provide the basis for concluding that the refueling cavity drain(s) would not become blocked with debris. Please identify the potential types and characteristics of debris that could reach these drains. In particular, could large pieces of debris be blown into the upper containment by pipe breaks occurring in the lower containment, and subsequently drop into the cavity? In the case that partial/total blockage of the drains might occur, do water hold-up calculations used in the computation of NPSH margin account for the lost (held-up) water resulting from debris blockage?*

RAI-22 Response: Table 22.1 shows the blowdown fraction of the various debris types to upper containment. The number in parenthesis is the representative quantity of debris from a break in Compartment B from the Debris Generation Calculation [22.1]. This was the bounding case as it had the greatest quantity of Cal-Sil/asbestos and fiberglass.

Table 22.1 – Blowdown Fractions of Debris to Upper Containment (Case 2)

Debris Type	Fines	Small Pieces	Unjacketed Large Pieces	Intact Blankets
Stainless Steel RMI	NA	0%	0%	NA
Cal-Sil with Asbestos	89% (13.1 ft ³)	0%	NA	NA
Temp-Mat	89% (6.9 ft ³)	76% (23.3 ft ³)	25% (3.3 ft ³)	25% (3.5 ft ³)
Thermal-Wrap	89% (80.7 ft ³)	76% (242.1 ft ³)	25% (27.0 ft ³)	25% (28.9 ft ³)
Phenolic Paint (inside ZOI)	89% (773 lbs)	NA	NA	NA
IOZ Paint (inside ZOI)	89% (109 lbs)	NA	NA	NA
Phenolic Paint (outside ZOI)	NA	NA	NA	NA
IOZ (outside ZOI)	NA	NA	NA	NA
Dirt/Dust	NA	NA	NA	NA
Latent Fiber	NA	NA	NA	NA

The physical properties of these debris types from the Debris Generation Calculation are shown below in Table 22.2 [22.1].

Table 22.2 – Physical Properties of Debris

Debris Type/Size	Material Bulk Density	Particulate/Individual Fiber Density	Characteristic Size
Cal-Sil/Asbestos	15 lb/ft ³	144 lb/ft ³	5 μm
Temp-Mat	9 lb/ft ³	162 lb/ft ³	9 μm
Thermal-Wrap	2.4 lb/ft ³	159 lb/ft ³	5.5 μm
Phenolic Paint	84 lb/ft ³	94 lb/ft ³	10 μm
IOZ Paint	223 lb/ft ³	457 lb/ft ³	10 μm

ATTACHMENT 1
 REGNPP GL 2004-02 THIRD SUPPLEMENTAL RAI RESPONSE

Appendix 1 of the debris transport calculation determined that the spray flow split to the refueling canal would be 14% [22.2]. Table 22.3 tabulates the quantity of debris that would transport to the refueling canal.

Table 22.3 – Quantity of Debris in the Refueling Canal

Debris Type	Fines	Small Pieces	Unjacketed Large Pieces	Intact Blankets
Cal-Sil with Asbestos	1.8 ft ³	NA	NA	NA
Temp-Mat	1.0 ft ³	3.3 ft ³	0.5 ft ³	0.5 ft ³
Thermal-Wrap	11.3 ft ³	33.9 ft ³	3.8 ft ³	4.0 ft ³
Phenolic Paint (inside ZOI)	108 lbs (1.3 ft ³)	NA	NA	NA
IOZ Paint (inside ZOI)	15 lbs (0.1 ft ³)	NA	NA	NA

Combining the above, there would be 3.2 ft³ of particulate, 12.3 ft³ of individual fibers, 37.2 ft³ of small pieces of fiber (< 6”), 4.3 ft³ of unjacketed large pieces (> 6”), and 4.5 ft³ of intact blankets (> 6”) in the refueling canal.

At Ginna, the refueling canal drain becoming blocked is a non-issue. Once water or debris has entered the refueling canal, there are three flow paths that can be taken.

1. The water/debris can drain down the sides of the reactor vessel into an inactive sump.
2. The water/debris can make its way down to the refueling canal to the drain, which drains to an inactive cavity.
3. The water/debris can remain in the reactor vessel, either by settling in an area, or by the drain becoming clogged and being forced to remain in the canal.

All debris and water introduced into the refueling canal, regardless of subsequent flow path, ends up residing in an inactive cavity. The amount of water that would be held in the refueling cavity would be relatively small as the containment sprays are the only source of water to this area and they are terminated upon switchover to recirculation (57 minutes after Safety Injection Actuation Sequence [22.3]). The Ginna water level calculation already assumes that all water reaching the refueling canal is held up [22.3].

RAI-22 References:

- 22.1 Calculation ALION-CAL-CONS-3237-02, “Ginna Reactor Building GSI-191 Debris Generation Calculation”, Revision 1.
- 22.2 Calculation ALION-CAL-GINNA-4376-03, “Ginna GSI-191 Debris Transport Calculation”, Revision 2.
- 22.3 Calculation DA-ME-2005-085, “NPSH for ECCS Pumps During Injection and Sump Recirculation”, Revision 2.

RAI-23: *Please provide the basis for concluding that the ratio of refueling cavity area to basement floor area is conservative for determining how much water will drain into the cavity. For example, is it*

ATTACHMENT 1
REGNPP GL 2004-02 THIRD SUPPLEMENTAL RAI RESPONSE

possible that spray drainage landing on other surfaces at or above the elevation of the refueling cavity, but not directly over the refueling cavity, may drain into the refueling cavity?

RAI-23 Response: The area ratio used for determining the containment spray holdup is with respect to the containment cross-sectional area, not the containment basement floor area. The ratio of the refueling cavity area to the containment cross-sectional area is the proportion of containment spray that is assumed to enter and to be held up in the refueling cavity. Using the containment cross-sectional area in this ratio is conservative, since containment spray flow that impacts the containment wall will flow to lower levels, and the length of containment wall that communicates with the refueling cavity is disproportionately smaller than the ratio of the refueling cavity to the containment cross-sectional area. Therefore, by assuming that the coverage only includes the containment cross-sectional area, the calculated amount of water that will land in the refueling cavity is conservatively increased. None of the water landing outside of the cavity will transport to the cavity, because there is a curb surrounding the refueling cavity preventing flow. Calculations show that the height of the water on the containment operating floor does not exceed the height of the curb. This water flows through grating and stairways to lower elevations. There are no other mechanisms for spray flow to enter the refueling cavity. Therefore, it is conservative to assume that the water landing in the cavity (by ratio to the containment cross-sectional area) is the total volume of water held up by the cavity.

RAI-24: *What is the volume of water assumed to be held up in the refueling cavity whether blocked, partially blocked or open?*

RAI-24 Response: The volume of containment spray water entering the refueling cavity is 17,932 gallons, of which 4,149 gallons flows to and is held up in the reactor cavity. Therefore, the volume of containment spray that is held up in the refueling cavity is 13,783 gal. [24.1]. This entire volume is assumed to be held-up and assumed not to drain to the active recirculation pool.

RAI-24 References:

24.1 DA-ME-2005-085, "NPSH for ECCS Pumps During Injection and Sump Recirculation," Rev. 2.

ATTACHMENT 1
 REGNPP GL 2004-02 THIRD SUPPLEMENTAL RAI RESPONSE

Seismic

The following response spectra from ME-338, Attachment G are used:

Reactor Containment Interior, Node #1206, 245 ft elevation

OBE horizontal / vertical Damping D = 2.0 %

SSE horizontal / vertical Damping D = 4.0 %

The Square Root of Sum of Squares combination method (SRSS) is used to combine modes. The same method is used to combine the results for the x, y, and z-direction.

Hydrodynamic Water Mass

mi: enclosed water mass

md: water displaced by the structures

mh: surrounding water mass

Water Mass Per Module, 16 Cartridges 400 mm Depth, 2x8 Pockets

Water mass		Module 2-8 cartridges	
		n = 16 (kg)	8 Pockets (lbm)
mi	x	900	1984.2
	y	1164	2566.2
	z	1164	2566.2
md	x	993	2189.2
	y	1257	2771.2
	z	1257	2771.2
mh	x	664	1463.9
	y	2296	5061.8
	z	2800	6172.9

Water Mass Per Module, 10 Cartridges 300 mm Depth, 2x8 Pockets

Water mass		Module 2-5 cartridges	
		n = 10 (kg)	8 Pockets (lbm)
mi	x	430	948.0
	y	603	1329.4
	z	603	1329.4
md	x	496	1093.5
	y	669	1474.9
	z	669	1474.9
mh	x	426	939.2
	y	1006	2217.9
	z	1046	2306.0

ATTACHMENT 1

REGNPP GL 2004-02 THIRD SUPPLEMENTAL RAI RESPONSE

Water Mass Per Module, 14 Cartridges 200 mm Depth, 2x7 Pockets

Water mass		Module 2-7 cartridges	
		n = 14 (kg)	7 Pockets (lbm)
mi	x	387	853.2
	y	593	1307.3
	z	593	1307.3
md	x	451	994.3
	y	657	1448.4
	z	657	1448.4
mh	x	297	654.8
	y	1561	3441.4
	z	1480	3262.8

Seismic Slushing

The hydrodynamic pressure due to slushing acting on the strainer modules is taken conservatively to $p_{SI} = p_w$ as the wall pressure for a completely constrained fluid mass due to seismic acceleration.

For OBE / SSE: $p_{SI} = \rho \cdot l \cdot a_{SSEh} = 1000 \text{ kg/m}^3 \cdot 1.5 \text{ m} \cdot 0.167 \cdot 9.81 \text{ m/s}^2 =$
 $p_{SI} = 2457 \text{ Pa} = 0.002457 \text{ MPa}$

Live Load (LL)

The top of the strainers and sump cover area is covered with checker plate to which the following live load (LL) applies:

LL strainer modules is 50 lb./ft² (0.00239 MPa)

LL sump cover area is 200 lb./ft² (0.00956 MPa)

Materials

SA-240 Type 304L Plate

T (°F)	T (°C)	Fy (ksi)	Fu (ksi)	S (ksi)	E (ksi)	α (1/°F)
70	21.1	25.00	70.00	16.70	28300	8.50E-06
80	26.7	25.00	70.00	16.70	28238	8.53E-06
100	37.8	25.00	70.00	16.70	28115	8.60E-06
120	48.9	24.08	69.22	16.70	27992	8.68E-06
150	65.6	22.70	68.05	16.70	27808	8.80E-06
195	90.6	21.53	66.30	16.70	27531	8.89E-06
200	93.3	21.40	66.10	16.70	27500	8.90E-06
245	118.3	20.32	63.90	16.70	27275	9.08E-06
250	121.1	20.20	63.65	16.70	27250	9.10E-06
275	135.0	19.70	62.43	16.70	27125	9.15E-06
286	141.1	19.48	61.89	16.70	27070	9.17E-06
300	148.9	19.20	61.20	16.70	27000	9.20E-06

Austenitic Bolts SA-193 B8M Class 2

ATTACHMENT 1
REGNPP GL 2004-02 THIRD SUPPLEMENTAL RAI RESPONSE

T (F°)	T (°C)	Size $t \leq \frac{3}{4}$ in		Size $\frac{3}{4}$ in $< t \leq 1$ in	
		Fy (ksi)	Fu (ksi)	Fy (ksi)	Fu (ksi)
70	21.1	95.00	110.00	80.00	100.00
80	26.7	95.00	110.00	80.00	100.00
100	37.8	95.00	110.00	80.00	100.00
120	48.9	91.84	110.00	77.82	100.00
150	65.6	87.10	110.00	74.55	100.00
195	90.6	79.99	110.00	69.65	100.00
200	93.3	79.20	110.00	69.10	100.00
245	118.3	75.56	109.28	67.48	99.37
250	121.1	75.15	109.20	67.30	99.30
275	135.0	73.13	108.80	66.40	98.95
286	141.1	72.23	108.62	66.00	98.80
300	148.9	71.10	108.40	65.50	98.60
400	204.4	65.50	105.90	59.60	96.30

Austenitic Bolts SA-193 B8 and B8M Class 1

T (F°)	T (°C)	B8 Class 1		B8M Class 1	
		Fy (ksi)	Fu (ksi)	Fy (ksi)	Fu (ksi)
70	21.1	30.00	75.00	30.00	75.00
80	26.7	30.00	75.00	30.00	75.00
100	37.8	30.00	75.00	30.00	75.00
120	48.9	29.00	74.20	29.18	75.00
150	65.6	27.50	73.00	27.95	75.00
195	90.6	25.25	71.20	26.11	75.00
200	93.3	25.00	71.00	25.90	75.00
245	118.3	23.83	68.84	24.78	74.06
250	121.1	23.70	68.60	24.65	73.95
275	135.0	23.05	67.40	24.03	73.43
286	141.1	22.76	66.87	23.75	73.19
300	148.9	22.40	66.20	23.40	72.90
400	204.4	20.70	64.00	21.40	71.90

RAI-26 References:

26.1 3SA-096.061, CCI Calculation, "Structural Analysis of Strainer and Support Structure," Rev. 1.

ATTACHMENT 1
REGNPP GL 2004-02 THIRD SUPPLEMENTAL RAI RESPONSE

RAI-27: Please list the actual load combinations evaluated in the structural analysis of the sump strainer assembly.

RAI-27 Response:

Load Combinations

Load Comb. Nr.	Temperature		Load Combinations	ASME Service Level
	(°F)	(°C)		
1	286	141.1	DL (pool dry)	A
2	80	26.7	DL + LL (pool dry)	A
3	286	141.1	DL + OBE (pool dry)	B
4	286	141.1	DL + SSE _I (pool dry)	C
5	275	135	DL + OBE (pool filled) + dP _{SI}	B
6	275	135	DL + SSE (pool filled) + dP _{SI}	C
7	68 (245)	20 (118.3)	DL + WD + OBE (pool filled) + dPD + dP _{SI}	B
8	68 (245)	20 (118.3)	DL + WD + SSE (pool filled) + dPD + dP _{SI}	C

Stress Limits at 20 °C are used for the Load combinations 7 and 8 in the analysis for the support structure.

Loads:

- DL Weight of strainers and supporting structures
- WD Weight of debris
- LL Live Load
- dPD Pressure difference across (0.022 MPa)
- dP_{SI} Sloshing Pressure (0.002457 Pa)
- OBE Operating basis earthquake
- SSE Safe shut down earthquake

RAI-28: Please indicate the edition/revision of the AISC and ASME Section III codes and the Regulatory Guides used in the structural analysis.

RAI-28 Response:

The following codes were used in the structural analysis of the Ginna sump strainers:

- ASME Boiler and Pressure Vessel Code, Section III, Division 1-Subsection NF Supports, Edition 2001, incl. Addenda 2003
- ASME Boiler and Pressure Vessel Code, Section II, Part D - Properties, Edition 2001, incl. Addenda 2003

ATTACHMENT 1

REGNPP GL 2004-02 THIRD SUPPLEMENTAL RAI RESPONSE

RAI-29: *Please indicate the components for which the equivalent static analysis was used and the components for which the dynamic analysis was used, and if any structural analysis software was used.*

RAI-29 Response: Equivalent static analysis was used for all components. The natural frequencies were determined for the strainer cartridges, the strainer module with 16 cartridges, and the sump cover.

Software used:

Program ANSYS, Rev. 11.0

Computer: PC, Windows ME resp. XP professional

Author: ANSYS Inc., Houston, TX, USA

Documentations: Vol. 4 User's Manuals,

ANSYS is verified according to the CCI N-III Quality Assurance Manual

RAI-30: *A calculation (Reference i) is listed in the list of references for Section 3.k in the supplemental response which may contain the structural qualification results and design margins for various components of the sump strainer structural assembly. However, none of the actual information was summarized or provided. Please provide a summary of this information. This summary should include interaction ratios and/or design margins for the structural components (structural members, plates, welds, concrete anchorages, and bolted connections, as applicable) of the strainer assembly that demonstrate existing margins between actual stress (force) and allowable stress (force) or other acceptance criteria for the different structural components of the strainer assembly for the load combinations considered.*

ATTACHMENT 1
REGNPP GL 2004-02 THIRD SUPPLEMENTAL RAI RESPONSE

RAI-30 Response:

Stress Summary

Shell and Plate

Description	Chapter	Stresses in Plates					Material	Utilization					
		σ_m	P_m	$\sigma_m + \sigma_n$	$P_m + P_n$	τ		Shear	mem	bend	shear		
Cartridges	Sidewalls Cartridge 200 mm	5.4.1	-	206.8 MPa 30000 psi	214.5 MPa 31111 psi	< 310.3 MPa 45000 psi	-	124.1 MPa 18000 psi	304	-	69.1%	-	
		Clips Cartridge 200 mm	5.4.2	5.6 MPa 812 psi	< 206.8 MPa 30000 psi	-	310.3 MPa 45000 psi	13.1 MPa 1900 psi	< 124.1 MPa 18000 psi	304	2.7%	-	10.6%
	Upper Cover Plate Cartridge 200 mm	5.4.3	-	206.8 MPa 30000 psi	-	310.3 MPa 45000 psi	35.4 MPa 5134 psi	< 124.1 MPa 18000 psi	304	-	-	28.5%	
	Cartridge Pockets Cartridge 200 mm	5.4.5	3.0 MPa 435 psi	< 206.8 MPa 30000 psi	205.7 MPa 29834 psi	< 310.3 MPa 45000 psi	-	124.1 MPa 18000 psi	304	1.5%	66.3%	-	
		Sidewalls Cartridge 300 mm	5.5.1	-	206.8 MPa 30000 psi	200.9 MPa 29138 psi	< 310.3 MPa 45000 psi	-	124.1 MPa 18000 psi	304	-	64.8%	-
	Clips Cartridge 300 mm		5.5.2	5.2 MPa 754 psi	< 206.8 MPa 30000 psi	-	310.3 MPa 45000 psi	5.5 MPa 798 psi	< 124.1 MPa 18000 psi	304	2.5%	-	4.4%
	Upper Cover Plate Cartridge 300 mm	5.5.3	-	206.8 MPa 30000 psi	-	310.3 MPa 45000 psi	48.4 MPa 7020 psi	< 124.1 MPa 18000 psi	304	-	-	39.0%	
		Cartridge Pockets Cartridge 300 mm	5.5.5	3.0 MPa 435 psi	< 206.8 MPa 30000 psi	207.0 MPa 30023 psi	< 310.3 MPa 45000 psi	-	124.1 MPa 18000 psi	304	1.5%	66.7%	-
	Sidewalls Cartridge 400 mm	5.6.1	-	206.8 MPa 30000 psi	193.2 MPa 28021 psi	< 310.3 MPa 45000 psi	-	124.1 MPa 18000 psi	304	-	62.3%	-	
		Clips Cartridge 400 mm	5.6.2	4.8 MPa 701 psi	< 206.8 MPa 30000 psi	-	310.3 MPa 45000 psi	4.6 MPa 667 psi	< 124.1 MPa 18000 psi	304	2.3%	-	3.7%
	Upper Cover Plate Cartridge 400 mm	5.6.3	-	206.8 MPa 30000 psi	-	310.3 MPa 45000 psi	61.0 MPa 8847 psi	< 124.1 MPa 18000 psi	304	-	-	49.2%	
	Cartridge Pockets Cartridge 400 mm	5.6.5	3.0 MPa 435 psi	< 206.8 MPa 30000 psi	206.9 MPa 30008 psi	< 310.3 MPa 45000 psi	-	124.1 MPa 18000 psi	304	1.5%	66.7%	-	
		Load Combination 2	Duct	6.6.1.1	41.0 MPa 5947 psi	< 115.1 MPa 16700 psi	128.0 MPa 18565 psi	< 172.7 MPa 25050 psi	-	69.1 MPa 10020 psi	304L	35.6%	74.1%
	Retaining Structure		6.6.1.2	67.0 MPa 9718 psi	< 115.1 MPa 16700 psi	72.0 MPa 10443 psi	< 172.7 MPa 25050 psi	-	69.1 MPa 10020 psi	304L	58.2%	41.7%	-
	Support Foot		6.6.1.3	49.0 MPa 7107 psi	< 115.1 MPa 16700 psi	73.0 MPa 10588 psi	< 172.7 MPa 25050 psi	-	69.1 MPa 10020 psi	304L	42.6%	42.3%	-
Checker Plate	6.6.1.4		62.0 MPa 8992 psi	< 115.1 MPa 16700 psi	96.0 MPa 13924 psi	< 172.7 MPa 25050 psi	-	69.1 MPa 10020 psi	304L	53.8%	55.6%	-	
Load Combination 8, Load Case 1	Duct	6.6.2.1	123.0 MPa 17840 psi	< 172.7 MPa 25050 psi	229.0 MPa 33214 psi	< 259.1 MPa 37575 psi	-	103.6 MPa 15030 psi	304L	71.2%	88.4%	-	
	Retaining Structure	6.6.2.2	154.0 MPa 22336 psi	< 172.7 MPa 25050 psi	173.0 MPa 25092 psi	< 259.1 MPa 37575 psi	-	103.6 MPa 15030 psi	304L	89.2%	66.8%	-	
	Support Foot	6.6.2.3	67.0 MPa 9718 psi	< 172.7 MPa 25050 psi	194.0 MPa 28137 psi	< 259.1 MPa 37575 psi	-	103.6 MPa 15030 psi	304L	38.8%	74.9%	-	
	Checker Plate	6.6.2.4	77.0 MPa 11168 psi	< 172.7 MPa 25050 psi	224.0 MPa 32488 psi	< 259.1 MPa 37575 psi	-	103.6 MPa 15030 psi	304L	44.6%	86.5%	-	
Load Combination 8, Load Case 2	Duct	6.6.3.1	90.0 MPa 13053 psi	< 172.7 MPa 25050 psi	202.0 MPa 29298 psi	< 259.1 MPa 37575 psi	-	103.6 MPa 15030 psi	304L	52.1%	78.0%	-	
	Retaining Structure	6.6.3.2	154.0 MPa 22336 psi	< 172.7 MPa 25050 psi	173.0 MPa 25092 psi	< 259.1 MPa 37575 psi	-	103.6 MPa 15030 psi	304L	89.2%	66.8%	-	
	Support Foot	6.6.3.3	59.0 MPa 8557 psi	< 172.7 MPa 25050 psi	185.0 MPa 26832 psi	< 259.1 MPa 37575 psi	-	103.6 MPa 15030 psi	304L	34.2%	71.4%	-	
	Checker Plate	6.6.3.4	60.0 MPa 8702 psi	< 172.7 MPa 25050 psi	149.0 MPa 21611 psi	< 259.1 MPa 37575 psi	-	103.6 MPa 15030 psi	304L	34.7%	57.5%	-	
Load Combination 8	Sealing Plates	6.6.4	-	206.8 MPa 30000 psi	290.1 MPa 42075 psi	< 310.3 MPa 45000 psi	-	124.1 MPa 18000 psi	304	-	93.5%	-	
	Support Foot A9	6.7.3.2	-	172.7 MPa 25050 psi	16.8 MPa 2437 psi	< 259.1 MPa 37575 psi	3.4 MPa 493 psi	< 103.6 MPa 15030 psi	304L	-	6.5%	3.3%	
Closing Modules	Load Combination 8	Retaining Plate A1	7.2.1	-	172.7 MPa 25050 psi	129.1 MPa 18725 psi	< 259.1 MPa 37575 psi	-	103.6 MPa 15030 psi	304L	-	49.8%	-
		Retaining Plate B3	7.3.1	-	172.7 MPa 25050 psi	127.9 MPa 18550 psi	< 259.1 MPa 37575 psi	-	103.6 MPa 15030 psi	304L	-	49.4%	-
		Retaining Plate B5	7.4.1	-	172.7 MPa 25050 psi	127.9 MPa 18550 psi	< 259.1 MPa 37575 psi	-	103.6 MPa 15030 psi	304L	-	49.4%	-
		Retaining Plate C1	7.5.1	-	172.7 MPa 25050 psi	129.1 MPa 18725 psi	< 259.1 MPa 37575 psi	-	103.6 MPa 15030 psi	304L	-	49.8%	-
Channel	Load Combination 8	Side Plates	8.1.1	1.3 MPa 189 psi	< 172.7 MPa 25050 psi	252.3 MPa 36593 psi	< 259.1 MPa 37575 psi	-	103.6 MPa 15030 psi	304L	0.8%	97.4%	-
		Lower- & Upperplates	8.1.2	-	172.7 MPa 25050 psi	49.5 MPa 7179 psi	< 259.1 MPa 37575 psi	-	103.6 MPa 15030 psi	304L	-	19.1%	-
		Support C4 - C5	8.2.2.1	134.0 MPa 19435 psi	< 172.7 MPa 25050 psi	202.0 MPa 29298 psi	< 259.1 MPa 37575 psi	-	103.6 MPa 15030 psi	304L	77.6%	78.0%	-
Sump Cover	Load Combination 8	Support A9 - C9	8.3.2.1	96.0 MPa 13924 psi	< 172.0 MPa 25050 psi	202.0 MPa 29298 psi	< 259.1 MPa 37575 psi	-	103.6 MPa 15030 psi	304L	55.8%	78.0%	-
		Girder Supports	9.2.4	34.5 MPa 5004 psi	< 172.7 MPa 25050 psi	57.5 MPa 8340 psi	< 259.1 MPa 37575 psi	-	103.6 MPa 15030 psi	304L	20.0%	22.2%	-
	Frame connector		9.3.4	23.0 MPa 3336 psi	< 172.7 MPa 25050 psi	57.5 MPa 8340 psi	< 259.1 MPa 37575 psi	-	103.6 MPa 15030 psi	304L	13.3%	22.2%	-
	Cover Plate 1	9.5.2.4	-	172.7 MPa 25050 psi	92.0 MPa 13343 psi	< 259.1 MPa 37575 psi	-	103.6 MPa 15030 psi	304L	-	35.5%	-	
		Cover Plate 2	9.5.3.4	-	172.7 MPa 25050 psi	68.3 MPa 9906 psi	< 259.1 MPa 37575 psi	-	103.6 MPa 15030 psi	304L	-	26.4%	-
			9.5.4.4	-	172.7 MPa 25050 psi	108.4 MPa 15722 psi	< 259.1 MPa 37575 psi	-	103.6 MPa 15030 psi	304L	-	41.8%	-
		Cover Plate 4	9.5.5.4	-	172.7 MPa 25050 psi	106.6 MPa 15461 psi	< 259.1 MPa 37575 psi	-	103.6 MPa 15030 psi	304L	-	41.1%	-
	9.5.6.4		-	172.7 MPa 25050 psi	69.0 MPa 10008 psi	< 259.1 MPa 37575 psi	-	103.6 MPa 15030 psi	304L	-	26.6%	-	
	Load Combination 2	Cover Plate 11	9.5.7.4.1	-	115.1 MPa 16700 psi	92.0 MPa 13343 psi	< 172.7 MPa 25050 psi	-	69.1 MPa 10020 psi	304L	-	53.3%	-
		Load Combination 8	Cover Plate 11	9.5.7.4.2	-	172.7 MPa 25050 psi	172.0 MPa 24946 psi	< 259.1 MPa 37575 psi	-	103.6 MPa 15030 psi	304L	-	66.4%

ATTACHMENT 1
REGNPP GL 2004-02 THIRD SUPPLEMENTAL RAI RESPONSE

Bolts

Description	Chapter	Bolt	Stresses in Bolts				Material	Utilization			
			f_t	F_{tb}	f_v	F_{vb}		tension	shear	combined	
Load Combination 2	Fixing Shear Pins	6.6.1.8.1	M8	-	144.8 MPa 21000 psi	0.7 MPa 102 psi	59.8 MPa 8680 psi	304L	-	1.2%	0.0%
	Pinhead Screws	6.6.1.8.3	M12	5.9 MPa 856 psi	< 227.5 MPa 33000 psi	5.9 MPa 856 psi	< 94.0 MPa 13640 psi	B8M Class 2	2.6%	6.3%	0.5%
	Cover plate connections	6.6.1.8.6	M12	2.3 MPa 334 psi	< 227.5 MPa 33000 psi	20.7 MPa 3002 psi	< 94.0 MPa 13640 psi	B8M Class 2	1.0%	22.0%	4.9%
	Mounting Brackets	6.6.1.8.7	M12	56.8 MPa 8238 psi	< 227.5 MPa 33000 psi	12.1 MPa 1755 psi	< 94.0 MPa 13640 psi	B8M Class 2	25.0%	12.9%	7.9%
Module Structure	Fixing Shear Pins	6.6.2.8.1	M12	-	181.0 MPa 26250 psi	46.3 MPa 6715 psi	< 74.8 MPa 10850 psi	304L	-	61.9%	38.3%
	Leveling Screws	6.6.2.8.2	M20	31.0 MPa 4496 psi	< 258.6 MPa 37500 psi	-	< 106.9 MPa 15500 psi	B8M Class 2	12.0%	-	1.4%
	Pinhead Screws	6.6.2.8.3	M12	13.0 MPa 1885 psi	< 284.4 MPa 41250 psi	54.5 MPa 7905 psi	< 117.6 MPa 17050 psi	B8M Class 2	4.6%	46.4%	21.7%
	Screws Duct	6.6.2.8.4	M20	6.1 MPa 885 psi	< 258.6 MPa 37500 psi	52.6 MPa 7629 psi	< 106.9 MPa 15500 psi	B8M Class 2	2.4%	49.2%	24.3%
	Shear connection Stud	6.6.2.8.5	M20	23.3 MPa 3379 psi	< 181.0 MPa 26250 psi	58.0 MPa 8412 psi	< 74.8 MPa 10850 psi	304L	12.9%	77.5%	61.8%
	Cover plate connections	6.6.2.8.6	M12	1.1 MPa 160 psi	< 284.4 MPa 41250 psi	9.3 MPa 1349 psi	< 117.6 MPa 17050 psi	B8M Class 2	0.4%	7.9%	0.6%
	Mounting Brackets	6.6.2.8.7	M12	56.6 MPa 8209 psi	< 284.4 MPa 41250 psi	16.6 MPa 2408 psi	< 117.6 MPa 17050 psi	B8M Class 2	19.9%	14.1%	6.0%
	Support Foot	6.6.2.8.9	M12	37.2 MPa 5395 psi	< 284.4 MPa 41250 psi	41.5 MPa 6019 psi	< 117.6 MPa 17050 psi	B8M Class 2	13.1%	35.3%	14.2%
	Leveling Screws	6.6.3.8.2	M20	22.4 MPa 3249 psi	< 258.6 MPa 37500 psi	-	< 106.9 MPa 15500 psi	B8M Class 2	8.7%	-	0.8%
	Pinhead Screws	6.6.3.8.3	M12	20.2 MPa 2930 psi	< 284.4 MPa 41250 psi	57.9 MPa 8398 psi	< 117.6 MPa 17050 psi	B8M Class 2	7.1%	49.3%	24.8%
	Screws Duct	6.6.3.8.4	M20	26.1 MPa 3785 psi	< 258.6 MPa 37500 psi	52.6 MPa 7629 psi	< 106.9 MPa 15500 psi	B8M Class 2	10.1%	49.2%	25.2%
	Load Combination 8, Load Case 2	Shear connection Stud	6.6.3.8.5	M20	40.8 MPa 5918 psi	< 181.0 MPa 26250 psi	52.0 MPa 7542 psi	< 74.8 MPa 10850 psi	304L	22.5%	69.5%
Load Combination 8, Load Case 2	Cover plate connections	6.6.3.8.6	M12	1.5 MPa 218 psi	< 284.4 MPa 41250 psi	8.1 MPa 1175 psi	< 117.6 MPa 17050 psi	B8M Class 2	0.5%	6.9%	0.5%
	Mounting Brackets	6.6.3.8.7	M12	57.7 MPa 8369 psi	< 284.4 MPa 41250 psi	14.1 MPa 2045 psi	< 117.6 MPa 17050 psi	B8M Class 2	20.3%	12.0%	5.6%
	Support Foot	6.6.3.8.9	M12	52.2 MPa 7571 psi	< 284.4 MPa 41250 psi	42.9 MPa 6222 psi	< 117.6 MPa 17050 psi	B8M Class 2	18.4%	36.5%	16.7%
	Support Foot A9	6.7.3.3	M12	95.6 MPa 13866 psi	< 284.4 MPa 41250 psi	64.6 MPa 9369 psi	< 117.6 MPa 17050 psi	B8M Class 2	33.6%	55.0%	41.5%
Closing Modules	Leveling Screws A1	7.2.3	M20	40.4 MPa 5860 psi	< 258.6 MPa 37500 psi	-	< 106.9 MPa 15500 psi	B8M Class 2	15.6%	-	2.4%
	Leveling Screws B3	7.3.3	M20	40.4 MPa 5860 psi	< 258.6 MPa 37500 psi	-	< 106.9 MPa 15500 psi	B8M Class 2	15.6%	-	2.4%
	Leveling Screws B5	7.4.3	M20	40.4 MPa 5860 psi	< 258.6 MPa 37500 psi	-	< 106.9 MPa 15500 psi	B8M Class 2	15.6%	-	2.4%
	Leveling Screws C1	7.5.3	M20	40.4 MPa 5860 psi	< 258.6 MPa 37500 psi	-	< 106.9 MPa 15500 psi	B8M Class 2	15.6%	-	2.4%
	Channel	General Parts	8.1.3	M8	59.0 MPa 8557 psi	< 284.4 MPa 41250 psi	50.7 MPa 7353 psi	< 117.6 MPa 17050 psi	B8M Class 2	20.7%	43.1%
Support Foot C4-C5		8.2.2.2	M20	45.3 MPa 6570 psi	< 258.6 MPa 37500 psi	78.8 MPa 11429 psi	< 106.9 MPa 15500 psi	B8M Class 2	17.5%	73.7%	57.4%
Shear connection Stud C4-C5		8.2.2.2	M20	42.0 MPa 6092 psi	< 181.0 MPa 26250 psi	42.0 MPa 6092 psi	< 74.8 MPa 10850 psi	304L	23.2%	56.1%	36.9%
Support Foot C4-C5		8.3.2.2	M20	39.2 MPa 5685 psi	< 258.6 MPa 37500 psi	85.6 MPa 12415 psi	< 106.9 MPa 15500 psi	B8M Class 2	15.2%	80.1%	66.5%
Shear connection Stud C4-C5		8.3.2.2	M20	36.3 MPa 5265 psi	< 181.0 MPa 26250 psi	51.0 MPa 7397 psi	< 74.8 MPa 10850 psi	304L	20.1%	68.2%	50.5%
Sump Cover	Main Beam Connection	9.1.7.3.1	M16	-	284.4 MPa 41250 psi	17.3 MPa 2509 psi	< 117.6 MPa 17050 psi	B8M Class 2	-	14.7%	2.2%
	Bottom Leveling Screws	9.1.7.3.2	M20	120.7 MPa 17506 psi	< 258.6 MPa 37500 psi	-	< 106.9 MPa 15500 psi	B8M Class 2	46.7%	-	21.8%
	Top Leveling Screws	9.1.7.3.2	M20	93.7 MPa 13590 psi	< 258.6 MPa 37500 psi	-	< 106.9 MPa 15500 psi	B8M Class 2	36.2%	-	13.1%
	Y-Junction	9.1.7.3.2	M16	-	284.4 MPa 41250 psi	81.1 MPa 11763 psi	< 117.6 MPa 17050 psi	B8M Class 2	-	69.0%	47.6%
	Base Support	9.1.7.3.2	M16	-	284.4 MPa 41250 psi	108.9 MPa 15795 psi	< 117.6 MPa 17050 psi	B8M Class 2	-	92.6%	85.8%
	Anchor Plate Girder Supports	9.2.5.1	M16	23.1 MPa 3350 psi	< 284.4 MPa 41250 psi	25.8 MPa 3742 psi	< 117.6 MPa 17050 psi	B8M Class 2	8.1%	21.9%	5.5%
	Girder	9.2.5.2	M16	-	284.4 MPa 41250 psi	24.1 MPa 3495 psi	< 117.6 MPa 17050 psi	B8M Class 2	-	20.5%	4.2%
	Girder Supports	9.3.5.1	M16	57.0 MPa 8267 psi	< 284.4 MPa 41250 psi	25.5 MPa 3698 psi	< 117.6 MPa 17050 psi	B8M Class 2	20.0%	21.7%	8.7%
	Beam	9.3.5.2	M16	-	284.4 MPa 41250 psi	56.1 MPa 8137 psi	< 117.6 MPa 17050 psi	B8M Class 2	-	47.7%	22.8%
	Frame Connector	9.4.1	M20	68.6 MPa 9950 psi	< 258.6 MPa 37500 psi	-	< 106.9 MPa 15500 psi	B8M Class 2	26.5%	-	7.0%
	Support Side Bumper	9.4.4	M16	-	284.4 MPa 41250 psi	50.0 MPa 7252 psi	< 117.6 MPa 17050 psi	B8M Class 2	-	42.5%	18.1%
	Cover Plate 1	9.5.8.2.1	M12	14.5 MPa 2103 psi	< 284.4 MPa 41250 psi	29.8 MPa 4322 psi	< 117.6 MPa 17050 psi	B8M Class 2	5.1%	25.3%	6.7%
	Cover Plate 4	9.5.8.2.2	M12	35.2 MPa 5105 psi	< 284.4 MPa 41250 psi	74.0 MPa 10733 psi	< 117.6 MPa 17050 psi	B8M Class 2	12.4%	62.9%	41.2%
	Cover Plate 9	9.5.8.2.3	M12	28.5 MPa 4134 psi	< 284.4 MPa 41250 psi	77.3 MPa 11211 psi	< 117.6 MPa 17050 psi	B8M Class 2	10.0%	65.8%	44.2%
	Cover Plate 11	9.5.8.2.4	M12	21.8 MPa 3162 psi	< 284.4 MPa 41250 psi	89.1 MPa 12923 psi	< 117.6 MPa 17050 psi	B8M Class 2	7.7%	75.8%	58.0%

ATTACHMENT 1
REGNPP GL 2004-02 THIRD SUPPLEMENTAL RAI RESPONSE

Buckling

Description	Chapter	Stresses in Plates		Material	Utilization
		f_a	F_a		
Module Structure Load Combination 2	Retaining Structure	6.6.1.7.1	1.9 MPa < 24.3 MPa 276 psi < 3524 psi	304L	7.8%
	Central Part of the Duct	6.6.1.7.2	2.1 MPa < 15.9 MPa 305 psi < 2306 psi	304L	13.2%
	Retaining Structure	6.6.2.7.1	8.4 MPa < 36.5 MPa 1218 psi < 5287 psi	304L	23.0%
	Central Part of the Duct	6.6.2.7.2	7.2 MPa < 23.9 MPa 1044 psi < 3459 psi	304L	30.2%
Channel Load Combination 8	Lower- & Upperplate	8.1.4	2.3 MPa < 41.2 MPa 334 psi < 5976 psi	304L	5.6%
	Side Plates	8.1.5	2.1 MPa < 85.2 MPa 305 psi < 12357 psi	304L	2.5%
Sump Cover Load Combination 8	Column Main Section	9.1.7.2.2	12.9 MPa < 61.5 MPa 1872 psi < 8920 psi	304L	21.0%
	Column Y-Section	9.1.7.2.2	11.0 MPa < 65.1 MPa 1598 psi < 9442 psi	304L	16.9%

Anchor Bolts

Description	Chapter	Size	Stresses in Bolts				Utilization		
			T	T_A	S	S_A	tension	shear	combined
Module Structure Load Combination 8	Module LC1	6.6.2.9	5.3 kN 1191 lbf	16.2 kN 3642 lbf	5.9 kN 1326 lbf	20.3 kN 4564 lbf	32.7%	29.1%	61.8%
	Module LC2	6.6.3.9	8.4 kN 1896 lbf	16.2 kN 3642 lbf	5.9 kN 1330 lbf	20.3 kN 4564 lbf	52.1%	29.1%	81.2%
	Support Foot A5/A6	6.7.2.1	9.1 kN 2050 lbf	16.2 kN 3642 lbf	5.5 kN 1242 lbf	20.3 kN 4564 lbf	56.3%	27.2%	83.5%
	Support Foot A9	6.7.3.1	8.9 kN 2003 lbf	16.2 kN 3642 lbf	5.2 kN 1167 lbf	20.3 kN 4564 lbf	55.0%	25.6%	80.6%
Closing Modules Load Combination 8	Anchor Bolts A1	7.2.4	4.7 kN 1062 lbf	16.2 kN 3642 lbf	4.6 kN 1030 lbf	20.3 kN 4564 lbf	29.2%	22.6%	51.7%
	Anchor Bolts B3	7.3.4	6.0 kN 1345 lbf	16.2 kN 3642 lbf	3.7 kN 839 lbf	20.3 kN 4564 lbf	36.9%	18.4%	55.3%
	Anchor Bolts C1	7.5.4	5.7 kN 1289 lbf	16.2 kN 3642 lbf	6.1 kN 1371 lbf	20.3 kN 4564 lbf	35.4%	30.0%	65.4%
Channel Load Combination 8	Anchor Bolts C4-C5	8.2.2.3	6.7 kN 1502 lbf	16.2 kN 3642 lbf	7.7 kN 1726 lbf	20.3 kN 4564 lbf	41.2%	37.8%	79.0%
	Anchor Bolts A9-C9	8.3.2.3	5.7 kN 1286 lbf	16.2 kN 3642 lbf	7.2 kN 1622 lbf	20.3 kN 4564 lbf	35.3%	35.5%	70.8%
Sump Cover Load Combination 8	Girders	9.1.7.4.2	1.3 kN 290 lbf	11.8 kN 2659 lbf	1.9 kN 418 lbf	14.8 kN 3331 lbf	10.9%	12.5%	23.5%
	Main Beams	9.1.7.4.2	2.1 kN 482 lbf	14.4 kN 3241 lbf	5.1 kN 1155 lbf	18.1 kN 4062 lbf	14.9%	28.4%	43.3%
	Floating Support	9.1.7.4.2	2.0 kN 458 lbf	16.2 kN 3642 lbf	7.1 kN 1604 lbf	20.3 kN 4564 lbf	12.6%	35.2%	47.7%
	Column-Base Support	9.1.7.4.2	13.0 kN 2927 lbf	14.4 kN 3241 lbf	0.3 kN 66 lbf	18.1 kN 4062 lbf	90.3%	1.6%	91.9%

Linear Type Supports

Description	Chapter	Stresses in linear type supports						Material	Utilization				
		f_a	F_a	f_{bx}	F_{bx}	f_{by}	F_{by}		axial	bending 1	bending 2	combined	
Sump Cover Load Combination 8	Main Beams and Girders	9.1.7.2.1	3.5 MPa 509 psi	155.1 MPa 22500 psi	40.5 MPa 5874 psi	170.6 MPa 24750 psi	33.1 MPa 4801 psi	170.6 MPa 24750 psi	304L	2.3%	23.7%	19.4%	45.4%
	Column Main Section	9.1.7.2.2	12.9 MPa 1872 psi	61.5 MPa 8920 psi	13.8 MPa 1997 psi	170.6 MPa 24750 psi	5.4 MPa 788 psi	170.6 MPa 24750 psi	304L	21.0%	8.1%	3.2%	32.2%
	Column Y-Section	9.1.7.2.2	11.0 MPa 1598 psi	65.1 MPa 9442 psi	16.7 MPa 2425 psi	170.6 MPa 24750 psi	1.0 MPa 142 psi	170.6 MPa 24750 psi	304L	16.9%	9.8%	0.6%	27.3%
	Side Bumper Support	9.4.3	-	-	11.0 MPa 1595 psi	193.9 MPa 28125 psi	-	-	304L	-	5.7%	-	5.7%

ATTACHMENT 1
REGNPP GL 2004-02 THIRD SUPPLEMENTAL RAI RESPONSE

RAI-31: *The Leak-Before-Break (LBB) concept, which was NRC-approved for Ginna for the main coolant loop piping under LOCA (see UFSAR Sections 3.6.1.3.2.13 and 5.4.11.1.2), was appropriately credited in the sump structural analysis as the rationale for not considering the dynamic effects of a break in this particular piping (submittal Section 3.k.1, page 72). However, the supplemental response did not specifically state that the sump was outside the ZOIs of the three pipe breaks postulated in Section 3.e.2 and Figure 3.e.2.1 (page 40) of the supplemental response. Considering this, please provide the following information regarding consideration of possible dynamic effects associated with high-energy line breaks in the sump structural analysis: (a) please examine the above stated break locations relative to the location of the sump and confirm/justify if these postulated breaks would or would not impose dynamic pipe break effects on the sump strainer assembly; and (b) please examine and confirm if there are or are not breaks of any other piping (e.g. safety injection, containment spray lines etc.) for which application of the leak-before-break concept may not have been approved but which may impose dynamic pipe break effects on the strainer assembly. If there are any such cases, please justify why the dynamic pipe break effects of such piping were not considered in the sump structural analysis.*

RAI-31 Response:

(a) The postulated pipe break locations that would result in the worst case debris generation are within the two steam generator compartments. A break in the 31" intermediate leg at the base of the steam generator in each steam generator compartment represents the two LBLOCA pipe break locations with the greatest potential for sump strainer debris loading. A pressurizer spray line break in steam generator compartment "B" represents the SBLOCA pipe break location with the greatest potential for sump debris loading. The containment sump "B" strainer modules are outside the 10 pipe diameters ZOI for any postulated pipe break location in steam generator compartment "A" or "B". Furthermore, the strainer modules are fully shielded by robust concrete walls and barriers that would protect the strainer modules from any jet impingement or pipe whip.

(b) Piping lines inside containment which normally or occasionally experience high energy service conditions (operating temperature > 200 F and/or operating pressure > 275 psig) were evaluated for the effects of potential pipe breaks [31.1]. All high energy lines in containment with the potential of causing the containment sump "B" strainer to fail to fulfill its design function are separated from the strainer modules by substantial distance and/or by robust concrete walls and barriers, resulting in no jet impingement or pipe whip effects from any postulated high energy line break.

RAI-31 References:

31.1 Ginna UFSAR Section 3.6.1, "Postulated Piping Failures in Fluid Systems Inside Containment".

RAI-32: *The supplemental response for Section 3.k is silent with regard to backflushing. Please indicate whether a back-flushing strategy was credited for Ginna. If credited, please provide a summary statement regarding the sump strainer structural analysis considering reverse flow, as requested in the fourth bullet of the guidance for Section 3.k in the Revised Content Guide for GL 2004-02.*

RAI-32 Response: A back-flushing strategy of the Ginna containment sump strainers has not been credited.

ATTACHMENT 1
REGNPP GL 2004-02 THIRD SUPPLEMENTAL RAI RESPONSE

RAI-33: *Please confirm that the downstream effects components and systems evaluation performed for Ginna used the guidance in WCAP-16406-P, Revision 1 and the NRC safety evaluation of WCAP-16406-P, Revision 1.*

RAI-33 Response: In 2007, Westinghouse performed downstream effects analyses for Ginna to support responses to the NRC regarding GSI-191 resolution. The analyses performed were based on WCAP-16406-P, Revision 1. At the time the work was done, the Pressurized Water Reactor Owners' Group (PWROG) was in possession of the NRC draft Safety Evaluation (SE). Westinghouse applied the methodologies developed in WCAP-16406-P, Revision 1 to reach the conclusions developed in the analytical work performed. Subsequently, the NRC-approved version of that WCAP was issued [33.1], which included the NRC final SE. The final SE included a list of Limitations and Conditions to which utilities must adhere when applying the methodologies in the WCAP. A review of the original analytical work was performed by Westinghouse to address the impact of the NRC's final SE to the evaluations done for Ginna using the methodology of Reference 33.1. The results of this review, as documented in Reference 33.2, definitively demonstrate Ginna's adherence to those Limitations and Conditions, with the following clarification:

The PWROG has submitted WCAP-16793-NP, Revision 0 [33.3] to the NRC. WCAP-16793-NP, Revision 0 is currently being revised to address NRC RAIs on that document, including the incorporation of debris capture testing for fuel. Ginna will address in-vessel downstream effects associated with GSI-191 after NRC issues a Safety Evaluation (SE) on Revision 1 WCAP-16793-NP. Within 90 days of issuance of the SE, a submittal will be made either demonstrating that Revision 1 of WCAP-16793-NP applies to Ginna, that Ginna is bounded by the information presented in Revision 1 of WCAP-16793-NP, and the in-vessel downstream effects are addressed; or providing a schedule for completing the in-vessel downstream effects evaluation for response to this Limitation/Condition to WCAP-16406-P. This Commitment is captured in Attachment 2.

RAI-33 References:

- 33.1 Westinghouse WCAP-16406-P-A, Rev. 1, "Evaluation of Downstream Sump Debris Effects in Support of GSI-191," March, 2008.
- 33.2 Westinghouse LTR-SEE-IV-09-25, Rev. 0, "Impact Evaluation – NRC Final Safety Evaluation Limitations & Conditions on WCAP-16406-P-A".
- 33.3 Westinghouse WCAP-16793-NP, Rev. 0, "Evaluation of Long-Term Cooling Considering Particulate, Fibrous, and Chemical Debris in the Recirculating Fluid," May 2007.

RAI-34: *The February 29, 2008, supplemental response discusses the assumptions for post-LOCA pH in the sump pool but did not provide the pH values for the containment spray. The corrosion rate of aluminum exposed to initial containment spray containing injected sodium hydroxide will be higher due to the increased pH before an equilibrium pH is reached in the sump. Please provide the containment spray pH values used as input for the WCAP-16530-NP chemical spreadsheet from the time that sodium hydroxide is injected into the containment spray until an equilibrium pH value is reached.*

ATTACHMENT 1

REGNPP GL 2004-02 THIRD SUPPLEMENTAL RAI RESPONSE

RAI-34 Response: The containment spray pH value used as input to the WCAP-16530-NP chemical effects spreadsheet is 9.76. This pH value was applied for the entire period in which containment spray is active [34.1]. During the times that containment spray is active, the chemical effects spreadsheet evaluates the impact of the spray, at the pH value specified, on all exposed aluminum.

RAI-34 References:

34.1 CN-SEE-I-07-16, "R. E. Ginna GSI-191 Chemical Effects Evaluation," Rev. 2.

RAI-35: *The February 29, 2008, supplemental response indicated that aluminum corrosion inhibition by silica leached from various sources was stated to not have been taken into account. However, the 71.3 kg of sodium aluminum silicate tested in February 2008, appears to be consistent with a silica refinement value shown in Table 3.o.1 in the February 29, 2008, supplemental response. Please clarify if aluminum corrosion inhibition by silica was credited. If silica inhibition credit was used to reduce the amount of aluminum containing precipitate, please address the following: (a) the types and amounts of plant debris assumed to provide the source of silicates, (b) the dissolved silicate concentration assumed to inhibit aluminum corrosion and the time assumed to reach that silicate concentration, (c) for cases where silicate inhibition was credited, discuss whether other breaks that produce less calcium silicate were considered to ensure that these breaks did not produce a more challenging head loss test by having a greater amount of chemical precipitate, and (d) how much of the amount of chemical precipitates in the head loss test was reduced by silicate inhibition.*

RAI-35 Response: The February 29, 2008, supplemental response made reference to chemical effects testing performed in November 2007. The November 2007 chemical effects testing used a conservative quantity of chemical precipitant (81 kg), as calculated following the WCAP-16530-P methodology. This quantity of precipitant did not credit the silicate inhibition of aluminum corrosion. Additional chemical effects testing was being conducted in late February to early March 2008, as the February 29, 2008, supplemental response was being prepared. The February 29, 2008 supplemental response did not discuss the results of these tests, since they had not been finalized. The July 25, 2008, Second Supplementary response discussed the results of the February / March 2008 chemical effects testing. The chemical precipitant quantity used in the February / March 2008 testing was 71.3 kg. At the time, the intent was to credit silicate inhibition of aluminum corrosion.

However, subsequent re-analysis of the Ginna chemical effects [35.1] shows that by re-proportioning the submerged/unsubmerged aluminum that was included as contingency (margin), a precipitant quantity of 71.3 kg would be generated without crediting silicate inhibition of aluminum corrosion. The original analysis assumed that 100% of the aluminum contingency (margin), which is not present in containment, would be submerged. Additionally, the same 100% contingency was conservatively added to the quantity of unsubmerged aluminum, thereby doubling the contingency. Modifying the contingency proportion to 18% submerged and 82% unsubmerged, results in a reduction of the precipitant generated from 81.0 to 71.3 kg, without crediting silicate inhibition of aluminum corrosion. This proportion of submerged/unsubmerged aluminum is reasonable given that the recirculation pool depth is less than 10% of the elevation to the containment operating floor. (This re-analysis highlights the compensating effects of conservatism embedded in the analysis that offset uncertainties that may be present in analytical methods, e.g., crediting silicate inhibition of aluminum corrosion). Therefore, the quantity of sodium

ATTACHMENT 1
REGNPP GL 2004-02 THIRD SUPPLEMENTAL RAI RESPONSE

aluminum silicate precipitant used during the Ginna head loss testing (1.398 kg (71.3 kg / 51.02 scaling factor)) does not credit silicate inhibition of aluminum corrosion.

RAI-35 References:

35.1 CN-SEE-I-07-16, "R. E. Ginna GSI-191 Chemical Effects Evaluation," Rev. 2.

RAI-36: *The February 29, 2008, supplemental response stated that licensee analysis of the Control Components, Incorporated (CCI) precipitate generation methodology concluded that approximately four times the precipitate that was expected per WCAP-16530-NP formed in the test loop. Therefore the chemical effects testing was considered flawed and additional testing was performed. Please describe the analysis that was performed and the basis for concluding that four times the predicted amount of chemical precipitate formed in the CCI test loop. In addition, please describe why the precipitate that formed in the test loop was not representative of what could form in the sump pool following a loss of coolant accident.*

RAI-36 Response: The Ginna chemical effects testing was first conducted in November 2007, using a method that CCI had developed and used exclusively up to that point. The CCI method used at that time did not follow the guidance provided in WCAP-16530-NP. The CCI method relied on the formation of precipitants within the test loop, as opposed to the WCAP methodology, which prescribes the formation of precipitants outside the test loop, for later addition to the test loop.

The CCI method of chemical precipitant preparation relied on an analysis and confirming bench top tests to determine the quantity of chemicals to be used to produce the chemical precipitants predicted by WCAP-16530-NP. These quantities of chemicals were scaled up to correspond to the volume of water in the test loop. The following quantities of chemicals were added to the test loop for the November 2007 Ginna chemical effects test [36.1].

100% Chemical Addition Amount	Quantity
Boric Acid	17.920 kg
Sodium Aluminate Solution, 36%	0.835 kg
Calcium Chloride Solution, 34%	4.151 kg
Sodium Silicate Solution, 38%	5.708 kg
Caustic Soda 30%	7.400 kg

The scaled quantity of precipitant (sodium aluminum silicate) to be generated and produced in the test loop, as a result of this chemical addition, was 0.794 kg (81 kg, as predicted through the WCAP-16530-NP methodology / 102.05, test loop scaling factor).

As a result of the unexpectedly high strainer head loss obtained during the November 2007 testing, Ginna embarked on an effort to understand the test results. An initial review of the testing methodology uncovered several concerns.

- 1) The quantities of chemicals added to the test loop to produce 0.794 kg of precipitant seemed excessive.

ATTACHMENT 1
REGNPP GL 2004-02 THIRD SUPPLEMENTAL RAI RESPONSE

- 2) Boric acid was added to the test loop, followed by the fibrous and particulate debris, without any consideration for the interaction of the boric acid and subsequent chemical addition on the fiber and particulates already in the test loop. Instead of adding an inert precipitant to the test loop, as prescribed by the WCAP, uncontrolled reactions in the test loop were allowed to take place. Adequate control of the quantity and morphology of precipitant generation in the test loop appeared to be lacking.
- 3) Calcium chloride solution was added to the test loop, where neither calcium, nor chloride is a required constituent element for the formation of sodium aluminum silicate. Ginna's initial suspicion that four times the precipitant that was required to be formed in the test loop is based on the quantities of calcium added to the test loop. With the addition of 4.151 kg of calcium chloride solution along with the quantities of calcium silicate insulation and calcium oxide from the stone flour already in the test loop, it was suspected that significant quantities of calcium precipitates were being formed.
- 4) The appearance of the precipitant was not as described in the available literature and that received anecdotally.

To further explore Ginna's initial concerns, an analysis of the CCI testing methodology by MPR, Associates, was conducted [36.2]. The analysis confirmed Ginna's concern that the CCI method was flawed and produced precipitants in excessive quantities. The following are observations and recommendations from the MPR report:

- 1) Perform head loss testing by preparing a separate solution of the desired precipitant following the methods in WCAP-16530-NP. The mixtures have been shown in other tests to achieve the desired precipitate quantity and morphology.
- 2) Sodium hydroxide buffer should have been added immediately after the boric acid to more correctly model the plant response. Sodium hydroxide buffer was added at the end of test to adjust the fluid pH. This is not consistent with the plant design. The test design does not appear to mimic the plant. Addition of sodium hydroxide is critical for controlling pH levels early in the accident.
- 3) There is no need for the calcium chloride solution to be added to the test loop.
- 4) The chemical compounds used in the CCI method appear to produce undesired precipitants. The choice of sodium aluminate solution as a source of aluminum deviates from the WCAP methodology, which relies on aluminum nitrate solution. The former dissolves in water to produce an alkaline aqueous solution, whereas the latter is an acidic aqueous solution. Aluminum hydroxide is a likely precipitant formed. The results of the head loss test shows that the circulating water was in the acidic range when the sodium aluminate solution was added. An excess of silicon does not appear to be available for aluminum to react with given the order by which the precursor solutions are added and the reaction kinetics of the aluminum hydroxide precipitation reaction. The first sodium silicate addition occurred about 15 hours after the sodium aluminate addition.

ATTACHMENT 1
REGNPP GL 2004-02 THIRD SUPPLEMENTAL RAI RESPONSE

- 5) With regard to the role of calcium in the precipitation process, the bench top analysis clearly shows that approximately 50% of the added calcium source will precipitate. However, the WCAP analytic methods show that only calcium phosphate is a candidate for precipitation and only in plants buffered with tri-sodium phosphate. No calcium precipitate is expected in a plant buffered with sodium hydroxide. The calcium precipitated from solution is an unexpected result. There are a number of pathways for calcium-based compounds to precipitate. Calcium oxide, which is readily available in stone flour (9.3% by mass) and reacts with water to form calcium hydroxide is a source of calcium precipitate when sodium hydroxide is present.

As discussed above, there are a number of reasons to believe that the test performed in November 2007 was not representative of what could form in the Ginna sump recirculation pool following an accident.

- 1) Excess calcium was added to the test loop, resulting in calcium precipitant formation.
- 2) The order and combination of the chemicals added to the test loop was not representative of the containment environment, which lead to the formation of aluminum hydroxide.
- 3) Boric acid was added to the test loop before any of the fiber and particulate debris. Sodium hydroxide buffer was not added to the test loop until the end of the test. This allowed for uncontrolled interactions in the test loop.

As a result of the evaluations performed, the November 2007 chemical effects testing was determined to be flawed and non-representative of the Ginna containment sump recirculation pool post-LOCA. Additional testing, strictly following the methods of WCAP-16530-NP, was conducted in February / March 2008. The results of these tests showed that the Ginna sump strainers have ample NPSH margin [36.3].

RAI-36 References:

- 36.1 Q.003.84 804, "Chemical Effect Head Loss Test Specification," Rev. 0.
- 36.2 MPR, Associates Inc. Letter Report, DRN: 0236-0708-001, "Review of Ginna and Calvert Cliffs Chemical Effects Testing," January 4, 2008.
- 36.3 3SA-096.077, "Head Loss Calculation Including Chemical Effects," Rev. 1.

ATTACHMENT 1

REGNPP GL 2004-02 THIRD SUPPLEMENTAL RAI RESPONSE

RAI-37: *Please indicate what aspects of the plant's licensing basis has changed and/or what new information will be added and considered to be part of the plant's licensing basis. Please provide a schedule for establishing a revised licensing basis.*

RAI-37 Response:

The design basis of the modified emergency sump strainer has been incorporated into the plant's current licensing basis. The Updated Final Safety Analysis Report and Technical Specification Bases have been revised to include this information as part of the modification implementation process. At this time, Ginna does not anticipate any additional licensing changes to achieve compliance with regulatory requirements listed in the Applicable Regulatory Requirements section of GL 2004-02.

ATTACHMENT 2

LIST OF REGULATORY COMMITMENTS

ATTACHMENT 2
SUMMARY OF REGULATORY COMMITMENTS

The following table identifies those actions committed to by Ginna LLC in this document. Any other statements made in this submittal are provided for informational purposes only and are not to be considered regulatory commitments. Please direct any questions you have in this matter to Mr. Thomas Harding at (585)771-5219.

COMMITMENT	COMPLETION DATE
Ginna LLC will provide the results of evaluations of in-vessel downstream effects for RAI Question #33 within 90 days of issuance of the NRC's Safety Evaluation of Revision 1 for WCAP-16793-NP.	Within 90 days of issuance of the final NRC SER on WCAP-16793-NP

ATTACHMENT 3

**SUMMARY OF CALCIUM SILICATE TYPES USED IN
CONTAINMENT AT US NUCLEAR PLANTS**

ATTACHMENT 3

SUMMARY OF CALCIUM SILICATE INSULATION TYPES USED INSIDE CONTAINMENT AT US NUCLEAR PLANTS

Summary of Calcium Silicate Insulation Types Used Inside Containment at US Nuclear Plants By Gordon H. Hart, P.E. December 31, 2007

Over the past 50 years or so of nuclear power plant construction and operation, several different types of calcium silicate pipe and block insulation have been used:

1. Type I, which contains asbestos fibers as reinforcement and is a Post Autoclave process;
2. Type II, which is free of asbestos fibers and is made by a filter press, pre-autoclave process (sometimes referred to as the Johns-Manville Process);
3. Type III, which is free of asbestos fiber and is made in a pour and mold process known as the Pabco Process, also a Post Autoclave process.

All three types start with an aqueous mixture, or slurry, of lime, diatomaceous earth (i.e., silica), and some type of reinforcing fibers (such as asbestos, wood pulp, rayon, polyester, glass, or other). This slurry is first heated and then poured into molds to be formed into the final shape of either blocks or curved sections to fit onto a pipe. Once formed into desired shapes and allowed to set for a short period of time for the chemical reaction to initiate, the Types I and III process sections are then processed in a high pressure steam vessel known as an autoclave where the chemical reaction to form calcium silicate crystals is completed. The Type II process sections, by contrast, are reacted prior to pouring the slurry into the molds as opposed to afterwards. In all three types, once removed from the molds and allowed to dry, moisture is replaced by air, resulting in an excellent thermal insulation material with a high compressive resistance.

Due to the high strength of the asbestos fibers, the Type I calcium silicate (contains asbestos reinforcing fibers), when it was made, was extremely hard and more durable than the other two types of Cal-Sil. However, when broken or pulverized, the asbestos fibers could become airborne, posing a health hazard. For this reason, no North American manufacturer of calcium silicate has made this type of insulation since 1972. At the time, however, there remained large quantities of this Type I insulation in warehouses so it was still installed on many projects where asbestos containing material was still allowed.

The Type II calcium silicate (that made by pre-autoclave process), the chemical reaction to form calcium silicate takes place while still in a liquid form; the material is then squeezed together for remove much of the water and form sections. By contrast, the Type III (that made by the post autoclave or Pabco Process), the chemical reaction takes place while in the molded shapes. In the end, the Type II product is somewhat harder than the Type III product and hence is more prone to staying together when immersed in a water bath. If the Type III blocks are broken into chunks and covered with water, they also will readily absorb the water but they may also eventually break apart into smaller pieces. By contrast, if the Type II blocks are broken into chunks and covered with water, the material readily absorbs the water but are less inclined to break into smaller pieces.